CENTRO DE INVESTIGACIONES EN ÓPTICA, A.C.

Photochemical synthesis of heparin-based gold nanoparticles and their use in Surface Enhanced Raman Spectroscopy.

PhD in Optical Sciences

María del Pilar Rodríguez Torres

Advisor: Dr. Luis Armando Díaz -Torres.

September 3rd 2015

León, Guanajuato,Mexico

Versión definitiva. Incluye cambios sugeridos por revisores

I, María del Pilar Rodríguez-Torres, declare that this thesis, submitted in fulfilment of the requirements for the award of Doctor of Philosophy, at Centro de Investigaciones en Óptica, A.C., is wholly my own work unless otherwise referenced or acknowledged. The document has not been submitted for qualifications at any other academic institution.

María del Pilar Rodríguez Torres.
September 2015.

_____

Dr. Luis Armando Díaz Torres.

PhD Advisor.

Examination comittee:

_____

Dr. Claudio Frausto Reyes

_____

Dr. Laura Susana Acosta Torres

_____

Dr. Luis Armando Díaz Torres

September 3rd, 2015, León, Guanajuato México.

DEDICATION

I dedicate my dissertation work to my family and many friends. A special feeling of gratitude to my loving parents, María de Jesús and Pablo, whose words of encouragement and push for tenacity ring in my ears and to my sister Lorena who has never left my side and is very special.

ACKNOWLEDGEMENTS

I want to thank Dr. Luis Armando Díaz Torres for being my advisor and teacher over the four years I have been here at Centro de Investigaciones en Óptica.

I thank the members of our lab group for their help and support throughout my research. I also want to thank the technicians and members (students and researchers) of other groups and laboratories besides mine for helping me out when in need . I want to add a special acknowledgement to Dr. Raúl Borja Urby for the UV reactor manufacturing with which the synthesis procedures were carried out all through the project.

I also thank my revision committee for the feedback given throughout this time as well as for the comments and corrections for this thesis work improvement.

Last but not least I thank all of my friends at CIO and outside it and of course, my family for all of their support they have given me over the years during my PhD stay and all my life. They have been there cheering me up when I needed it the most.

Contents

Summary.

This dissertation deals with gold nanoparticle green synthesis in aqueous solution using heparin, as a reducing and stabilizing agent, without other reagents through photochemistry, and their usage as surface enhanced Raman colloidal substrates. This work is divided in four parts: The first one is about proposing the photochemical synthesis method used to prepare the heparin-based gold nanoparticles in aqueous solution using UVA light (λ=366 nm). Two types of experiments were carried out: The nanoparticles were synthesized using reactive and pharmaceutical-grade heparins. Nanoparticle characterization was carried out with UV-Vis spectroscopy and Scanning Electron Microscopy. In the second one, a nanoparticle formation mechanism is proposed with the aid of UV-Vis and FTIR spectroscopies and pH measurements. In the third part, surface enhanced Raman activity is investigated, finding that reactive-grade heparin gold nanoparticles yield good Raman signals and the pharmaceutical-grade ones do not. The probe molecules used were differently charged dyes: Methylene Blue (-), Rosebengal (+) and Neutral Red (+-); as well as proteins (GP120 and Bovine Serum Albumin). There are no reports on heparin-gold nanoparticles being used for this purpose to our knowledge. In the final section, this dissertation´s contributions are presented as a closure to the research that was performed.

Introduction.

Green chemistry is the design of chemical products and processes that reduce or eliminate the use and/or generation of hazardous substances. In the case of nanotechnology, it implies producing nanomaterials and products without harming the environment or human health, and producing materials that provide solutions to environmental problems. It relies on the principles of green chemistry and green engineering to make nanomaterials without toxic reagents, at low temperatures using less energy and renewable inputs wherever possible, and using lifecycle thinking in all design and engineering stages. All this turns out into making current manufacturing processes for nanomaterials and products more environmentally friendly and even unexpensive. The 12 basic principles of green chemistry are cited below [1]:

1. It is better to prevent waste than to treat or clean up waste after it is formed.

2. Synthetic methods should be designed to maximize the incorporation of all materials used in the process into the final product.

3. Wherever practicable, synthetic methodologies should be designed to use and generate substances that possess little or no toxicity to human health and the environment.

4. Chemical products should be designed to preserve efficacy of function while reducing toxicity.

5. The use of auxiliary substances (for example, solvents, separation agents and so on) should be made unnecessary wherever possible and innocuous when used.

6. Energy requirements should be recognized for their environmental and economic impacts and should be minimized. Synthetic methods should be conducted at ambient temperature and pressure.

7. A raw material feedstock should be renewable rather than depleting wherever technically and economically practicable.

8. Unnecessary derivatization (blocking group, protection/deprotection, and temporal modification of physical/chemical processes) should be avoided whenever possible.

9. Catalytic reagents are superior to stoichiometric reagents.

10. Chemical products should be designed so that at the end of their function they do not persist in the environment and break down into innocuous degradation products.

11. Analytical methodologies need to be further developed to allow for real time ,in-process monitoring and control prior to the formation of hazardous substances.

12. Substances and the form of a substance used in a chemical process should be chosen so as to minimize the potential for chemical accidents, including releases, explosions and fires.

The green preparation of nanoscale structures can be accomplished through bottom-up or top-down methods. In the bottom-up approach, small building blocks are assembled into larger structures: like in chemical synthesis, colloidal aggregation and self-assembly. In the top-down approach, large objects are modified to give them smaller features, for example, lithographic techniques (ion beam), film deposition and growth and mechanical techniques (machining and grinding) [2,3].

One green way to achieve nanoparticle (NP) production is through light irradiation, which is what is presented and is a bottom-up approach. Photochemistry plays an important role in noble metal nanoparticle synthesis because it generates zero-valent metal atoms (M^0) through the direct photoreduction of a metal source (metal salt or complex), or the reduction of metal ions using

photochemically generated intermediates such as excited molecules and radicals (so it is a bottom-up approach), which in the end lead to nanoparticle generation. Photochemical synthesis is suitable for the selective fabrication of metal NPs [4]. Other advantages this approach has are: reaction selectivity and controllability as well as shape conversion using different wavelengths [5].

Heparin is used as the reducing and capping agent for the gold nanoparticle synthesis. It is a material belonging to the glycosaminoglycans family, it is usually stored within the secretory granules of mast cells and released only into the vasculature at sites of tissue injury [6]. When produced artificially it is used for anticoagulation purposes. It is highly sulfated and has a high negative charge due to the sulfo and carboxyl gropus along its structure. Also, it is a mixture of linear anionic polysaccharides having 2-O-sulfo-α-L-iduronic acid, 2-deoxy-2-sulfamino-6-O-sulfo-α-D-glucose, β-D-glucuronic acid,2-acetamido-2-deoxy-α-D-glucose, and α-L-iduronic acid as major saccharide units. These are joined through 1→4 glycosidic linkages [7] .The presence and frequency of these saccharide units vary with the tissue source from which heparin is extracted, in our case it comes from porcine intestinal mucosa.

Nanoparticle synthesis procedures using heparin have already been developed: Non-metallic [8-12], and noble-metal [13-16] , however most of these synthesis methods but are based on either room-temperature [8-12] or thermal approaches [14-16]. In some cases, heparin is conjugated to the nanoparticles after they have been synthesized by other methods [8,13]. Heparin is sometimes conjugated to other materials before nanoparticles are synthesized [9-12] or used directly for nanoparticle synthesis directly without any modification [15,16] . In all cases, the nanoparticles have quasispherical and spherical forms. The uses of these nanoparticles are related to disease treatment [10], drug delivery [8,9,14], tumor targeting [11-13]; but when it comes to the heparin-

based noble metal nanoparticle production, the applications are focused on the anticoagulant activity they possess for angiogenesis [14] and citotoxicity [13] studies, as well as for cancer-cell imaging [19]. Other published approaches just mention how nanoparticles are synthesized and the advantage posed by the fact they are already functionalized by heparin, but no applications are mentioned [15,16] . Neither a photochemical approach for synthesizing heparin-based gold nanoparticles nor their subsequent use as Surface Enhanced Raman substrates has been reported so far.

Raman scattering is a spectroscopic technique used to observe vibrational, rotational, and other low-frequency modes in a system. It relies on inelastic scattering, or Raman scattering of monochromatic light, usually from a laser in the visible, near infrared, or near ultraviolet range. The laser light interacts with molecular vibrations, phonons or other excitations in the system, resulting in the energy of the laser photons being shifted up or down. The shift in energy gives information about the vibrational modes in the system. Light from the illuminated spot is collected with a lens and sent through a monochromator. Wavelengths close to the laser line due to elastic Rayleigh scattering are filtered out while the rest of the collected light, with a frequency shifted from the incident one (Stokes or anti-Stokes) is dispersed onto a detector. Surface-enhanced Raman spectroscopy or surface-enhanced Raman scattering (SERS) is a surface-sensitive technique that enhances Raman scattering by molecules adsorbed on rough metal surfaces or nanostructures [17]. SERS is considered to rely on two enhancing mechanisms, the electromagnetic and the chemical one. The electromagnetic enhancement is a result of the amplification of the light by the excitation of the localized surface plasmon resonances. This light concentration occurs preferentially in the gaps, crevices or sharp features of plasmonic materials with nanoscale features [17].

The chemical enhancement involves charge transfer mechanisms, where the excitation wavelength is resonant with the metal-molecule charge transfer electronic states [18].

Heparin was chosen as the synthesis material because it is reactive to UV light, it acts as a reducing and capping agent. During the synthesis process, heparin suffers changes, structurally speaking, which allow nanoparticle growth, coverage, and most importantly, functionalization. As it was mentioned above, there are already heparin-based nanoparticle synthesis protocols but the one presented here is different and new, because it is photochemistry-oriented , has not been used before, the shapes obtained are not just spherical or quasispherical, the obtained gold nanoparticles are functionalized without having to modify heparin, and because it is a green approach which finally leads to SERS applications.

References.

[1] Anastas P.T., Kirchhoff M.M., (2002), Origins, current status, and future challenges of Green Chemistry, Acc. Chem. Res.,35,686-694.

[2] Vadlapudi V., Kaladhar D.S.V.G..K.,(2014), Review: Green Synthesis of Silver and Gold Nanoparticles, Middle-East Journal of Scientific Research, 19 ,6, 834-842.

[3] Lockwood D.J (Series editor), Rotello V. ,(2004), Nanoparticles: Building blocks for nanotechnology. 1st edition, Springer, United States of America.

[4] Sakamoto M., Fujistuka M., Majima T.,(2009), Light as a construction tool of metal nanoparticles: Synthesis and mechanism, Journal of Photochemistry and Photobiology C: Photochemistry Reviews, 10, 1, 33–56.

[5] Kim F., Song J.H., Yang P.,(2002), Photochemical Synthesis of Gold Nanorods, Journal of the American Chemical Society , 124, 14316-14317.

[6] Hirsch J.,Warkentin T.E., Shaughnessy S.G., Anand S.S., Halperin J.L., Raschke R., Granger C., Ohman E.M,., Dalen J.E.,(2001), Heparin and low-molecular-weight heparin.Mechanism of action, pharmacokinetics, dosing, monitoring, efficacy, and safety,CHEST, 119,1, 63S-94S.

[7] Baxter Healthcare Corporation, (no year), *Heparin sodium injection USP*, Deerfield, Ill, USA.

[8] Chung Y.I., Taea G,Yuk S.H., (2006), A facile method to prepare heparin-functionalized nanoparticles for controlled release of growth factors, Biomaterials ,27,2621–2626.

[9] Park K., Lee G.Y., Kim Y.S., Yu M., Park R.W.,Kim I.S., Kim S.Y., Byun Y.,(2006), Heparin–deoxycholic acid chemical conjugate as an anticancer drug carrier and its antitumor activity, Journal of Controlled Release 114 ,300–306.

[10] Chang C.H, Huang W.Y., Lai C.H., Hsu Y.M., Yao Y.H., Chen T.Y.,Wud J.Y., Peng S.F., Lin Y.H. ,(2011), Development of novel nanoparticles shelled with heparin for berberine delivery to treat Helicobacter pylori, Acta Biomaterialia 7 ,593–603.

[11] Chung Y.I., Kim J.C., Kim Y.H., Tae G.,Lee S.Y.,Kim K., Kwon I.C., (2010), The effect of surface functionalization of PLGA nanoparticles by heparin- or chitosan-conjugated Pluronic on tumor targeting, Journal of Controlled Release 143, 374–382.

[12] Nurunnabi Md, Khatun Z., Lee Y.K.,(2012), Heparin-based nanoparticles for cancer targeting and noninvasive imaging, Quantitative Imaging in Medical Surgery ,2,3,219-226

[13] Lee K., Lee H., Bae K.H., Park T.G.,(2010), Heparin immobilized gold nanoparticles for targeted detection and apoptotic death of metastatic cancer cells, Biomaterials 31, 6530-6536.

[14] Kemp M.M., Kumar A., Mousa S., Dyskin E., Yalcin M., Ajayan P., Lindhardt R.J., Mousa S.A., (2009), Gold and silver nanoparticles conjugated with heparin derivative possess anti-angiogenesis properties, Nanotechnology, 20, 45, 1-7.

[15] Guo Y.,Yan H., (2008), Preparation and characterization of heparin-stabilized gold nanoparticles, Journal of Carbohydrate Chemistry,27,5, 309-319.

[16] Huang H.,Yang X.,(2004), Synthesis of polysaccharide-stabilized gold and silver nanoparticles: a green method, Carbohydrate Research 339, 2627–2631.

[17] Haynes C.L., McFarland A.D., Van Duyne R.P., (2005), Surface Enhanced Raman Spectroscopy, Analytical Chemistry, 77, 17, 338A-346A.

[18] Sharma B., Frontiera R.R., Henry A.I., Ringe E, Van Duyne R.P., (2012), SERS: Materials, applications and the future, Materials Today, 15,1/2, 16-25.

[19] Lee K., Lee H., Bae K.H., Park T.G.,(2010), Heparin immobilized gold nanoparticles for targeted detection and apoptotic death of metastatic cancer cells, Biomaterials 31, 6530-6536.

Chapter 1.

On the synthesis methodology and characterization techniques.

In this chapter, the photochemical synthesis of heparin-based gold nanoparticles in solution by photochemistry and heat to contrast both methods is described. Nanoparticle characterization was performed by UV-Vis spectroscopy, Scanning Electron Microscopy (SEM) and Transmission Electron Microscopy (TEM). Characterization of the heparin-based products was used to investigate their properties.

Noble metal heparin nanoparticles have been synthesized already using wet chemistry methods [1-3], but there are only two methods by which gold nanoparticles are prepared using heparin as a reducing and stabilizing agent [2,3], both of them involve heating solutions at boiling temperatures and then the dropwise addition of heparin, in one of them, heparin is used directly as purchased [3] and in the other, heparin is modified [2]. Here, results obtained by using both UVA radiation and heating will be compared.

1.1 Heparin-based gold nanoparticle synthesis.

Two kinds of heparin were used for the photochemical synthesis of gold nanoparticles in solution: 1) Pharmaceutical grade (5000 IU/mL, 10 mL) from PISA laboratories, Mexico and 2) reactive-grade heparin sodium powder (195.9 USP units/mg, 1 g) from Sigma-Aldrich. The metal precursor, chloroauric acid ($HAuCl_4$) was also purchased from Sigma-Aldrich. Benzyl alcohol was from KARAL, SA de CV, Mexico. All reagents were used without any further modification

or purification. Samples were centrifuged 4 times at 13,500 rpm in a SIGMA 2-6 centrifuge and redispersed in deionized water.

A different solvent was used for each synthesis type:

- When pharmaceutical-grade heparin gold nanoparticles were synthesized, the necessary amount of solution was taken directly from the bottle and then $HAuCl_4$ was added. So, the solvent was the excipient (The PISA water/benzyl alcohol mixture formulation).
- As for reactive-grade heparin gold nanoparticles, a deionized water/benzyl alcohol mixture at 1:106 ratio was prepared to be dissolved in it, and $HAuCl_4$ was added afterwards. Ghasemi et al [4] studied the content of benzyl alcohol in pharmaceutical preparations and the benzyl alcohol UV-Vis spectrum they obtained was used to compare it with the spectrum taken from the pharmaceutical-grade heparin excipient. Then, the deionized water/benzyl alcohol mixture ratio was determined as to match the absorption spectrum of the pharmaceutical-grade heparin´s excipient (black line in figure 1.1) . Thus by using UV-Vis spectroscopy, a solution with almost the same heparin concentration as the pharmaceutical-grade heparin was prepared for the reactive-grade heparin synthesis solvent (red line in figure 1.1). All reactive grade heparin experiments were carried out under the same conditions.

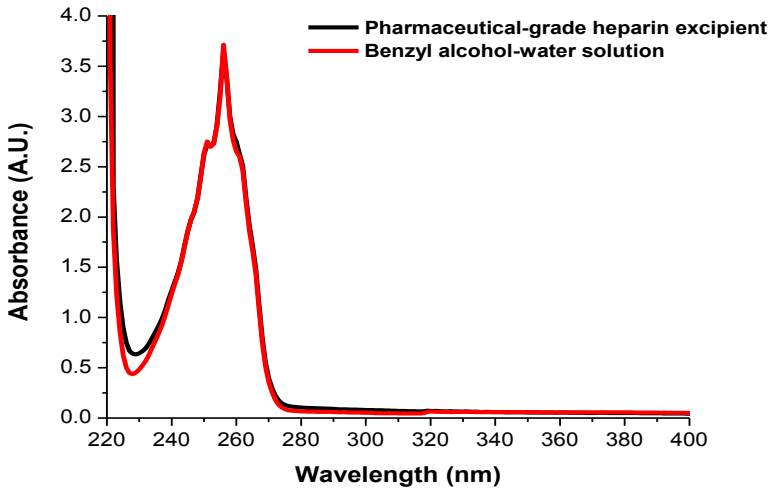

Figure 1.1 UV-Vis spectra of solvents used for each type og gold nanoparticle synthesis. The black line indicates the pharmaceutical-grade heparin excipient while the red line represents the solution prepared for reactive-grade heparin dissolution.

Gold nanoparticles synthesized with reactive-grade heparin were also prepared using deionized water as a solvent, too.

The device used for solution irradiation was a home-made UV reactor of cylindrical shape (shown in figure 1.2), its walls were made of aluminium with holes pierced vertically, within which there were 3 black light lamps in vertical position, on top of it a fan was placed to prevent overheating inside it during the reactions. The temperature reached in experiments was in the range of 35-38°C (such data being monitored by means of a thermocouple). The 10 mm quartz cell used in all the syntheses was placed in the center of the reactor and at a distance of 6 cm from each lamp. The experimental setup for the syntheses is shown in figure 1.2 .Samples were irradiated for 7 hours.

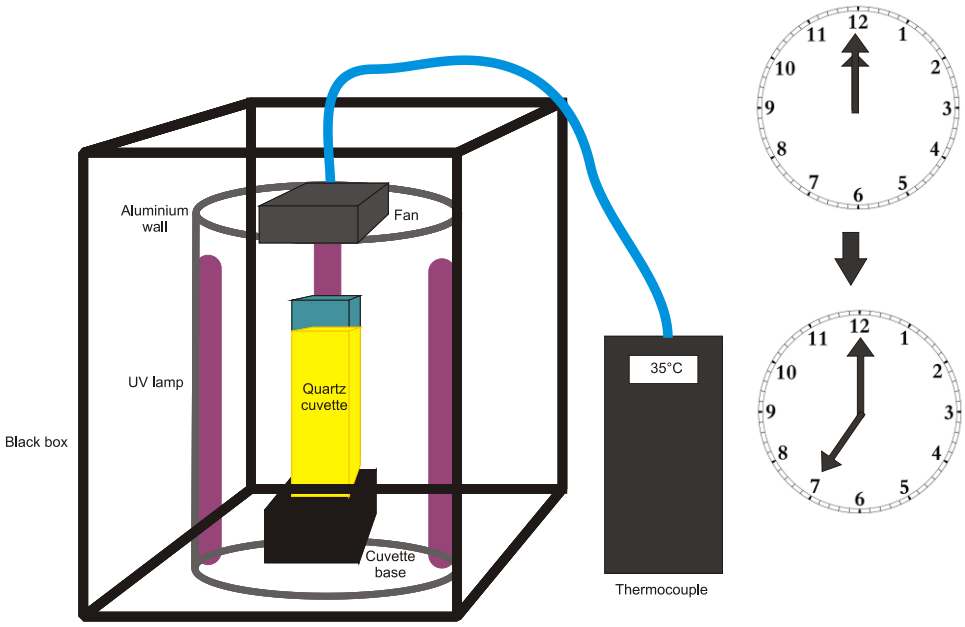

Figure 1.2 Setup for photochemical synthesis of heparin-based gold nanoparticles.

Black light lamps (4 W, 160 mm long) were purchased from TECNOLITE (Mexico), they are made of black light blue (dark blue) glass, which transmits UVA radiation, but gives only a minimum of visible light, such lamps are usually used in industry and criminology, for instance. They emit radiation at 366 nm, as shown in the emission spectrum in figure 1.3.

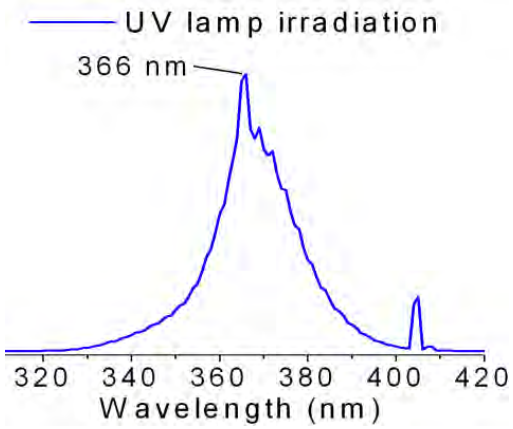

Figure 1.3 Emission spectra of the UV lamps used for heparin-based gold nanoparticle synthesis.

The wavelength of these lamps was chosen because they produce the least harm to skin and eyes, the easiness to get them, as well as their low price.

All the protocol was thought and conceived as a green alternative, from the reactants used and materials the UV reactor was made of, up to the lamps type used, considering low costs as well.

1.2 Photochemical synthesis of gold nanoparticles.

First, a mixture solution containing all reaction components is prepared as follows: Inside a volumetric flask, water is poured, then specific liquid amounts of $HAuCl_4$ and then heparin of either reactive grade (dissolved in either water or a water-benzyl alcohol mixture) or the pharmaceutical-grade one (in benzyl alcohol/water excipient) are added. The mix is then agitated by hand for the constituents to be well blended. Afterwards, the as-prepared solution is poured inside the quartz cell.

A fixed concentration for both reactants: heparin of either type and chloroauric acid was chosen:

Heparin: 0.833 mM

$HAuCl_4$: 0.840 mM

The syntheses were prepared and named as follows:

RGHEPWAU: Reactive-grade heparin based synthesis using just water as solvent.

RGHEPBAWAU: Reactive-grade heparin based synthesis using water-benzyl alcohol as solvent.

PGHEPAU: Pharmaceutical-grade heparin based synthesis using water-benzyl alcohol as solvent.

1.3 Characterization and Discussion.

1.3.1 UV-Vis spectroscopy.

All UV-Vis spectra for colloids were taken with a UV-Vis Cary 250 60 spectrometer using 1 mm quartz cuvettes.

The UV-Vis spectra for the three samples are shown in figures 1.4, 1.5 and 1.6.

Figure 1.4a (RGHEPWAU sample) shows the gold nanoparticle synthesis in which water was used as solvent (no benzyl alcohol was added), and the plasmon peak is at 532 nm. The work performed by Chirea et al. [5] with nanowires is shown as well for comparison, and as it can be seen the UV-Vis spectra of the nanoparticles synthesized by them are similar to the one obtained in this work, but the plasmon peaks are located at 515 and 518 nm. Also, their synthesis was performed by the reduction of $HAuCl_4$ in ethaline and reline using $NaBH_4$ (sodium borohydride).

Figure 1.5 (RGHEPBAWAU sample) displays the colloid prepared using reactive-grade heparin dissolved in benzyl alcohol and water, such spectrum shows a peak at 532 nm and a bump at its right side at 647 nm, implying that nanoparticles are aggregated [6].In the work done by Zhang et al. [7], melamine-modified gold nanoparticles in a Tris-HCl buffer in the presence of carbonate; and when increasing the Tris concentration, aggregation of nanoparticles is observed, one of the spectra obtained by this group is very similar to the heparin-based gold colloid´s obtained in this work. The differences observed are that in their case the peak at the right is located at 640 nm , while in our case it is at 647 nm, as for the other one in their work it is found at 518 nm, while in this work it is found at 532 nm.

Finally, figure 1.6a depicts the synthesis prepared using pharmaceutical-grade heparin whose solvent is benzyl alcohol and water (excipient), the spectrum shows two peaks, the first one at 531 nm (transversal mode) and the second one at 827 nm (longitudinal mode) , this indicates nanoparticles are anisotropic in shape [8]. The work done by Norman et al [9] is shown for comparison in figure 1.6b; in their synthesis method, gold reduction is carried out using sodium sulfide (Na_2S) and the stabilizing the obtained nanoparticles with either PVP (polyvinylpirrolidone) or PVA (polyvinyl alcohol), the UV-Vis spectrum of these nanoparticles is

shown in figure 1.6b, the transversal plasmon peak is located at 540 nm meanwhile the longitudinal one varies between 720 and 920 nm; which differs from this work in 9 nm for the transversal peak and approximately 100 nm for the longitudinal one.

As it can be seen, all the three samples have no resemblance to each other.

a)

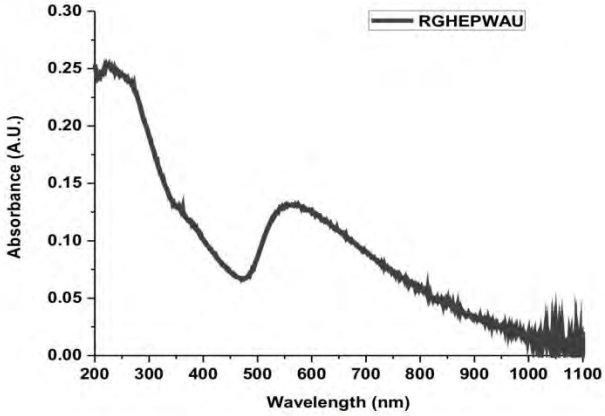

b)

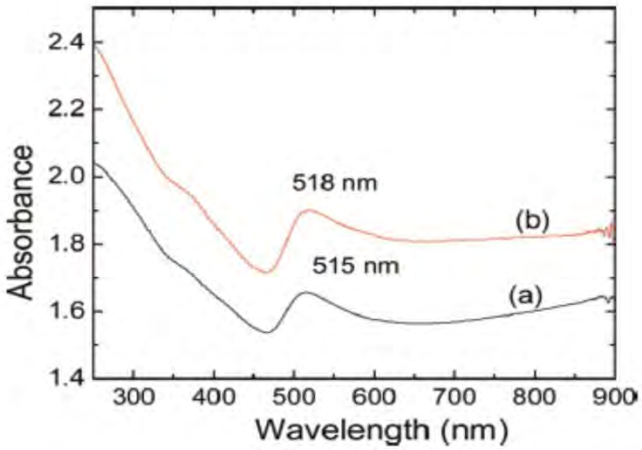

Figure 1.4a and b a) UV-Vis spectrum of gold nanoparticles synthesized only with water as solvent. b) UV-Vis spectrum of gold nanoparticles obtained by Chirea et al [5].

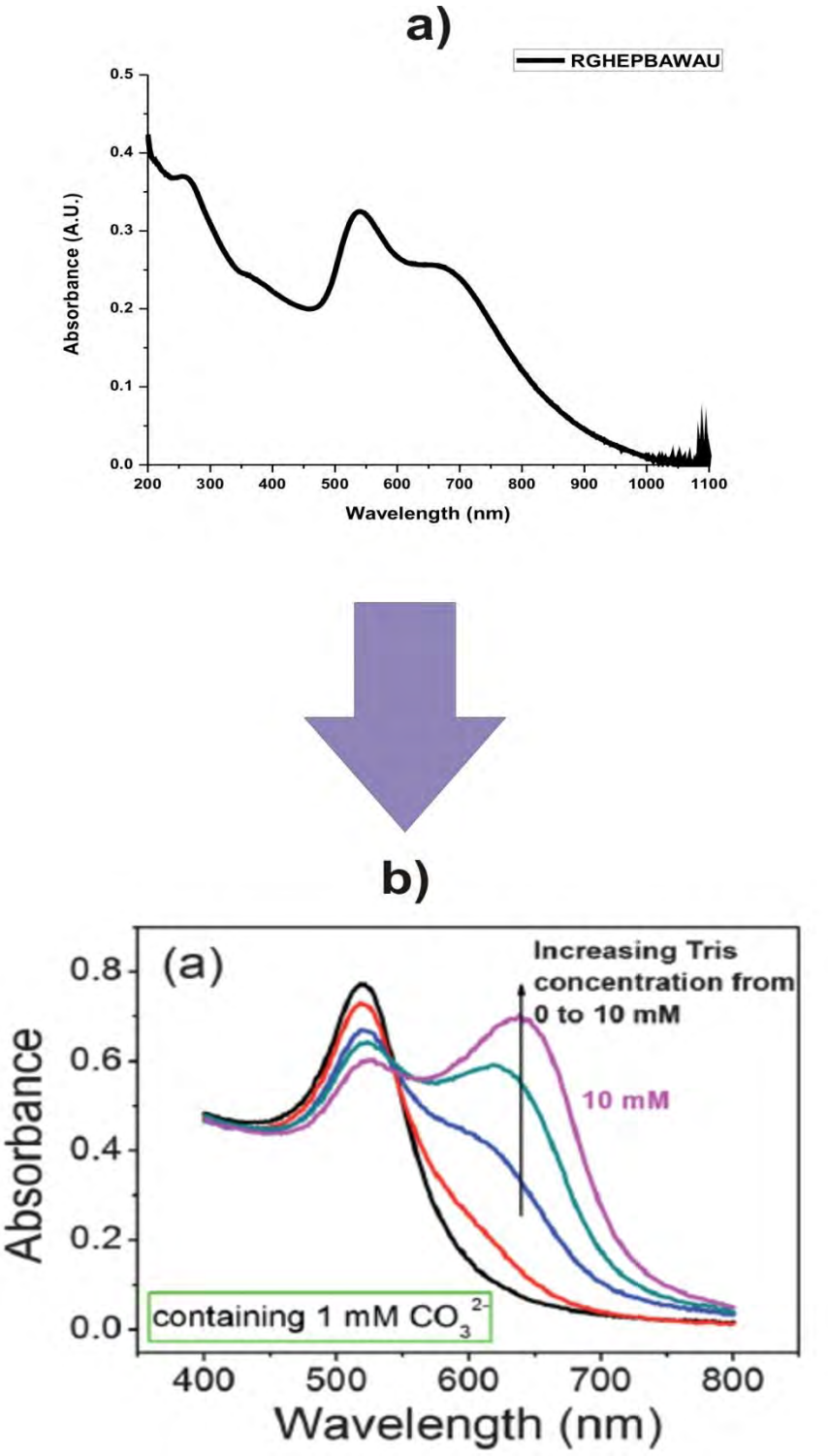

Figure 1.5a and b. a) UV-Vis spectrum of gold nanoparticles synthesized with water-benzyl alcohol as solvent, b) UV-Vis spectrum of gold nanoparticles obtained by Zhang et al [7].

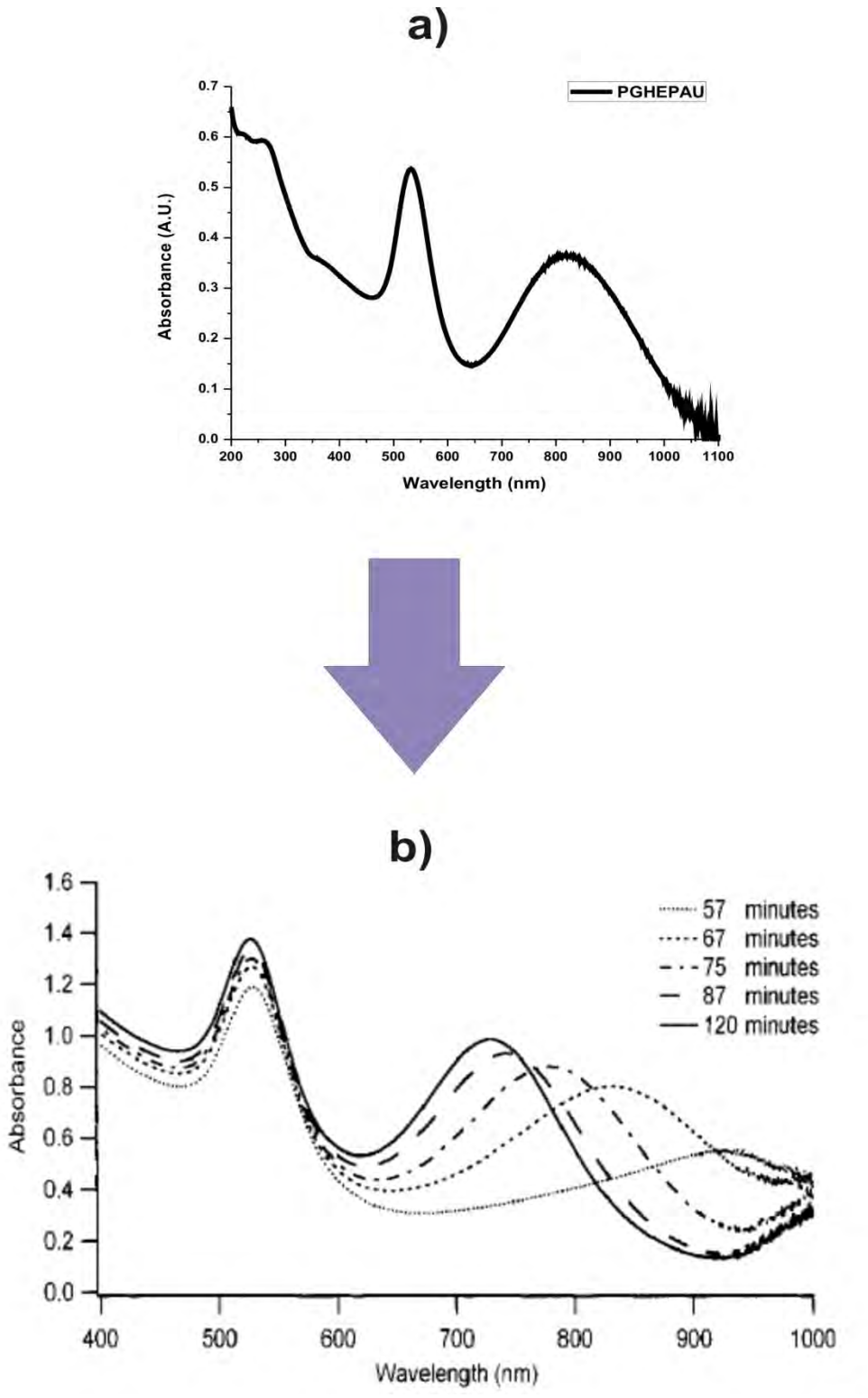

Figure 1.6a and b a) UV-Vis spectrum of gold nanoparticles synthesized with water-benzyl alcohol as solvent (excipient), b) UV-Vis spectrum of gold nanoparticles obtained by Norman et al [9].

A picture with the three solutions is shown below in figure 1.7. The tones among them are different .The RGHEPWAU sample has a grey-blue dark hue, RGHEPBAWAU is purple and PGHEPAU is wine. This confirms the findings from the UV-Vis spectra from each sample, the differences in shades demonstrates that nanoparticle shapes should not be the same.

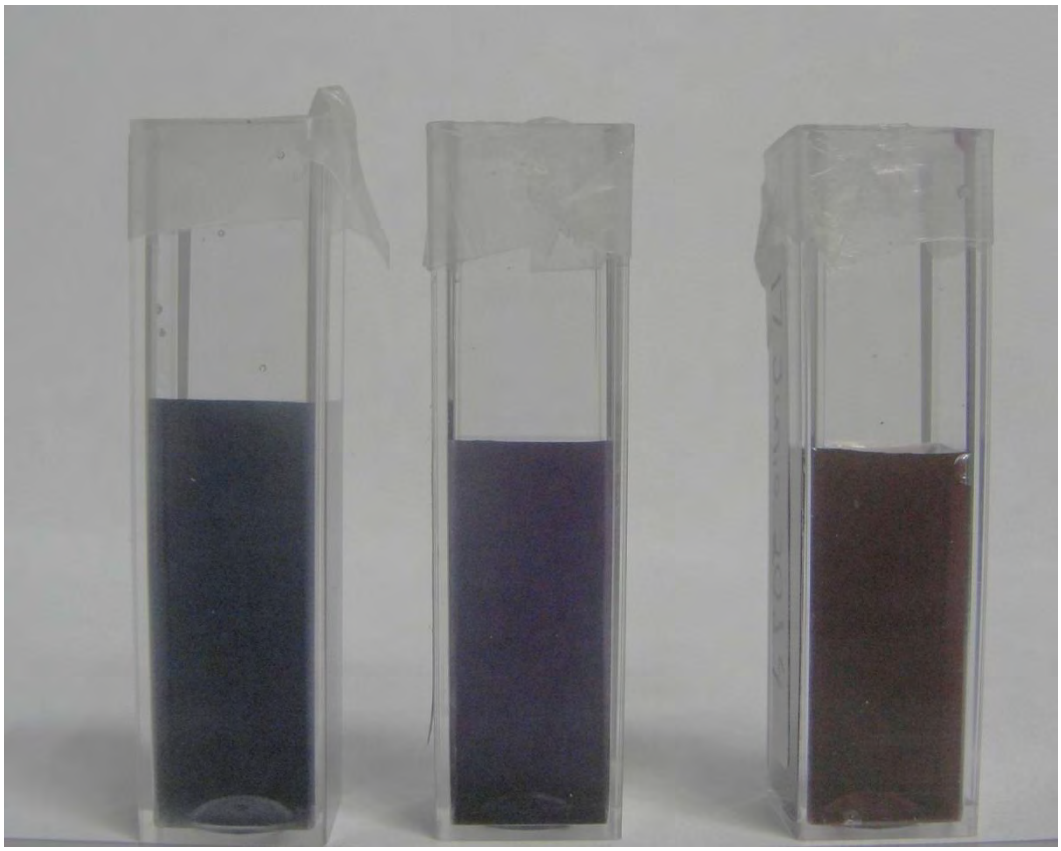

Figure 1.7 Photograph of the photochemically synthesized nanoparticle syntheses: The first one the gold nanoparticles synthesized with reactive-grade heparin in deionized water, the second with reactive-grade heparin in water-benzyl alcohol and the third one with pharmaceutical-grade heparin in its excipient (water-benzyl-alcohol).

1.3.2 Scanning electron microscopy.

SEM images were obtained with a JEOL JSM-7800F Extreme-resolution Analytical Field Emission 252 microscope. The colloids were prepared for characterization by washing silicon

wafers thoroughly with soap, water and ethanol and then dropping 10 μL of each synthesized solution and letting it dry in the dark. SEM results along with nanoparticle histograms are presented in figures 1.8a, 1.8b and 1.8c.

In the RGHEPWAU sample (figure 1.8a), big aggregates are formed by different-sized quasispherical products that have a polydisperse distribution ranging from 30-70 nm.

The PGHEPAU sample (figure 1.8b) shows nanoparticles with either a quasispherical shape, or triangular and trapezoidal plates (very few ones). Sizes vary from 45-60 nm for the quasispherical products while triangles are about 45-75 nm.

The RGHEPBAWAU sample in figure 1.8c shows a less disperse nanoparticle size distribution than in the previous cases, there are quasispherical particles with sizes in the 30-35 nm range, some triangles are present as well, but they are present in much less amount.

These SEM findings are in agreement with the results obtained from the UV-Vis spectra presented in the previous section because the UV-Vis spectrum from the RGHEPWAU sample (reactive-grade heparin based gold nanoparticles synthesized in water) shows only one broad peak tilted to the left as it would be expected for nanowires, as shown by Chirea et al [5]., the only difference in this thesis work is that instead of forming networks like in their case, nanoparticles form clusters. On the other hand, for the RGHEPBAWAU (reactive-grade heparin based gold nanoparticles synthesized in benzyl-alcohol/water) there are aggregated nanoparticles, and two peaks one beside the other in the visible in the UV-Vis spectrum, which is in good agreement with what was found by Zhang et al [7]. The PGHEPAU sample (pharmaceutical-grade based gold nanoparticles) has a peak in the near IR region besides the one found in the visible, showing that nanoparticle shapes are anisotropic, as also shown by Norman et al.[9] ,also the histograms obtained from the SEM images show that nanoparticle distribution is polydisperse ,as expected from nanoparticles synthesized with polysaccharides [10, 11].

a)

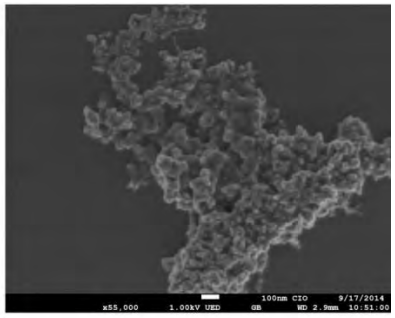
x55,000 1.00kV UED GB WD 2.9mm 10:51:00

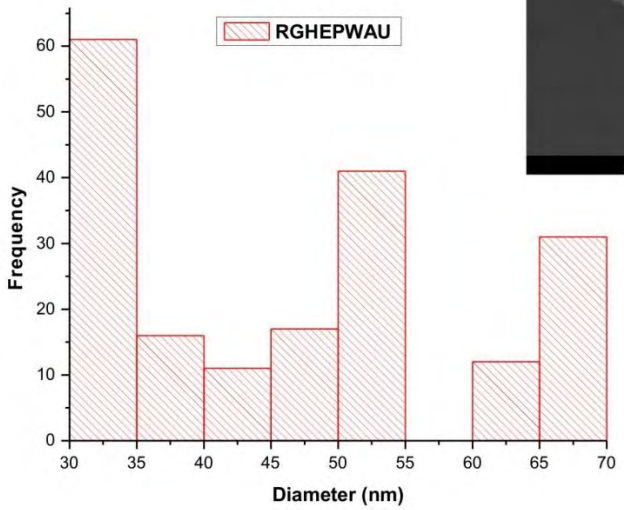
RGHEPWAU
Frequency
Diameter (nm)
0
10
20
30
40
50
60
30
35
40
45
50
55
60
65
70

b)

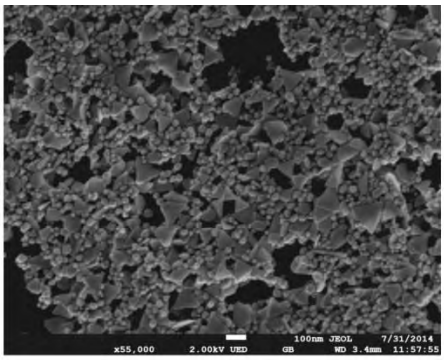
x55,000 2.00kV UED GB WD 3.4mm 11:57:55

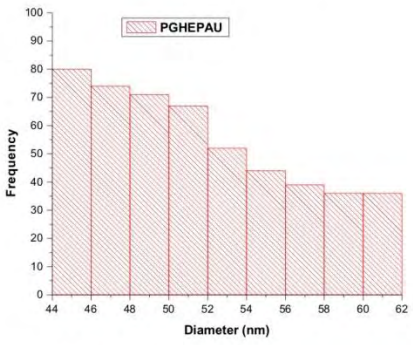
PGHEPAU
Frequency
Diameter (nm)
0
10
20
30
40
50
60
70
80
90
100
44
46
48
50
52
54
56
58
60
62

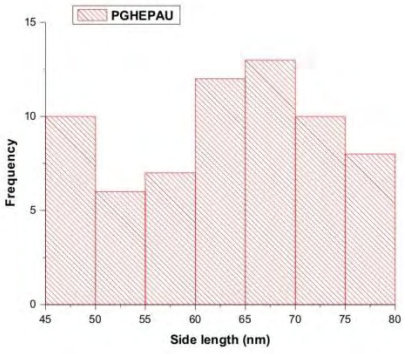
PGHEPAU
Frequency
Side length (nm)
0
5
10
15
45
50
55
60
65
70
75
80

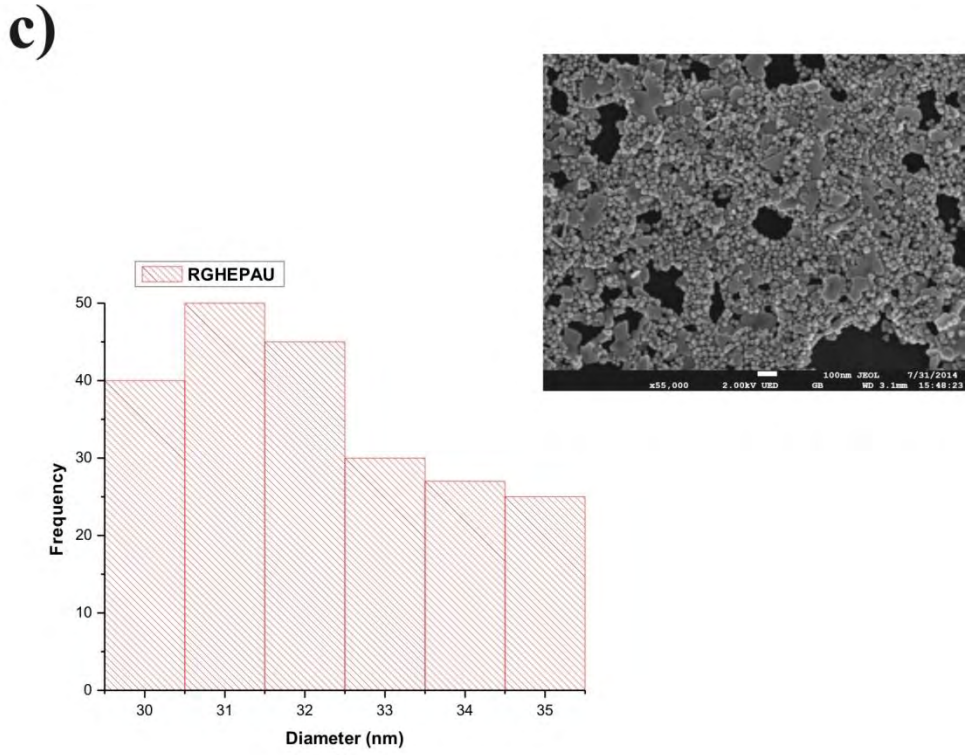

Figure 1.8 SEM images and histograms: : a)Reactive-grade heparin AuNPs in water, b)Pharmaceutical-grade heparin AuNPs in water/benzyl alcohol (excipient) , the first histogram shows the quasispherical nanoparticles diameter and the second one the side length corresponding to the triangle-shaped nanoparticles and c) Reactive-grade heparin AuNPs in water/benzyl alcohol mixture.

1.3.3 Reproducibility.

Samples were synthesized three times to check up on how reproducible they are, they were named PGHEPAU1, PGHEPAU2 and PGHEPAU3. The results are shown in the UV-Vis spectra in figure 1.8. As it can be seen, the transverse mode does not vary, but the longitudinal one shows differences. Table 1 is included to point out exactly the peak shifts indicating that the longitudinal mode of the samples is shifted (817±12.55 nm).

Table 1. UV-Vis absorption peaks for transverse and longitudinal modes in the pharmaceutical-grade gold nanoparticles syntheses.

SAMPLE	Transverse mode position (nm)	Longitudinal mode position (nm)
PGHEPAU1	532	800
PGHEPAU2	532	825
PGHEPAU3	532	828

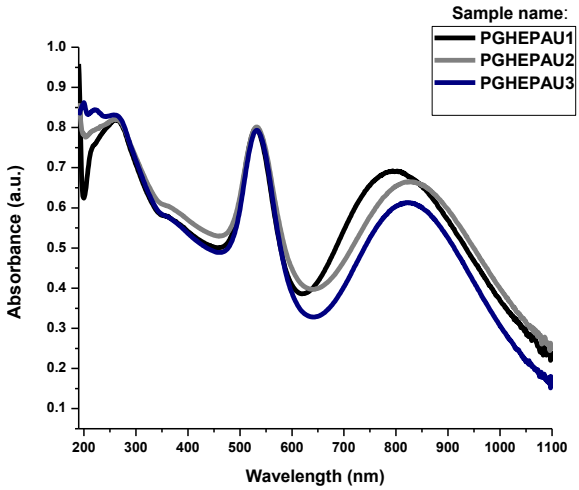

Figure 1.9 UV-Vis spectra of synthesized pharmaceutical-grade gold nanoparticles.

Samples synthesized with reactive-grade heparin were named RGHEPAU1, RGHEPAU2 and RGHEPAU3. The results are shown in the UV-Vis spectra in figure 1.9. The transverse mode peak position does not vary much, but the longitudinal one shows variations. Table 2 is included to point out exactly the peak shifts.

The longitudinal mode of these samples is shifted, too (668±12.83 nm).

Table 2. UV-Vis absorption peaks for transverse and longitudinal modes in the reactive-grade gold nanoparticles syntheses.

SAMPLE	Transverse mode position (nm)	Longitudinal mode position (nm)
RGHEPAU1	536	679
RGHEPAU2	536.5	675
RGHEPAU3	535	650

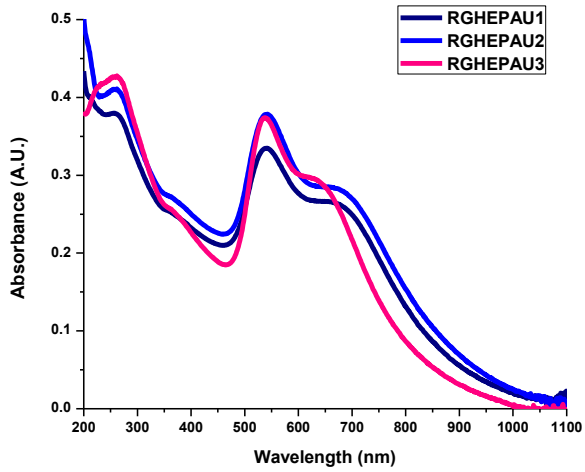

Figure 1.10 UV-Vis spectra of synthesized reactive-grade gold nanoparticles.

1.3.4 Stability.

Stability of nanoparticles is defined in terms of their ability to stay in the same chemical composition and in the same shape and size. But due to their small size, as time passes by, dissolution and redeposition of ions on the particles surface may occur [12]. The first process results in complete loss of the particles and the second one in particle growth (Ostwald ripening) [13].

UV-Vis spectra of the photochemically synthesized heparin Au NPs were taken (of each sample type) to check out their plasmon peak variations, black lines belong to samples as the original samples, this is, samples whose UV-Vis spectra were taken the day they were synthesized. The results are shown in figures 1.10a, b and c. Samples were stored in the dark and wrapped in aluminum foil right after they were synthesized to avoid light exposure.

These results show that the sample prepared in water (figure 10a) has its original plasmon peak at 532 nm and after 4 months, it red shifts towards 562 nm, this is a 30 nm difference value, also there is a peak-broadening. The sample prepared using pharmaceutical-grade heparin shows that the transverse mode peak does not change from its 532 nm value and the longitudinal mode peak blue-shifts from 825 nm to 820 nm (figure 1.10b). The sample prepared using reactive-grade heparin in water/benzyl alcohol, shows that its peaks, originally located at 536 nm and 679 nm, shift to 531 nm and 683 nm (figure 1.10c). Red-shifting in UV-Vis spectra means that nanoparticles agglomerate, this is because the conduction electrons near each particle surface become delocalized and are shared among neighboring nanoparticles [14]. Blue-shifting is, in general, an indicator of decreasing nanoparticle size, but it can also be due to the oxidation of colloidal gold due to its reaction with dissolved oxygen in water. Partial oxidation causes blue-shifting, too, because of the absorbance of gold (chloroauric acid), in the UV [15]. All samples exhibit a decrease in absorbance, this being due to nanoparticle destabilization, or that stable nanoparticles are being depleted, causing that the plasmon peak(s) broaden or forming peaks at longer wavelengths [14].

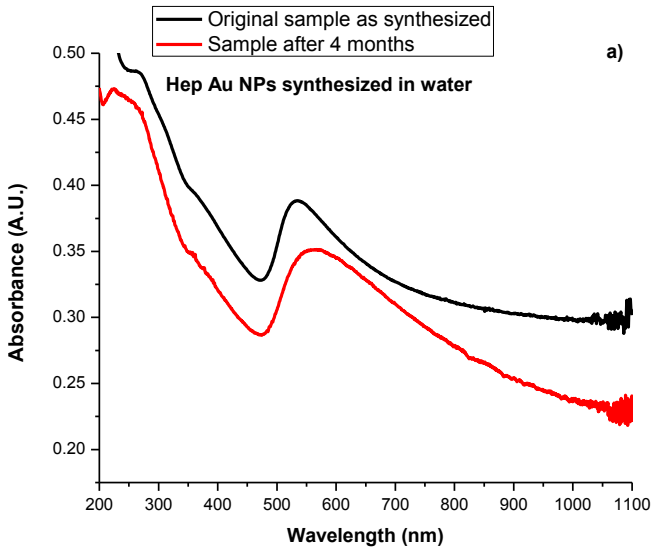

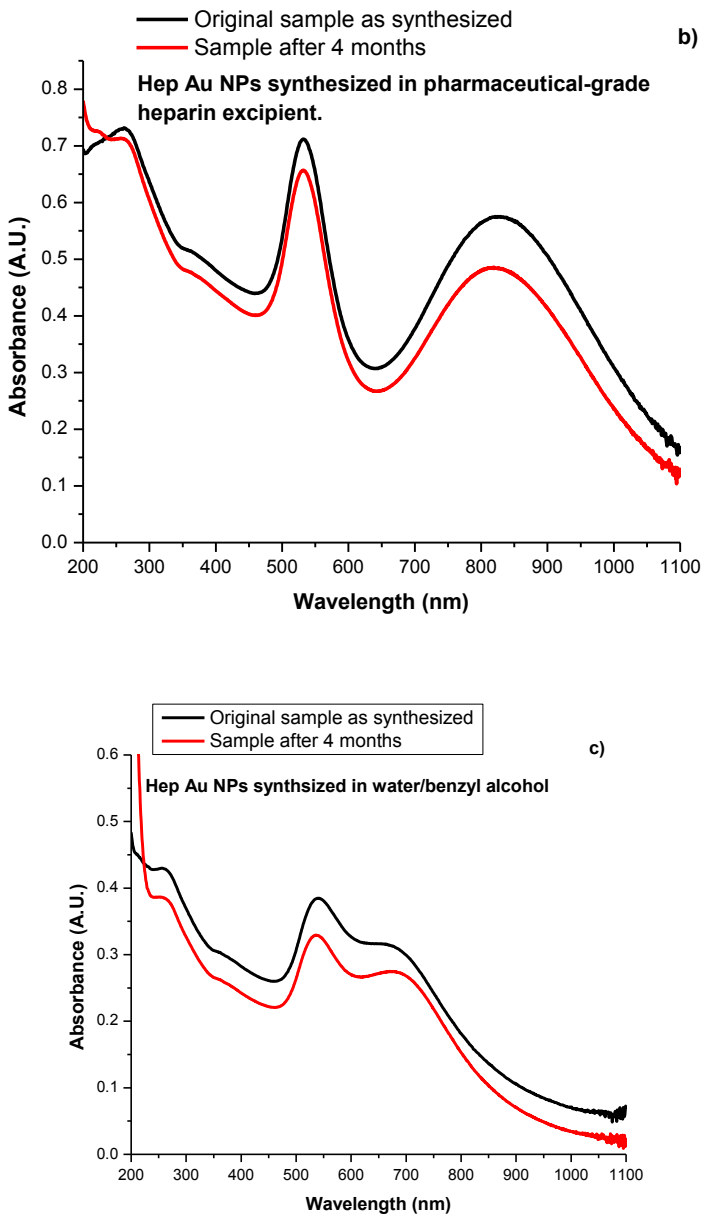

Figures 1.11 UV-Vis spectra of a sample from each gold nanoparticle synthesis type to show how stable samples remain in a 4-month period: a) Reactive-grade heparin AuNPs in water, b) Pharmaceutical-grade heparin AuNPs in water/benzyl alcohol (excipient) and c) Reactive-grade heparin AuNPs in water/benzyl alcohol mixture.

1.4 Heat-based synthesis of gold nanoparticles.

First, a mixture solution containing all reaction components is prepared as follows: Inside a volumetric flask, water is poured, then specific liquid amounts of $HAuCl_4$ and then heparin of

either reactive grade (dissolved in either water or a water-benzyl alcohol mixture) or the pharmaceutical-grade one (in benzyl alcohol/water excipient) are added. The mix is then agitated by hand for the constituents to be blended well. These heat-based syntheses were prepared at 38°C, which is the highest temperature that is reached inside the UV-reactor when the gold nanoparticles are photochemically synthesized.

Afterwards, the as-prepared solution is poured in a dark vial, which is also wrapped in aluminum foil to ensure light avoidance. Then, the solution was placed to heat on a hot plate for 7 hours, after the synthesis procedure, the obtained solution was centrifuged the same way photochemical syntheses were (4 times at 13,500 rpm) and then re-dispersed in deionized water. Also, they were wrapped in aluminum and stored and kept in the dark.

The same heparin and chloroauric acid concentrations used for the photochemical syntheses were used for these experiments:

Heparin: 0.833 mM

$HAuCl_4$: 0.840 mM

The syntheses were prepared and named as follows:

RGHEPWAU38: Reactive-grade heparin based synthesis using just water as solvent.

RGHEPBAWAU38: Reactive-grade heparin based synthesis using water-benzyl alcohol as solvent.

PGHEPAU38: Pharmaceutical-grade heparin based synthesis using water-benzyl alcohol as solvent (excipient).

1.4.1 UV-Vis spectroscopy.

Figure 1.12a displays the gold nanoparticle samples prepared with reactive-grade heparin in water .The sample that was heated shows a depression at 485 nm and a peak at 600 nm . The nanoparticles formed by UV irradiation present a plasmon peak at 532 nm.

Samples prepared using pharmaceutical-grade heparin (figure 1.12 b) show that when the heparin-gold solution is treated with heat, there is basically no plasmon peak formed in the 500-600 nm range, which is the region gold nanoparticles usually have their absorbance maximum. Also the solution tone is light yellow, it did change its color a little bit because the original solution was a little bit darker. This may indicate that some gold reduction might have taken place but it was not completed, no zero-valent metal was formed to produce nanoparticles. On the contrary, the sample which was UV-treated shows two plasmon peaks at 532 and 827 nm..

Reactive-grade heparin gold nanoparticles prepared in benzyl alcohol/water are shown, in figure 1.12c. The heparin-gold mixture shows different tendencies, the heat-treated sample shows two peaks, one at 200 nm, another at 598 nm, this indicated that gold nanoparticles have been formed but there was not a complete reduction of gold by heparin, which is noticeable because no plasmon peaks are formed in the wavelength regions nanoparticles are supposed to have their plasmon peaks. There is just a bump of weak intensity and big broadness. On the other hand, the sample that was UV irradiated shows a well-defined shape of the plasmon peaks belonging to the gold nanoparticles that were synthesized, they are found at 537 and 647 nm, also, the region between 200-400 nm shows that gold was reduced during the synthesis procedure and that some heparin was attached to the nanoparticles by taking a look at the peak formed at 267 nm.

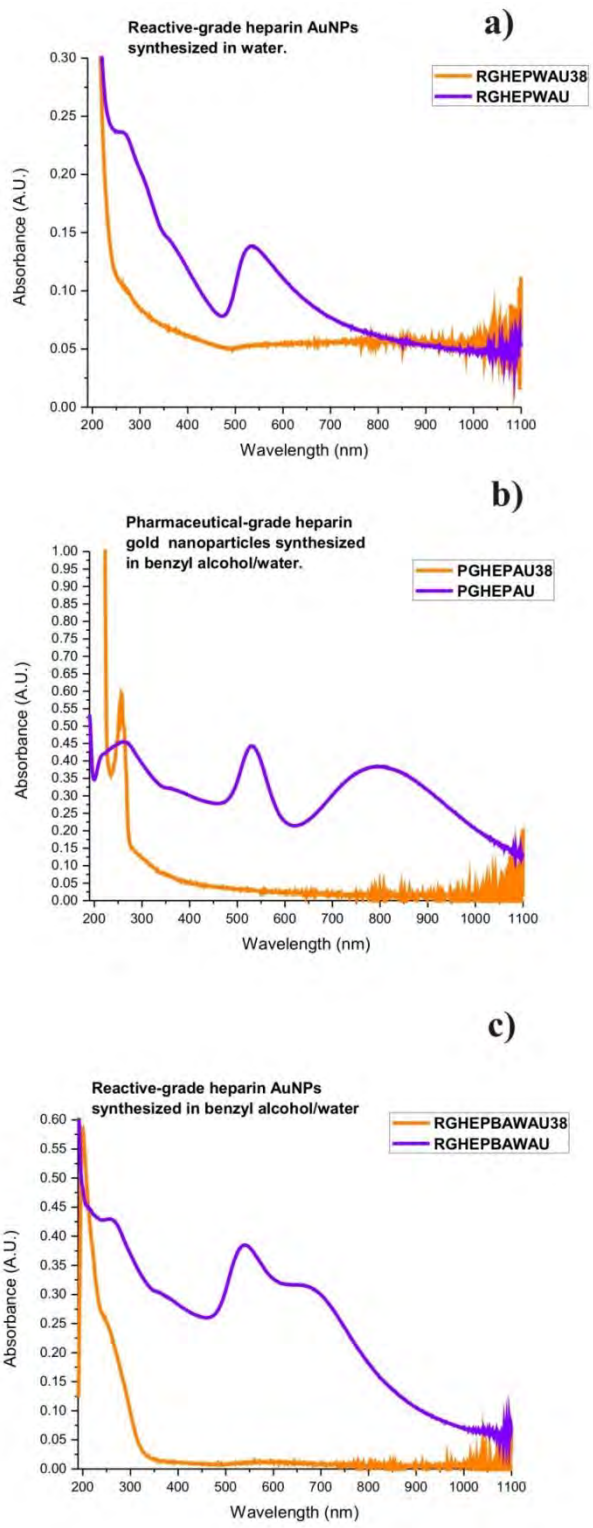

Figure 1.12 UV-Vis spectra of syntheses using heat (T=38 °C, orange lines) and their UV-light generated counterparts (violet lines) for comparison: a)Reactive-grade heparin AuNPs in water, b)Pharmaceutical-grade heparin AuNPs in water/benzyl alcohol (excipient) and c) Reactive-grade heparin AuNPs in water/benzyl alcohol mixture.

A picture of the three solutions is shown below in figure 1.13. The tones among them are quite different. The RGHEPWAU38 sample has a transparent light gray hue, RGHEPBAWAU38 is violet and PGHEPAU38 is light yellow. This confirms the findings from the UV-Vis spectra from each sample, the differences in shades demonstrates that nanoparticle forms should not be the same among these samples.

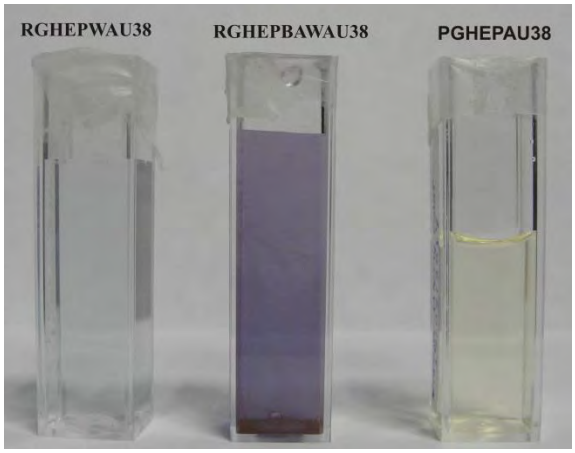

Figure 1.13 Photograph of the heat-based gold nanoparticle syntheses.

1.4.2 Scanning electron microscopy.

Scanning Electron Microscopy was performed on the samples prepared just with heat and with UV light, their SEM images are shown to contrast them.

The results indicate that in the RGHEPWAU38 sample (figure 1.14a), aggregates are formed; the structures that make them up are irregular in shape. Also, the aggregates are micron sized, but they are not even the same size when compared to each other: Some of them are really huge and others are not. As for the sample generated with UV light (figure 1.14b), aggregates are formed, but the structures that make them up are spherical and quasispherical.

The PGHEP38 sample (figure 1.14c) shows rectangular shapes and some other ones that might have had the tendency to become rectangles, but that during the synthesis procedure, it was not

possible they did so. These particles range from 210-500 nm. In the same SEM image, much smaller nanostructures can be observed: some of them resemble the bigger structures already mentioned and some other are pseudospherical, their distribution ranges 33-66 nm. The UV synthesized sample, PGHEPAU (figure 1.14d), although it shows some polydispersity, the predominant products are pseudospherical, and their size varies between 45-60 nm, and the plate-like nanostructures present are in the 45-75 nm range.

The samples prepared with reactive-grade heparin dissolved in benzyl-alcohol/water, RGHEPBAW38 (figure 1.14e) and RGHEPAU (figure 1.14f), also show different trends: When the heparin-gold solution is heated, bisquit shapes (100-330 nm), pseudospheres of 50-70 nm and elongated structures (60-140 nm) are present. The UV irradiated sample´s distribution is much more uniform and the pseudospherical products ranging between 30-35 nm, some other bigger shapes which are triangular are present as well but they are not predominant.

It can be concluded that nanoparticles obtained at 38°C, grow bigger and with more polydisperse distributions than the nanoparticles synthesized by UV-light, which show a less polydisperse distribution. In general, metal nanoparticles synthesized with polysaccharides yields polydisperse distributions, but possess biological activity and biocompatibility [16].

1.4.3 Comparison with an experiment which compares the photochemical and thermal approaches for nanoparticle synthesis.

In the work published by Alvarado et al [17], Cobalt Oxyhydroxide Nanocrystals are synthesized by the thermal and photochemical methods in order to compare both. They conclude that the photochemical method is the best way to prepare the nanocrystals either under UV (350 nm) or Visible (575 nm) irradiation because the thermal reaction (carried out in the dark, in a similar fashion to this thesis work) proceeded much more slowly and produced larger (~250 nm)

polydisperse Co(O)OH aggregates, which did not happen when using the photochemical route that yielded nanocrystals of 3 nm.

These results are similar to the ones obtained here because when using heat for nanoparticle synthesis, clusters and big products (along with some smaller ones) are acquired. But when using light, even though the nanoparticle distribution is polydisperse the obtained particles are much more defined and smaller than when light is not used in the synthesis, as shown in the SEM images from figure 1.14 below.

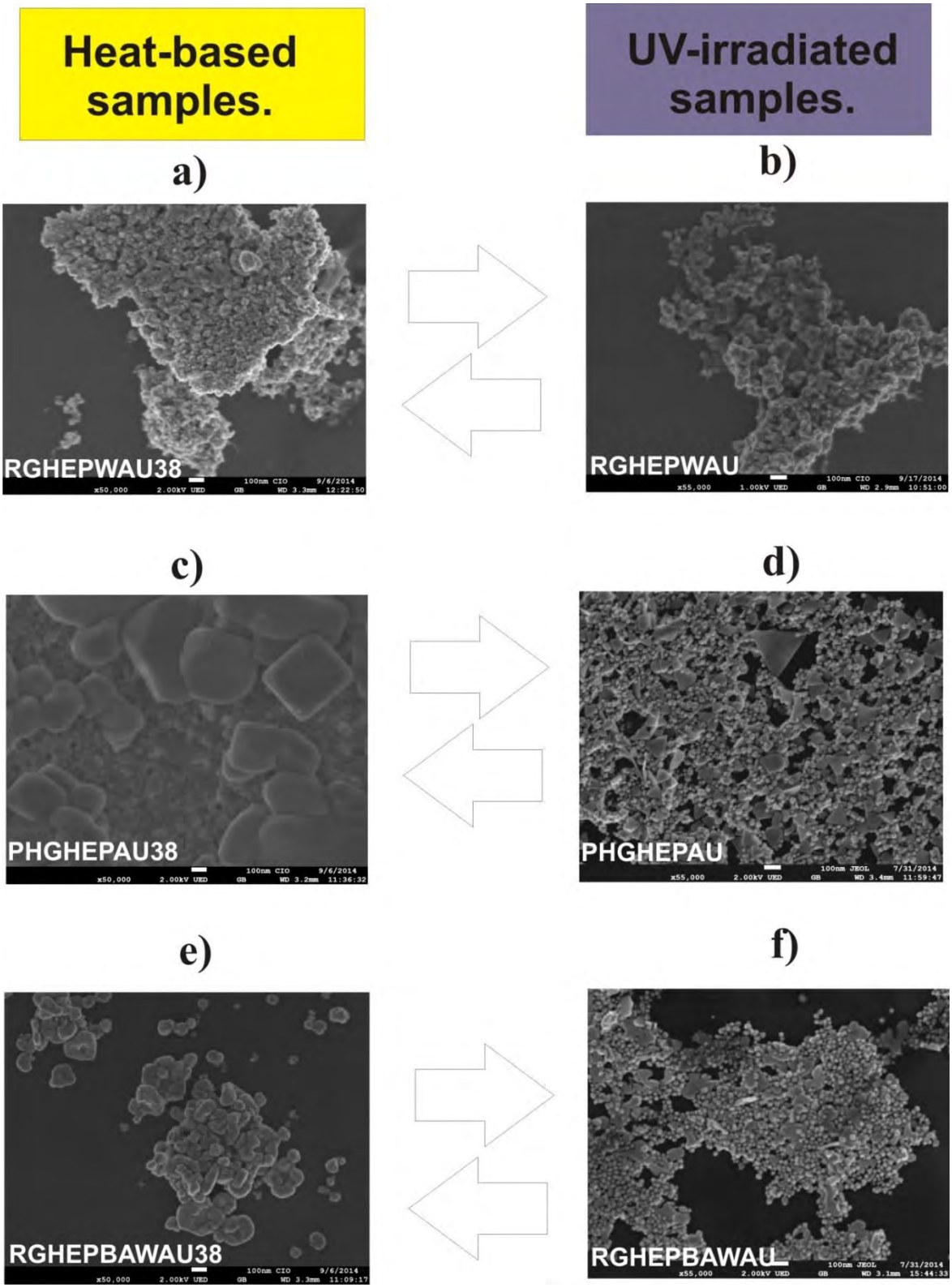

Figure 1.14 SEM images from heat-based samples: a,c, and e and their UV-light synthesized counterparts: b, d and f.

References:

[1] Lee K., Lee H., Bae K.H., Park T.G.,(2010), Heparin immobilized gold nanoparticles for targeted detection and apoptotic death of metastatic cancer cells, Biomaterials 31, 6530-6536.

[2] Kemp M.M., Kumar A., Mousa S., Dyskin E., Yalcin M., Ajayan P., Lindhardt R.J., Mousa S.A., (2009), Gold and silver nanoparticles conjugated with heparin derivative possess anti-angiogenesis properties, Nanotechnology, 20, 45, 1-7.

[3] Guo Y.,Yan H., (2008), Preparation and characterization of heparin-stabilized gold nanoparticles, Journal of Carbohydrate Chemistry,27,5, 309-319.

[4] Ghasemi J., Niazia A., Ghobadib S.,(2005), Simultaneous Spectrophotometric Determination of Benzyl Alcohol and Diclofenac in Pharmaceutical Formulations by Chemometrics Method, Journal of the Chinese Chemical Society, 52, 1049-1054.

[5] Chirea M., Freitas A., Vasile B.S., Ghitulica C. ,Carlos M. Pereira C.M.,Silva F., (2011), Gold Nanowire Networks: Synthesis, Characterization, and Catalytic Activity; Langmuir 2011, 27, 3906–3913.

[6] Wang A.J., Guo H., Zhang M., Zhou D.L., Wang R.Z., Feng J.J.,(2013), Sensitive and selective colorimetric detection of cadmium(II) using gold nanoparticles modified with 4-amino-3-hydrazino-5-mercapto-1,2,4-triazole180, 11-12, 1051-1057.

[7] Zhang J, Xu X., Yang X.,(2012), Role of Tris on the colorimetric recognition of anions with melamine-modified gold nanoparticle probe and the visual detection of sulfite and hypochlorite, Analyst, 137, 3437-3440.

[8] Hao E., Schatz G.C., Hupp J.T.,(2004), Synthesis and Optical Properties of Anisotropic Metal Nanoparticles, Journal of Fluorescence,14, 4, 331-341.

[9] Norman T.J. Jr., Grant C.D., Magana D., Zhang J.Z., (2002), Near Infrared Optical Absorption of Gold Nanoparticle Aggregates, Journal of Physical Chemistry B , 106, 7005-7012.

[10] Rajeshkumar S., Malarkodi C., Gnanajobitha G.,Paulkumar K.,Vanaja M., Kannan C., Annadurai G.,(2013), Seaweed-mediated synthesis of gold nanoparticles using Turbinaria conoides and its characterization, Journal of Nanostructure in Chemistry 2013, 3:44.

[11] Maity S, Sen I.K., Islam S.S.,(2012) , Green synthesis of gold nanoparticles using gumpolysaccharide of Cochlospermum religiosum (katira gum)and study of catalytic activity, Physica E 45 ,130–134.

[12] Zhou J., Ralston J. , Sedev R., Beattie D.A.,(2009), Functionalized gold nanoparticles: Synthesis, structure and colloid stability, Journal of Colloid and Interface Science, 331,2, 15, 251–262.

[13] Voorhees P.W.,(1985), The Theory of Ostwald Ripening, Journal of Statistical Physics, 38, 112,231-249.

[14] Nanocomposix,(2012), *UV/VIS/IR SPECTROSCOPY ANALYSIS OF NANOPARTICLES,*San Diego,California,USA.

[15] Dang T.M.D., Le T.T.T., Fribourg E.B., Dang M.C., (2011), The influence of solvents and surfactants on the preparation of copper nanoparticles by a chemical reduction method, Advances in Natural Sciences: Nanoscience and Nanotechnology, 2, 025004.

[16] Park Y., Hong Y.N., Weyers A., Kim Y.S., Linhardt R.J.,(2011), Polysaccharides and phytochemicals: a natural reservoir for the green synthesis of gold and silver nanoparticles, IET Nanobiotechnology, 5, 3, 69–78.

[17] Alvarado S.R., Guo Y.,Purnima T., Ruberu, A., Bakac, A., Vela J.,(2012), Photochemical versus Thermal Synthesis of Cobalt Oxyhydroxide Nanocrystals; The Journal of Physical Chemistry C , 116, 10382−10389.

Chapter 2.

Nanoparticle formation mechanism.

This chapter is devoted to explaining heparin´s structure and how metal nanoparticles are formed using the UV-based photochemical method proposed. Characterization was performed by UV-Vis and FTIR spectroscopy and pH measurements.

2.1 Heparin general information.

Heparin is a material which is a member of the glycosaminoglycans (GAGs) family. Glycosaminoglycans are large complex hydrocarbon structures that interact with a wide range of proteins involved in physiological and pathological processes. They are also referred to as mucopolysaccharides because of their viscous, lubricating properties, as found in mucous secretions [1].

Glycosaminoglycans in aqueous solution are surrounded by a shell of water molecules, which makes them occupy an enormous hydrodynamic volume in solution. When a solution of GAGs is compressed, the water squeezes out and the GAGs are forced to ocuppy a smaller volume. When the compression is removed they regain their original hydrated volume because of the repulsion arising from their negative charges [1].

Glycosaminoglycans are linear sulphated, negatively-charged polysaccharides that have molecular weights between 10-100 kDa. There are two main types of GAGs. Non-sulphated GAGs include hyaluronic acid (HA), whereas sulphated GAGs include chondroitin sulphate (CS), dermatan sulphate (DS), keratan sulphate (KS), heparin and heparan sulphate (HS).

Glycosaminoglycans chains are composed of disaccharide repeating units called disaccharide repeating regions. The repeating units are composed of uronic acid (D-glucuronic acid or L-iduronic acid) and an amino sugar (D-galactosamine or D-glucosamine). Hence, GAGs differ according to the type of hexosamine, hexose or hexuronic acid unit they contain, as well as the geometry of the glycosodic linkage between these units. Chondroitin sulphate and dermatan sulphate which contain galactosamine, are called galactosaminoglycans, whereas heparin and heparan sulphate , which contain glucosamine, are called glucosaminoglycans. The amino sugar may be sulphated on carbons 4, 6 or the non-acetylated nitrogen; however, the sugar backbone of GAGs can be sulphated at various positions. As a result, a simple octasaccharide can have over 1 000 000 different sulphation sequences. Glycosaminoglycans also vary in the geometry of the glycosidic linkage (α or β).At physiological pH (7.4), all carboxylic acid and sulphate groups are deprotonated, giving GAGs very high negative charge densities, an in the case of heparin it has the highest negative charge density of any known biomolecule [1-3].

It has to be mentioned that some glycosaminoglycans specifically hyaluronic acid, hyaluron sulfuric acid, and heparin suffer degradation in their structure under the influence of UV irradiation as investigated by Balazs et al. [4]. This implies a change in their structure, for instance, breakage of the glycosydic bondage that joins the main disaccharide unit, a decrease in viscosity and reducing power increase.

Heparin consists of repeating units of 1→4 linked pyranosyluronic acid and 2-amino-2-deoxyglucopyranose (glucosamine) residues. The uronic acid residues typically consist of 90% L-idupyranosyluronic acid (L- iduronic acid) and 10% D-glucopyranosyluronic acid (D-glucuronic acid).The amino group of the glucosamine residue may be substituted with an acetyl or sulphate or remain unsubstituted. The 3- and 6- positions of the glucosamine residues can either be substituted with an O-sulphate group or remain unsubstituted. The uronic acid, which

can be either L-iduronic or D-glucuronic acid, may also contain a 2-O sulphate group. Heparin tends to have an extended configuration because of its highly hydrophilic nature arising from its extensive degree of sulphation [2, 3].

2.2 Experimental.

First, the irradiation experiments carried out were using only heparin solutions, no $HAuCl_4$ was added. Three solutions were prepared and irradiated for 7 hours in separate experiments in order to confirm heparin´s degradation and to propose a mechanism that explained nanoparticle formation according to the changes observed when monitoring heparin changes.

These samples are distinguished from each other by the following names:

1. **PHGHEP**: Pharmaceutical-grade heparin in benzyl alcohol (excipient).
2. **RGHEPW**: Reactive-grade heparin dissolved in water.
3. **RGHEPBAW**: Reactive-grade heparin dissolved in water and benzyl alcohol.

2.3 Discussion.

2.3.1 UV-Vis spectroscopy analysis of heparins under UV irradiation.

The UV-Vis results obtained from the irradiated heparins are discussed first: Absorbance spectra were taken every hour from the beginning to the end of the irradiation experiments for each heparin type.

Both heparins present peaks in the UV region due to the aldehyde groups present in their basic structure. It should be noted that most pharmaceutical-grade heparins usually contain different excipients, for example, distilled water and other substances like sodium chloride to render isotonic; and also sodium hydroxide and/or hydrochloric acid for pH adjustment. In our case, the excipient was determined to be benzyl alcohol [4] as mentioned in chapter one. Peaks in both cases tend to grow in intensity, and some others come out as it will be discussed later. According

to Bazals et al. [5], this may be due to the fact that the increase in absorbance is promoted in more alkaline media than in acidic media, indicating radical formation as well.

The PGHEP sample, whose UV-Vis spectrum is shown in figure 2.1, has five peaks: 224, 248, 253, 260 and 266 nm, in the 300-350 nm region although a peak is not formed, it can be seen that an elevation grows very little in intensity, forming a shoulder at about 308 nm as the solution is UV-irradiated.

Sample RGHEPBAW (figure 2.2) depicts a tendency similar to the previous experiment with only small differences. Its peaks are found to be at 210, 225, 253 and 260 nm. Shoulders are formed at 266 and 356 nm as light is passing through the sample with time. In the pharmaceutical-grade heparin, the peak at 266 nm is already formed from the time irradiation begins and in RGHEPBAW although it is not sharp, at the beginning it only has a broad appearance, at the end of the experiment it has a more defined form. Figure 2.1 corresponding to the pharmaceutical-grade heparin has similar features.

Finally, for RGHEPW in figure 2.3, there are only two peaks: one at 194 nm and another which is formed as UV irradiation is taking place, at 254 nm as it can be seen in its absorption spectrum in figure 2.4. This spectrum has nothing to do with the two previous samples because no other peaks more than these two are recognizable, they seem to have been screened by the water spectrum. As it was mentioned previously, when heparin is dissolved in water, water molecules tend to surround it which makes it occupy an enormous hydrodynamic volume in solution.

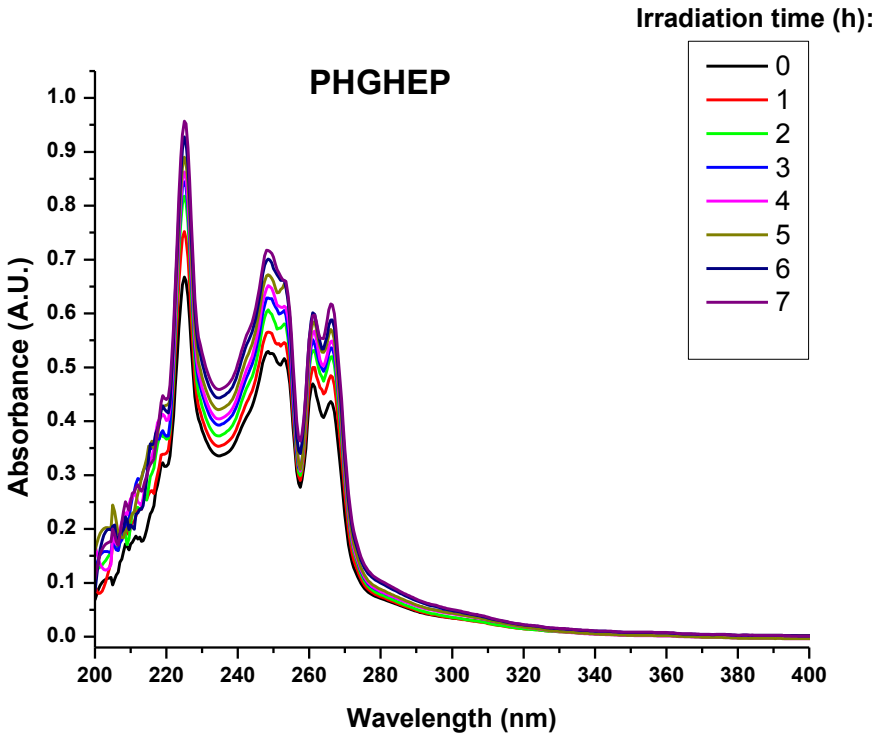

Figure 2.1 UV-Vis spectra of pharmaceutical-grade heparin irradiated for seven hours.

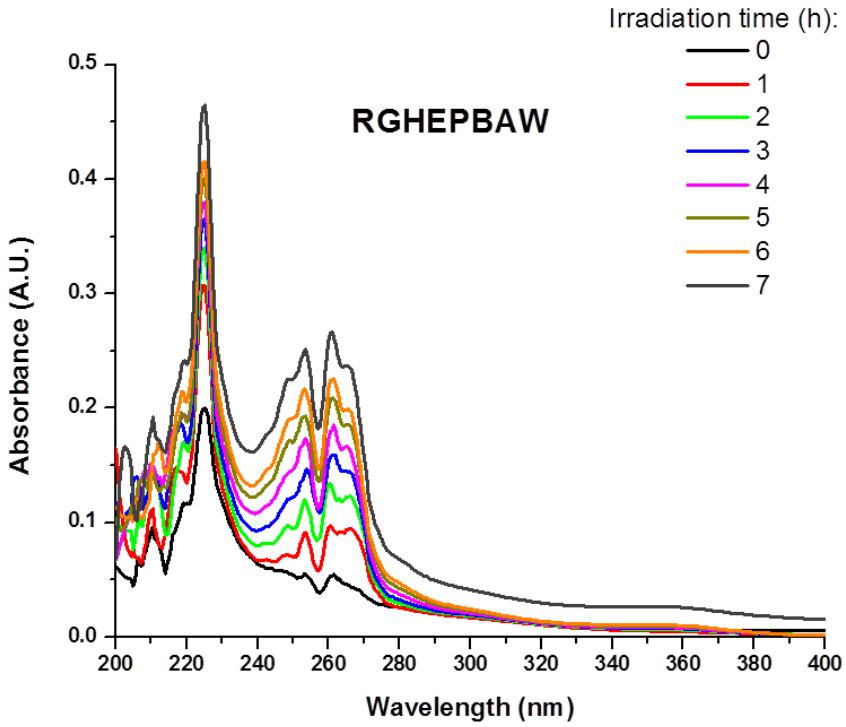

Figure 2.2 UV-Vis spectra of reactive-grade heparin irradiated for seven hours.

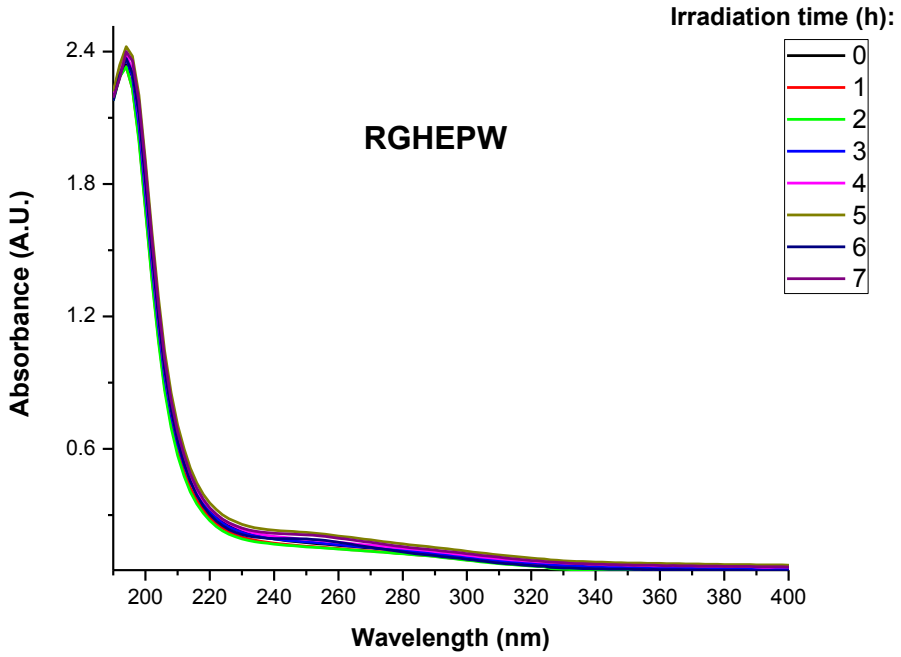

Figure 2.3 UV-Vis spectra of reactive-grade heparin dissolved in water irradiated for seven hours.

2.3.2 FT-IR analysis.

For infrared spectra measurements, a Perkin Elmer Spectrum BX FTIR system was used. Solid samples were prepared by mixing heparin powder with KBr (potassium bromide), in a heparin to KBr ratio of 1:100, and milling them to form a very fine and homogeneous powder to make a pellet for obtaining the spectra. Pharmaceutical-grade heparin, as well as both UV-irradiated and non-irradiated heparin solutions, were dried at 45 °C for 6 h, and mixed with dry KBr powder.

FTIR studies before and after UV irradiation taken for both heparin kinds show vibrational and absorption peaks, see figure 2.4 .The spectra tend to depict some differences. One thing to take into account is the fact that heparin even when dried is still hydrophilic, which means that some peaks may correspond to solvent retention and even impurities, considering heparin synthesis yields heterogeneous products even when being the same origin. The peak at 3,467 cm^{-1} in both

heparins corresponds to hydroxyl group vibrations. Carboxyl and sulfate groups are responsible for the acidic character of heparin, their location is approximately at 1,645 cm^{-1} and 1,648 cm^{-1} in pharmaceutical and reactive-grade heparins, respectively. The band at approximately 1,260 cm^{-1} in pharmaceutical-grade heparin and the one at 1,236 cm^{-1} in reactive-grade heparin display different structures; these peaks and their absorption intensity are normally related to symmetric vibrations of S=O bonds [6]. The latter has a less intense and broader peak in the 800–880 range which is the sulfated sugar region [7]. It is noted that peaks corresponding to the values of 800 and 816 and 820 cm^{-1} (in pharmaceutical-grade heparin and reactive-grade heparin, respectively) belong to the iduronate residue 2-0-sulphate group and to the 6-0-sulphate group of the glucosamine residue, such bands are overlapped in pharmaceutical-grade heparin split into two separated contributions in reactive-grade heparin but with lower absorption. Outside the mentioned range, the peak at approximately 941 cm^{-1} indicates vibrations of components which are part of the glycosidic linkages and also belong to C–O–S stretching (in glucosamine) [8].

Figures 2.4a to d depict the changes in both heparins after UV irradiation. The peak for the sulfate groups diminishes for pharmaceutical-grade heparin. This may indicate the appearance of other absorbing materials. The peaks that correspond to the glycosidic linkages in both heparins show an absorption decrease which is in agreement with the fact that they break during irradiation as expected. The peaks corresponding to S=O vibrations pose contrasting characteristics, because in the pharmaceutical-grade heparin there is less absorption after UV irradiation, contrary to what happens in reactive-grade heparin. This may be the result of major vibration in these bonds, from which it might be inferred that there are more atoms in this heparin chain which makes it bigger and heavier. The sulfate groups absorptions due to iduronate and glucosamine decrease in absorption but the peaks that are part of the D-glucosamine residue tend

to be more defined, something that may be explained by suggesting an increase in the reducing end groups [9].Figures 2.4a and c show the general structure of both heparin types.

Fig 2.4b and 2.4d are the insets corresponding to the different types of heparins, and as it can be seen, the changes are more evident in the glucosamine and the iduronate sulphated residues. This being due to the fact that the glucosamine monosaccharide is a reducing sugar [10].

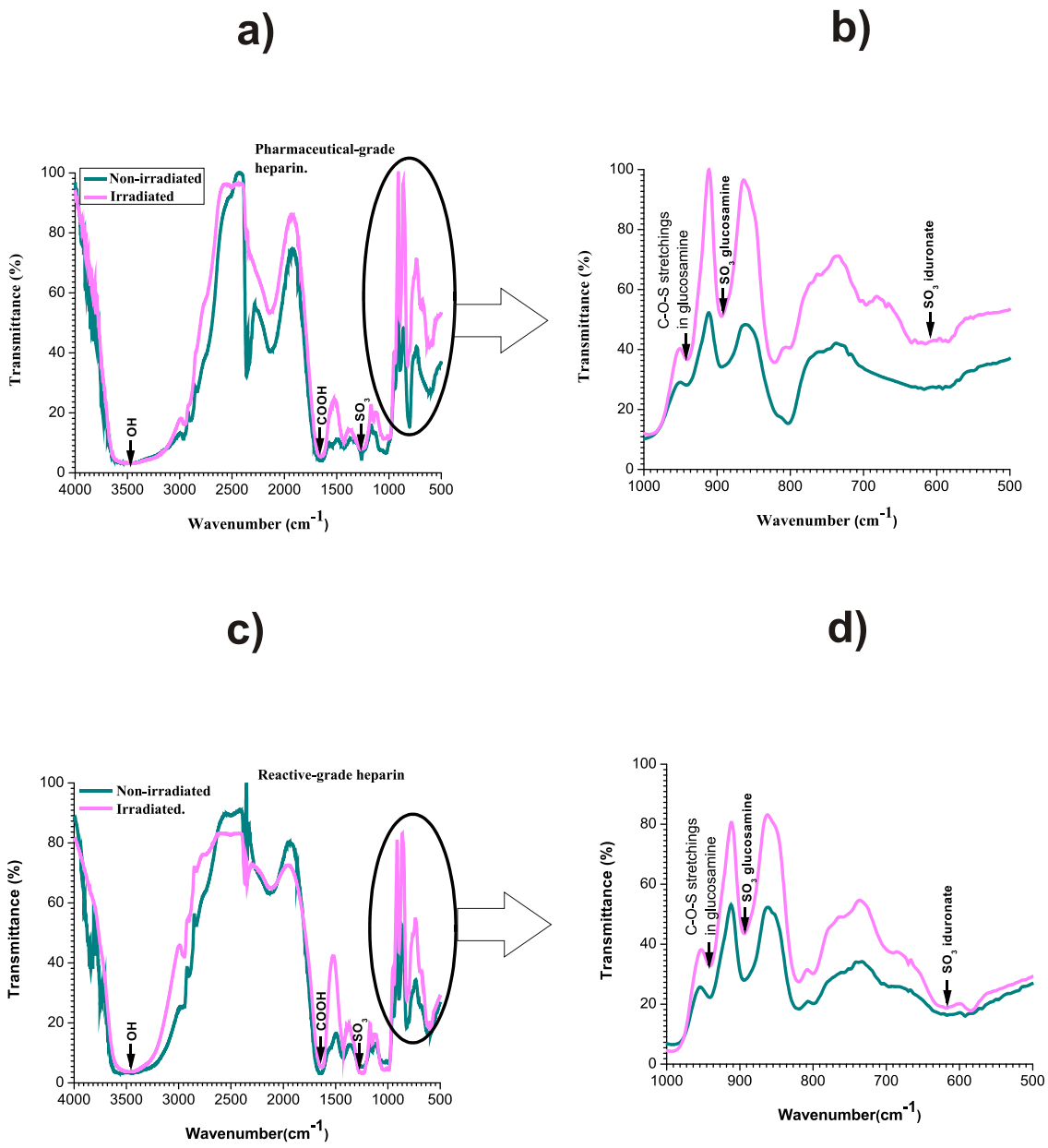

2.4a-d FTIR of non-irradiated and UV-irradiated heparin (pharmaceutical-grade and reactive-grade).

2.3.3 pH measurements.

The initial pH value for reactive-grade heparin dissolved in water was 7.2 which corresponds to an alkaline value, and from then on, it continued to go down reaching a final value of 6.85; the same heparin kind dissolved in benzyl alcohol had an initial value of 7.07, very close to the neutral domain and ended in 6.68, while for the pharmaceutical-grade preparation it went from

6.99 to 5.9. That is the reason why there is more UV-absorbing material generation as stated by Balazs et al. [5] and was verified in the UV–vis spectra .From these observations and relating them to the UV-Vis spectra studies, it might concluded that benzyl alcohol aids the reduction process in the nanoparticle synthesis and water does not.

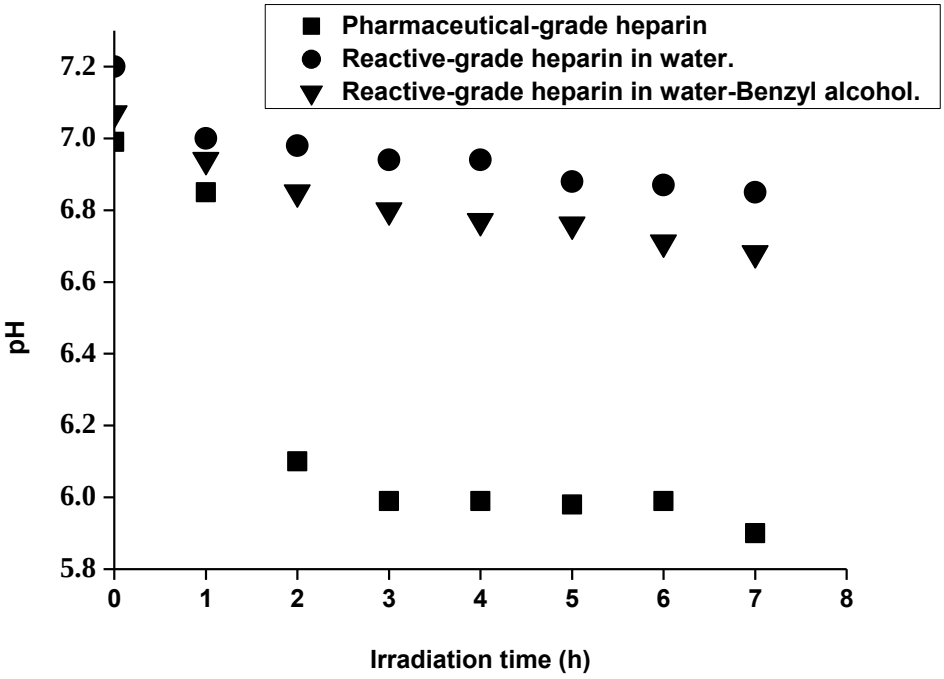

Figure 2.5 pH measurements of UV-irradiated heparins.

2.4 Heparin/$HAuCl_4$ interaction in solution.

A $HAuCl_4$ solution, whose UV-Vis spectrum is shown in figure 2.6, it was prepared to check out where its absorbance peaks are, and they are located at 203 and 315 nm, this last band belonging to the metal-to-ligand charge transfer transition of the $HAuCl_4^-$ complex [11] . Its tone is yellowish since no reduction reaction has taken place . Such spectrum will be taken as a reference as observations about the changes it suffered (as the metal precursor) in the synthesis process later on.

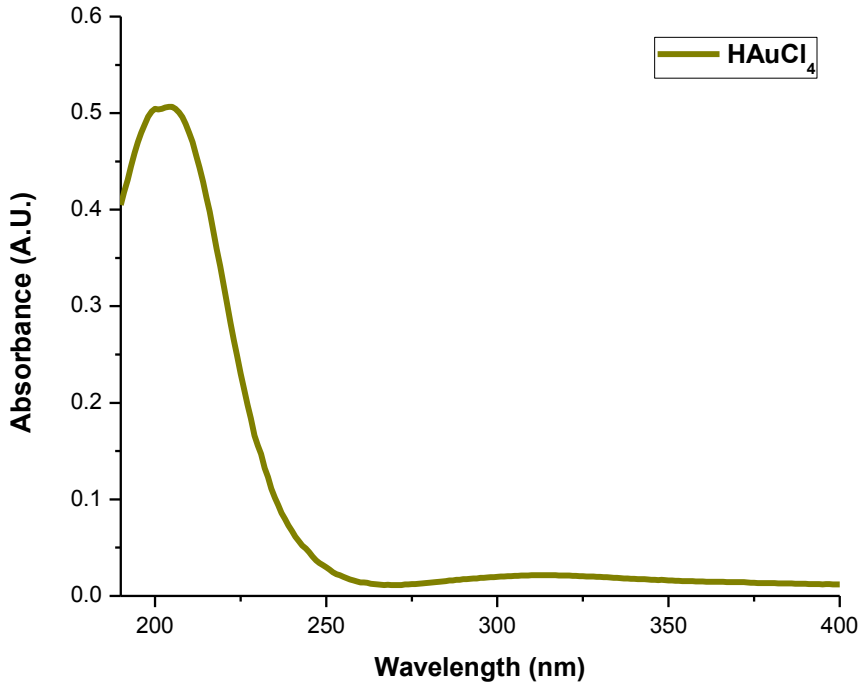

Figure 2.6 Chloroauric acid solution UV-Vis spectrum.

Figure 2.7a, b and c shows the mixtures of each heparin type and the gold solution precursor ($HAuCl_4$). Such experiments were carried to give way to analyze how the aqueous solution from which gold nanoparticles are generated is affected by UV light irradiation.

Glycosaminoglycans are a class of typical anionic polyelectrolytes that exhibit the property of binding or strong interaction with small inorganic cations, with cationic molecular species, and with cationic groups or regions of macromolecules [12], so the way the metal cation, in this case, Au^{+3}, interacts with heparins will be analyzed. The photoreduction of $HAuCl_4^-$ in aqueous solution provides nanoparticles, and in the method proposed in this thesis such reduction takes place not by direct photoreduction of the gold aqueous solution but via photosensitization which means that a photoactive reagent (heparin, in our case) is used to generate intermediates by

photoreduction. The intermediates reduce the co-existing metal source to produce the Au^0 (zerovalent metal) which gives place to nanoparticle formation [13].

The spectra of reactive and pharmaceutical-grade heparins shown in figures 2.6a and c are quite similar, and there are three contributions (since water has been subtracted from spectra): From Heparin, $HAuCl_4$ and Benzyl alcohol. In the case of reactive-grade heparin, its main peaks are located at 210, 225, 253 and 260 and for the pharmaceutical-grade one, they are found at 224, 248, 253, 260 and 266nm (as mentioned previously). When the heparin-gold in solution complex is formed the resulting peaks are at 190, 192, 205, 254 nm (reactive-grade heparin) and at 190, 192 (less prominent than in reactive-grade heparin) ,206 and 254 nm. By comparing the separate products (heparin and $HAuCl_4$) peaks and the ones formed in the complex, it is observed that the resulting shape is a result of the interaction between heparin and the gold precursor and from benzyl alcohol (it has a peak at 254 nm as already seen in Chapter 1) .As for the reactive-grade heparin dissolved in water and mixed with chloroauric acid, the individual components spectra do not differ much from the resulting complex spectrum. As stated at the beginning of this chapter, when glycosaminoglycans in aqueous solution are surrounded by a shell of water molecules, they occupy an enormous hydrodynamic volume in solution and when such solution is compressed , the water squeezes out and the GAGs are forced to ocuppy a smaller volume. In reference to the spectra displayed in figure 2.7b this could mean that water, when it is the only solvent, and due to the fact that it encloses heparin molecules, then its spectra becomes predominant being that the reason why no peaks are observed (also taking into account there is no benzyl alcohol present), which in turns also affects nanoparticle synthesis not aiding heparin in nanoparticle defined growth.

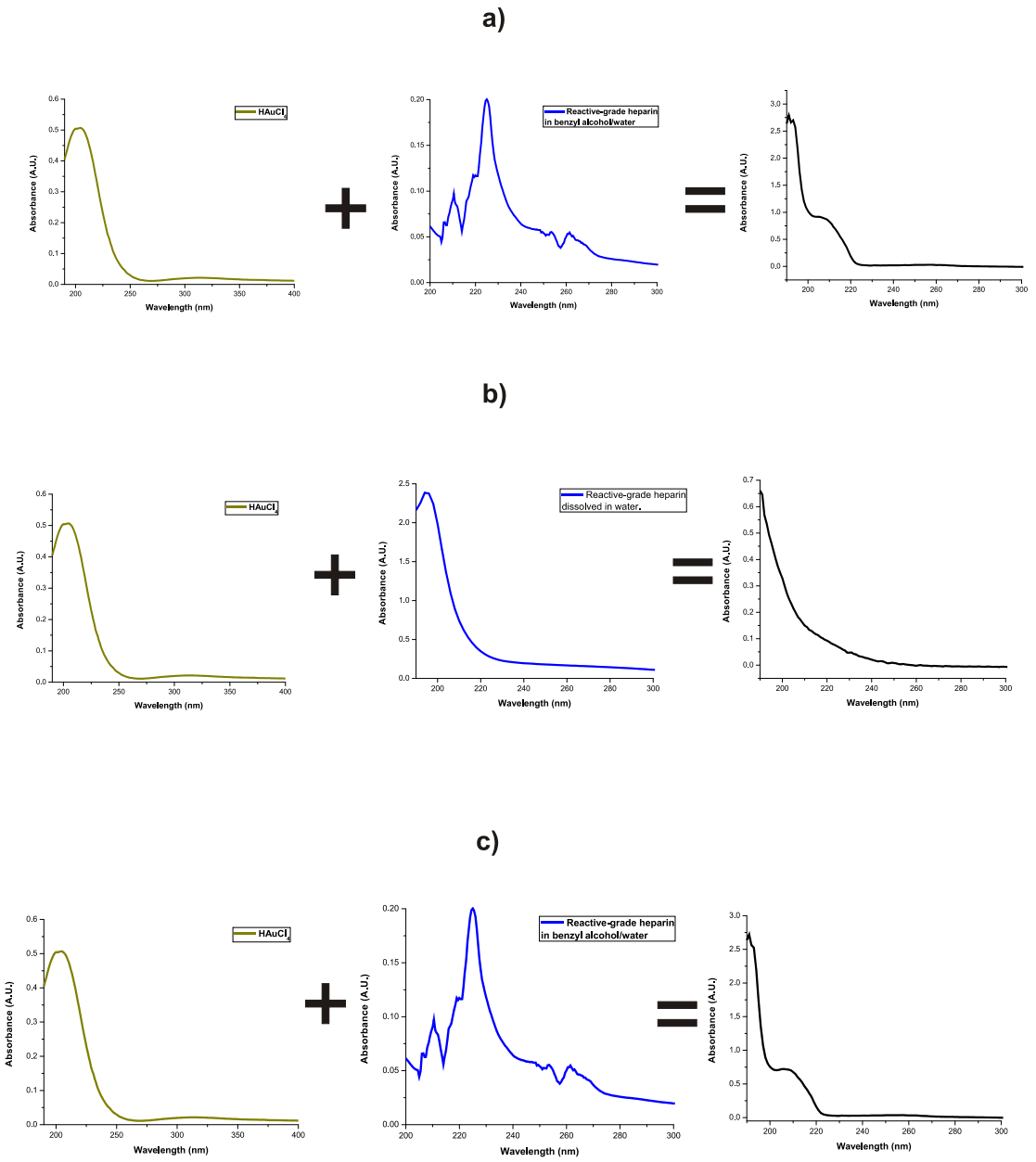

Figure2.7a, b and c Chloroauric acid and heparins aqueous individual solutions and the resulting complex from mixing them.

2.5 Concentration variation.

Both, heparin (reactive-grade and pharmaceutical-grade) and $HAuCl_4$ concentrations were varied in order to find out how such changes affected nanoparticle synthesis.

2.5.1 Reactive-grade heparin gold nanoparticle syntheses.

First, the chloroauric acid concentration, $HAuCl_4$, was increased from 0.0833 mM up to 0.4165 mM with heparin fixed at 0.0312 mM. Figures 2.8a,b and c show the UV-Vis spectra of samples A1, A2 and A3 for increasing $HAuCl_4$ concentrations of 0.0833, 0.333 and 0.4165 mM, respectively. The solutions tones changes from light purple to blue-grayish, suggesting a change in gold oxidation and the type of metal nanoparticles formed.

A possible explanation for the change from spheres to nanowire networks could be the fact that when the metal precursor concentration is very low, nanoparticles are formed, but the lack of stabilizer tends to form aggregated, elongated and bigger-sized structures. Taking into account that the gold concentration was being increased, the preferential growth in some directions is reached. This could explain the changes in shapes and the increase in length and decrease in diameter, indicating that there is not enough capping agent to passivate the nanoparticles surface.

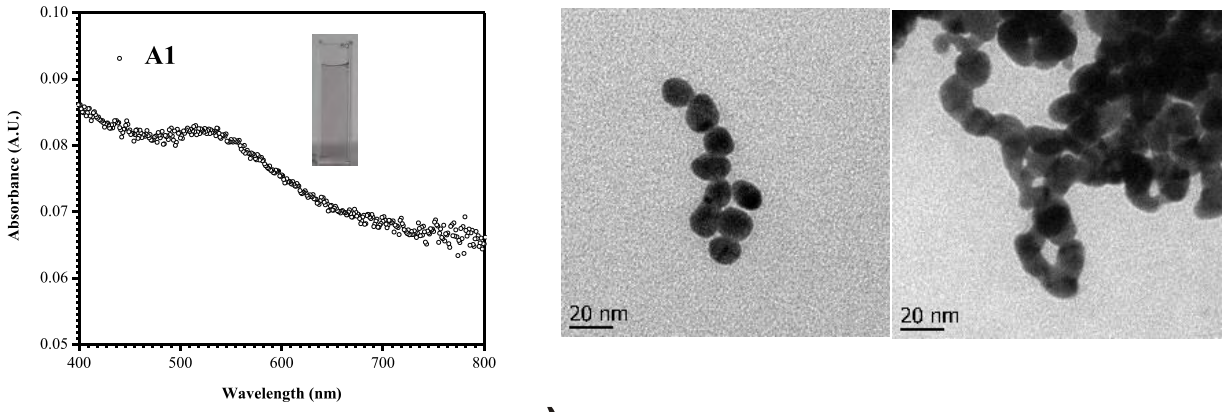

a)

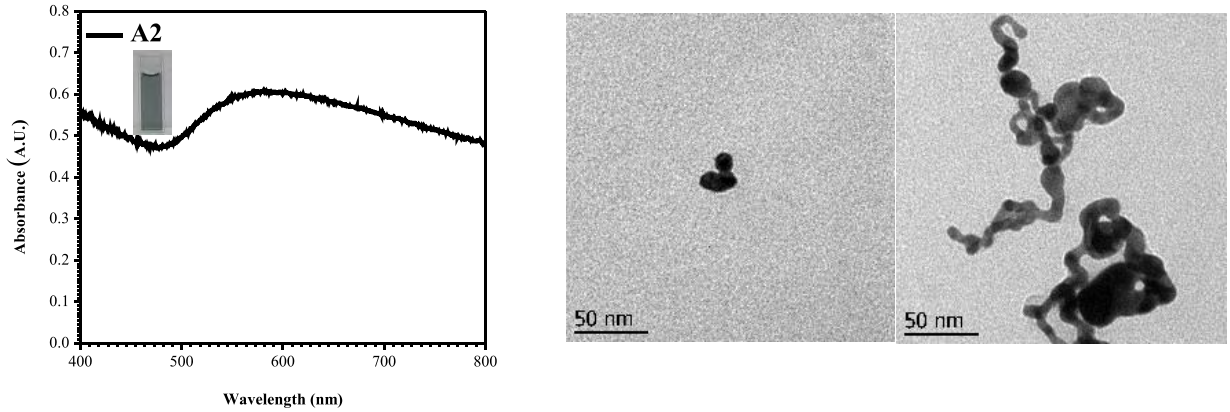

b)

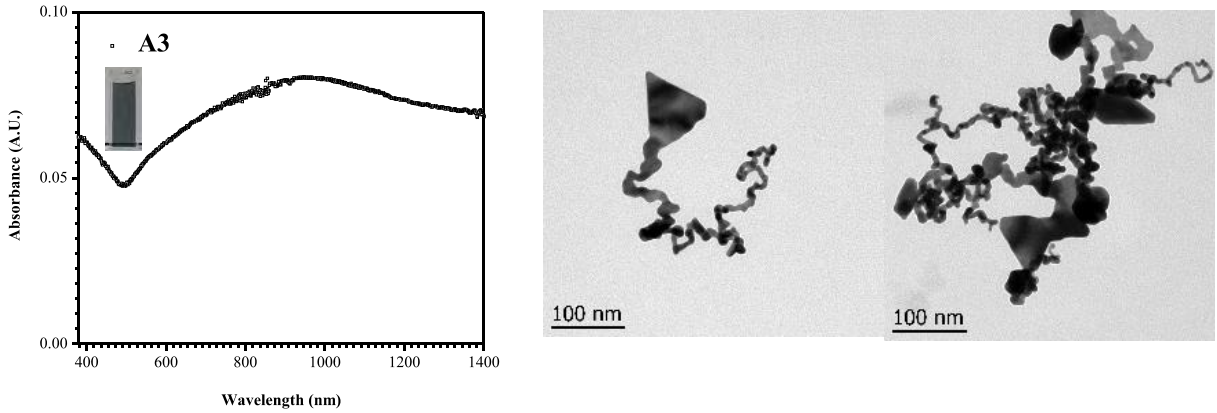

c)

Figure 2.8a,b and c UV-Vis spectra and TEM micrographies of samples with a fixed reactive-grade heparin concentration and a $HAuCl_4$ increasing concentration**.**

As the heparin concentration increases (figure 2.10), the assemblies begin to connect to each other forming networks of different sizes. The reason for this may come from the fact that heparin starts to enclose nanoparticles as well as to stabilize them, so this causes the individual clusters formed to gather in networks, and at the same time it induces growth for some nanoparticles in some preferential directions. Their aggregation inside the wires is probably a result of the heparin encapsulation, mentioned before, that is not letting the nanoparticles grow outside the wire but inside it; and in consequence inducing their aggregation in some parts. There is a noticeable difference at the highest concentration, there are still formed networks but now some parts of them break apart from that main structure, in a tap-pole shaped nanoparticles. That could make a slight dispersion contribution to the SPR peak observed in the UV–Vis spectrum in Fig. 2.9.

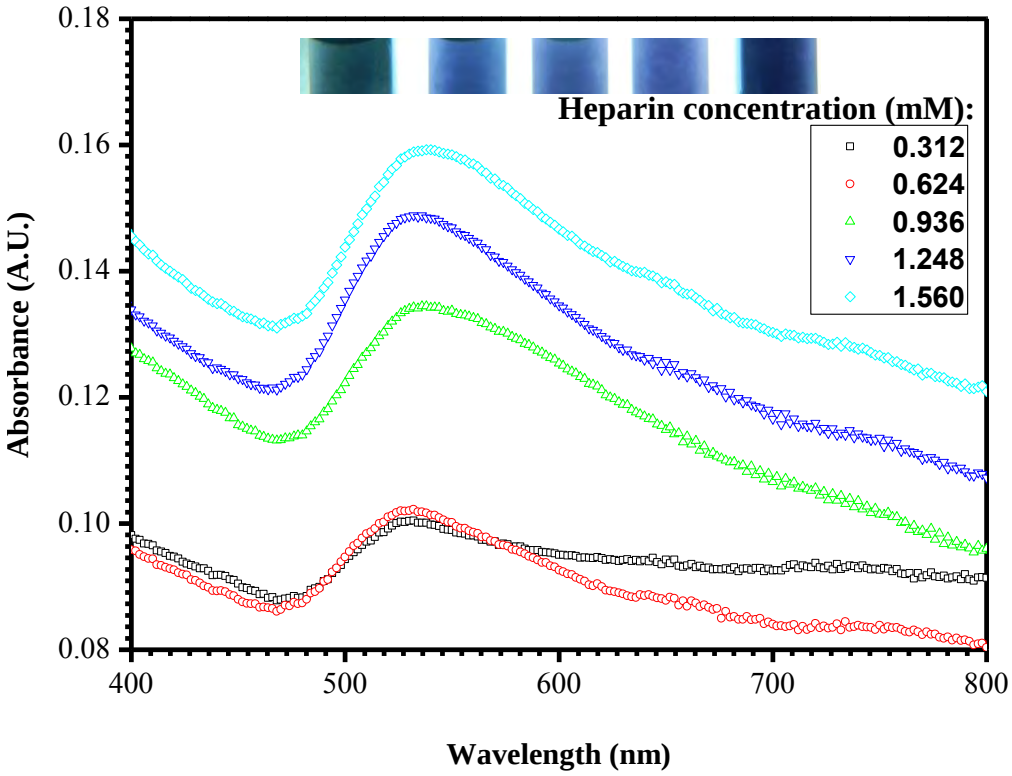

Figure 2.9. UV-Vis spectra of reactive-grade heparin gold nanoparticles with a 0.833 mM $HAuCl_4$ fixed concentration and a varying heparin one.

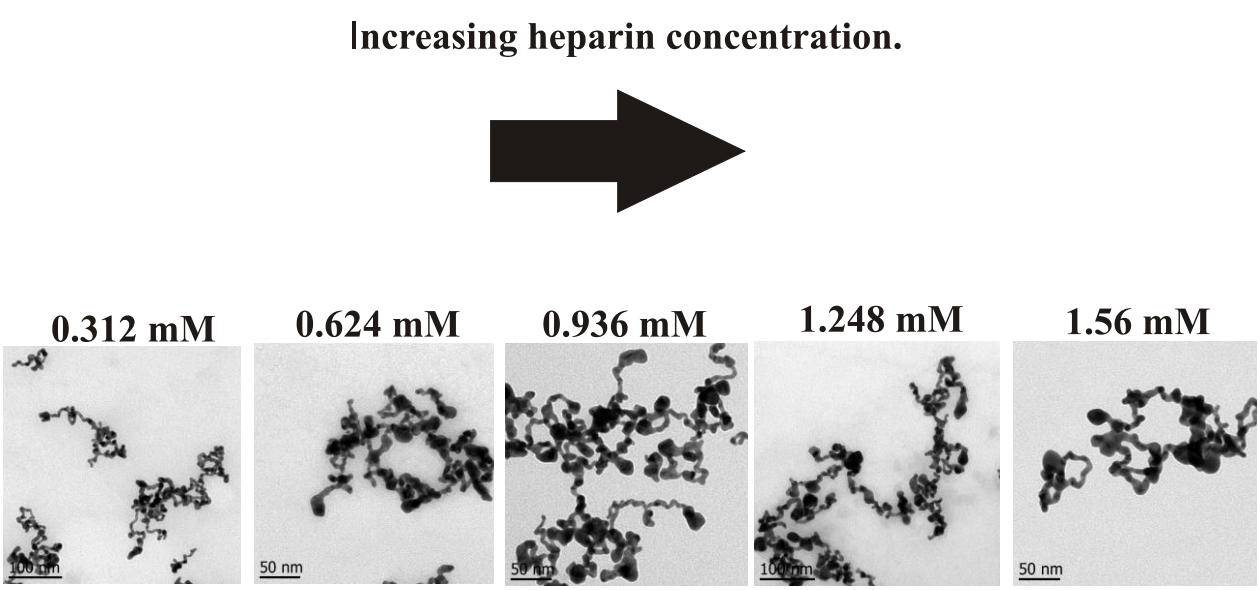

Figure 2.10 TEM micrographies of AuNPs with a 0.833 mM HAuCl4 fixed concentration and varying the heparin one.

2.5.2 Pharmaceutical-grade heparin gold nanoparticle syntheses.

Pharmaceutical-grade heparin possesses a 0.833 mM concentration in its vial, so the concentrations used for increasing gold concentrations are 0.0833 and 0.4165 mM (keeping heparin at 0.0312 mM) and for increasing heparin concentrations (keeping gold at 0.833 mM) are 0.312, 0.5, and 0.7 mM.

Non-spherical gold nanoparticles present multiple absorption bands correlating with their multiple axes, and they can support both propagating and localized surface plasmon resonances.

The number of SPR peaks usually increases as the symmetry of nanoparticles decreases; spherical nanoparticles exhibit only one peak, whereas two and three peaks are often observed in nanorods, nanodisks, and triangular plates, respectively [14]. Nanoplates have been previously

synthesized by photochemical methods [15,16] with similar results. In our case, when first modifying the gold concentration, it is observed that for the HEP1 sample, few nanoparticles are

generated and they are small, ranging from 13 to 20 nm. For sample HEP2 the situation is completely different because the nanoparticle sizes go up abruptly most likely due to the fact that the capping effect coming from heparin is not enough to stop their growth as shown in figure 2.11.

Also, another thing is that in contrast with reactive-grade heparin experiments, there is now a shape change. The particles show anisotropic features but instead of wire-like nanoparticles we obtained plates, faceted, pseudospherical and even some trapezoidal products that in principle do not coalesce among them to form more complex agglomerates.

Other aspects indicating differences from the nanoparticles synthesized with reactive-grade heparin are the solutions tones and their UV–vis spectra, the solutions shade change from a light pink to light violet which are shown in figure 2.11 as well.

For sample HEP1, there are three peaks: at 539, 626, and 718 nm and for HEP2 at 547, 642, and 737 nm, the appearance of three peaks can be explained due to the presence of tip-pointed nanoparticles which contribute to their plasmon resonance. Additionally, the plasmon peak red-shift indicates the nanoparticles sizes are bigger.

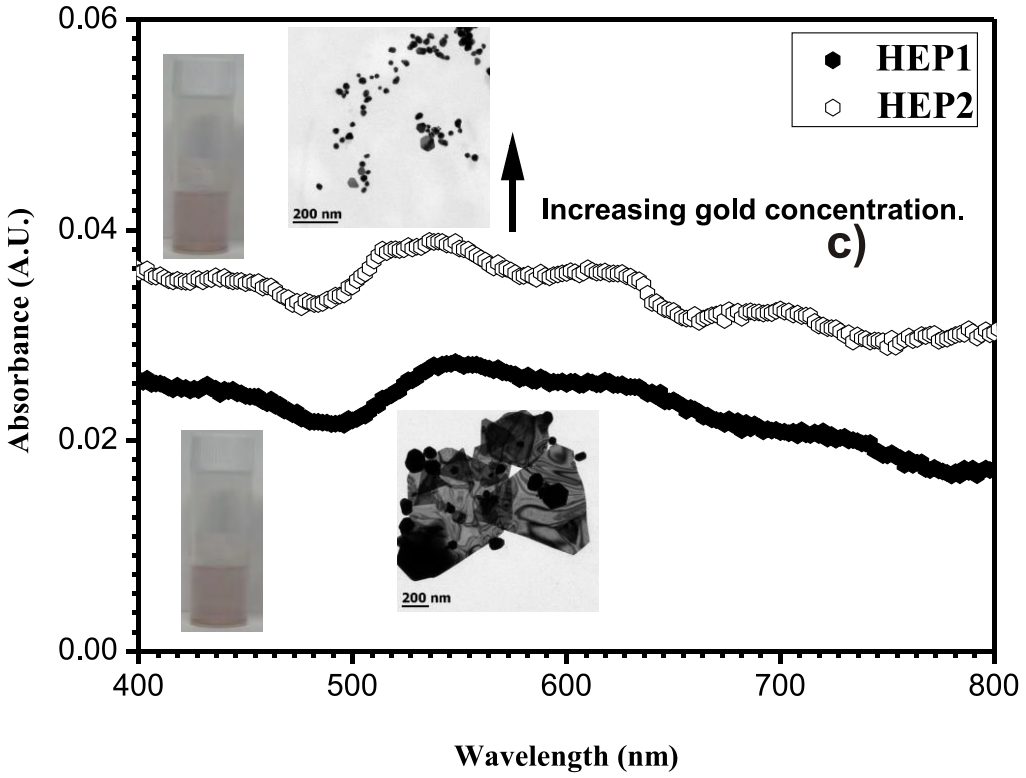

Figure 2.11 UV-Vis spectra and TEM micrographies of samples with a fixed pharmaceutical - grade heparin concentration and a HAuCl4 increasing concentration.

When pharmaceutical-grade heparin concentration was changed, the nanoparticles still show anisotropic features just like when the Au content is varied, the only difference resides in the size distribution as can be observed in figure 2.12.

As the heparin concentration rises, there is more encapsulating and size-limiting effects on the particles obtained as observed from the TEM images (Fig. 2.12). In the case of the HEP5 sample, it is noted that some really small nanoparticles are present due the heparin reducing power (besides its stabilizing role).

The plate sizes for these three syntheses with increasing heparin concentration vary from 100 up to 800 nm and for the other shapes from 20 to 50 nm. Figure 2.12 shows the solutions tones as

well as their UV–vis spectra. Unlike the previous case when decreasing heparin concentration case, for the three syntheses, the first peaks are located between 480 and 630 nm, and the second one between 700 and 900 nm , both peaks tend to blue-shift as the heparin concentration is increased indicating the nanoparticles diminish their size. Also, the FWHM for the first peak decreases from 8 to 58 nm indicating that the nanoparticle distribution is narrower, besides this peak sharpness indicates that a great contribution from the quasispherical nanoparticles is present.

Similar mixed products have been obtained by Zhang et al [17] .

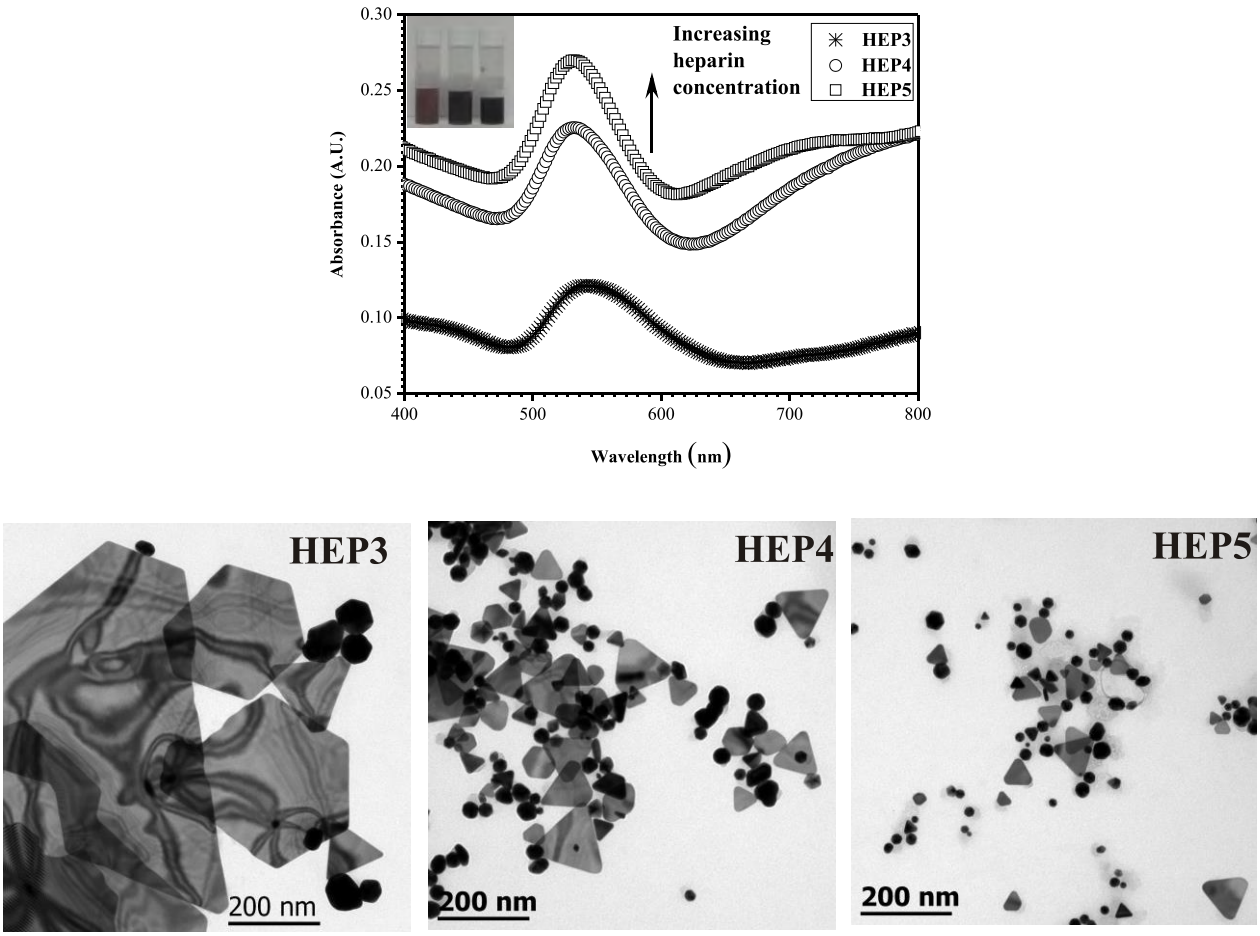

Figure 2.12 UV-Vis spectra of reactive-grade heparin gold nanoparticles with a 0.833 mM HAuCl4 fixed concentration and a varying heparin one.

2.6 Energy dispersive spectroscopy analysis.

EDS analyses were perfomed to find out what heparin functional groups are attached to the nanoparticles surface. Pharmaceutical-grade and reactive-grade heparin samples were prepared the same way they were for the Scanning Electron Microscope analysis.

Results are shown in figures 2.13a and b, it can be seen that there are peaks belonging to Silicon (which is discarded as a peak belonging to nanoparticles because the sample was prepared on a silicon wafer), gold, oxygen, sodium and sulfur.

Sulfur´s presence is due to the sulphate groups present in heparin, sodium´s because in both heparin´s cases they are sodium salts and oxygen may be part of the carboxylate and hydroxyl groups that are part of heparin´s structure.

In the case of reactive-grade heparin gold nanoparticles, the amount of oxygen, sodium and sulphur is bigger than in the case of the pharmaceutical grade ones. Sodium possesses a positive charge, and Sulphur and the hydroxyl and carboxylate groups are negatively charged, and there is there is one thing to take into account: The fact that hydroxyl groups are said to anchor metal ions tightly onto heparin via ion-dipole interactions, and act as passivation contacts for the stabilization of the nanoparticles by strong bonding interaction with their surface metal atom [22]. Therefore, if OH ions promote adhesion to the gold surface via the carboxylate group they are part of. then the surface must be “covered” by sulphate, carboxylate and sodium ions, being predominantly negatively charged, in addition to this, sulphate groups attach to the nanoparticle surface as well because gold forms covalent bonds with sulfur [18]. This conclusion is in good agreement with the results found by Ping et al [19] ; in their work, a gold heparinized sensor surface is studied for the detection of the low-density lipoprotein (LDL). To get to know what

groups are attached to the gold surface, they characterized it by X-ray photoelectron spectroscopy (XPS) and it from it, it was found that the heparin-modified gold surface shows several additional peaks corresponding to sulphur, nitrogen and oxygen.

a)
Reactive-grade heparin

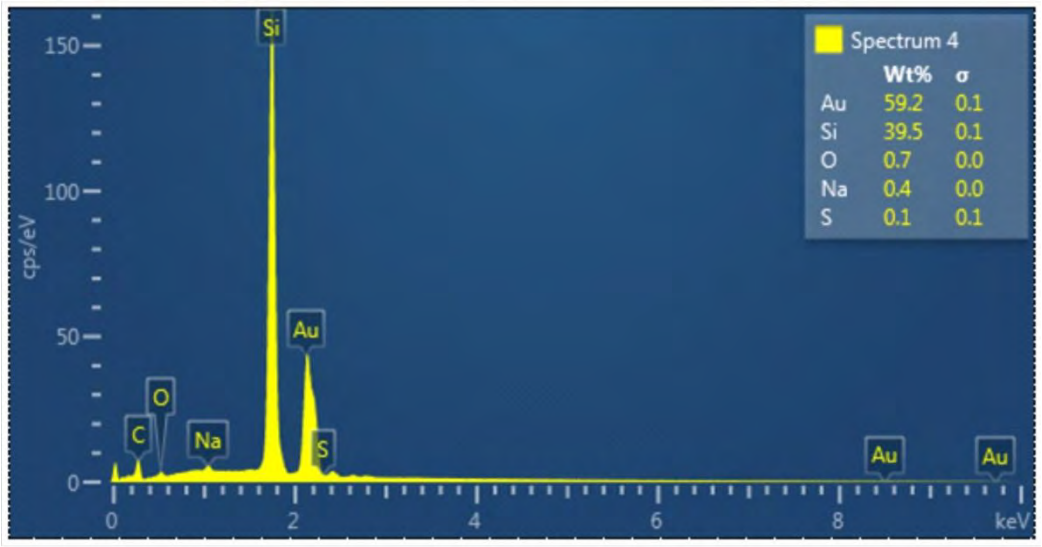

b)
Pharmaceutical-grade heparin

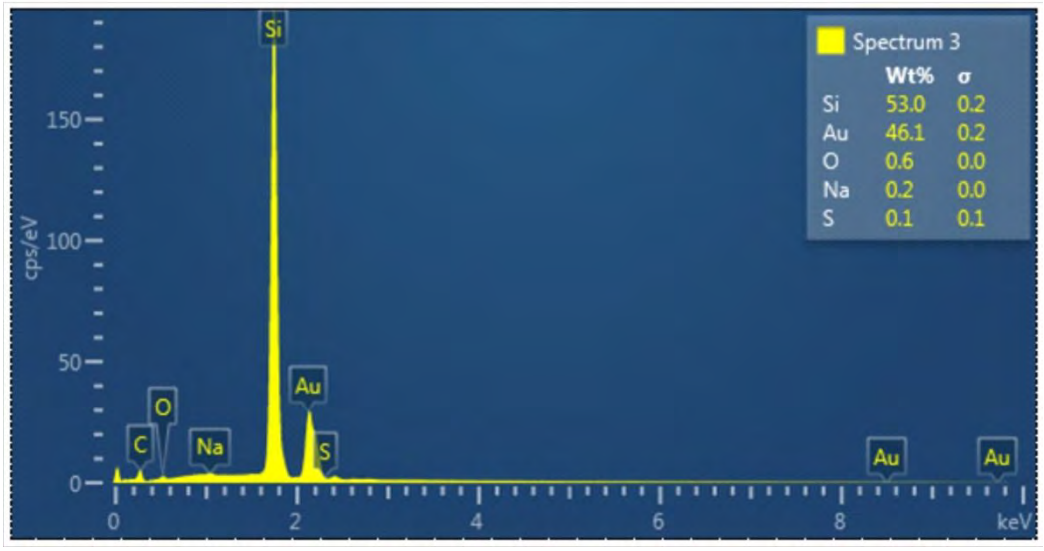

Figure 2.13 a and b a) EDS analysis graphs for reactive-grade heparin AuNPs and for b) pharmaceutical-grade heparin AuNPs.

2.7 Nanoparticle formation under UV irradiation.

Heparin is a polysaccharide formed by disaccharide basic units (iduronic acid and glucosamine) which are repetitive along its structure with varying sulfation degree and that becomes hydrolized when dissociated. This means that the glycosidic bond that joined them is broken because H and OH ions are donated by water. When this happens, these disaccharides units are separated (this occurs to the whole chain composed by these two monosaccharide units).Once there has been hydrolysis, the glucosamine monosaccharide turns to its hemiacetal form, this is, in its linear form,and the iduronic acid takes this form as well. In this hemiacetal form, the aldehyde present in the glucosamine residue, which is reactive in the UV range, promotes its own oxidation, which at the same time allows the reduction of gold ions when present in solution, and thus this process leads to nanoparticles generation and growth [20].

Thus, from the above results, it is possible that the differences between the types of nanoparticles produced by the two heparins (taking into account solvent differences as well) as photosensitive agents, might be due to the fact that pharmaceutical-grade heparin has a more acidic nature than the pharmaceutical-grade one making nanoparticle growth take place in different directions. pH might induce a change in the orientation and conformation of the heparin molecules when the synthesis is being carried out and this leads to different nanoparticle generation [20].

Although experiments related to water/benzyl alcohol mixtures for reactive-grade heparin nanoparticle solutions are not mentioned, benzyl alcohol structure is shown in figure 2.13, it is an aromatic alcohol formed by a benzyl group, the OH, hydroxyl group, attached to it. Multiple OH groups offer stability, solubility and resistance to high salt concentrations when they are located on the nanoparticles surface [21]. This might be the reason why in the samples mentioned in chapter 1, pharmaceutical-grade heparin and reactive-grade heparin dissolved in water/benzyl alcohol, show a much better stability after 4 months than the ones prepared using reactive-grade

heparin dissolved in water. Also, OH, groups are also found in heparin structure, but they are found in less amount, so, when heparin is dissolved in benzyl alcohol and water, there is an excess of them and that might aid nanoparticle synthesis as well as stability and functionality.

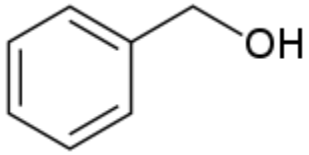

Figure 2.14 Benzyl alcohol structure.

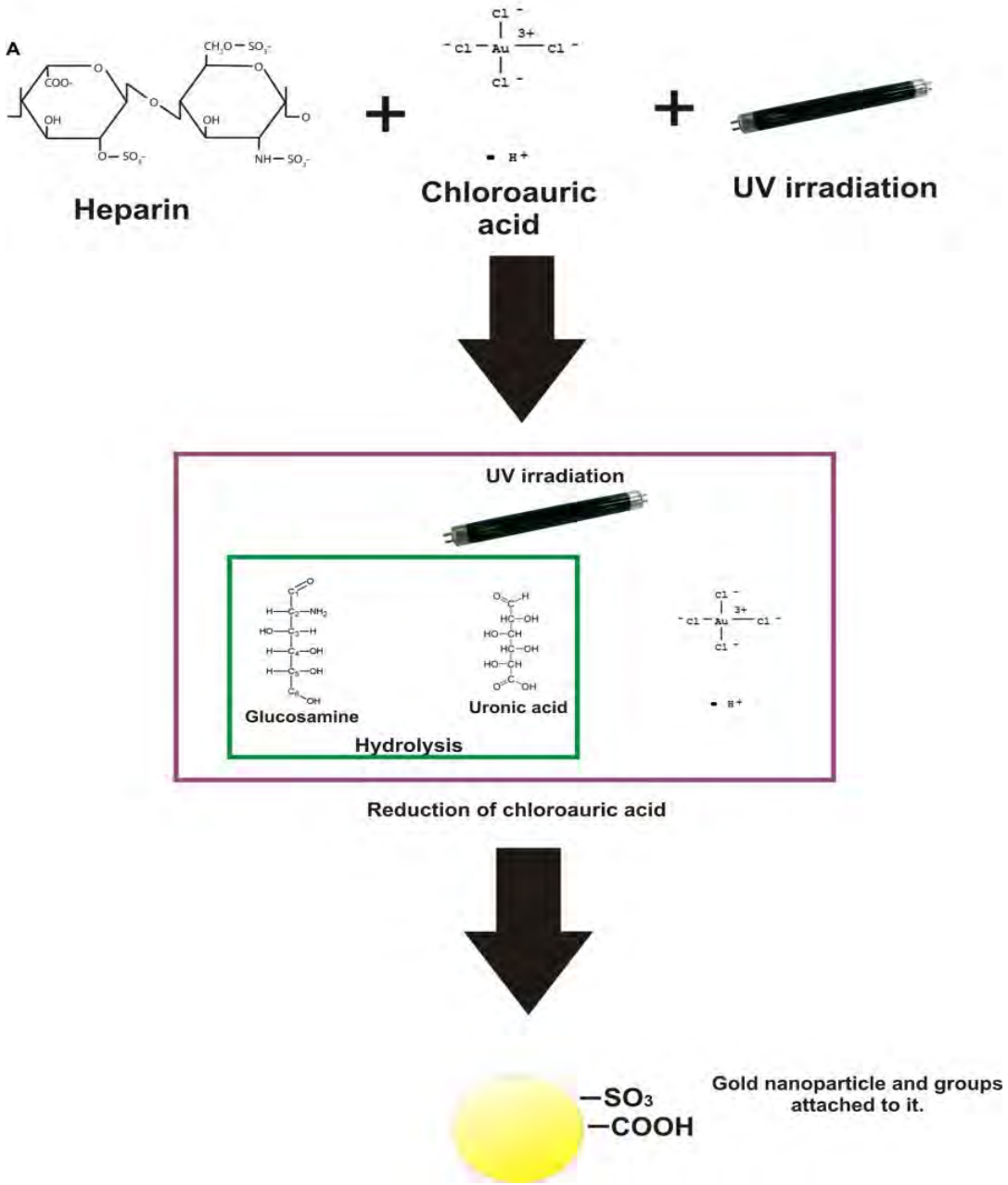

Figure 2.15 Heparin-based nanoparticle formation mechanism.

2.8 Comparison with previous heparin-based gold nanoparticle synthesis methods.

It has been mentioned previously in this work that there are several methods to synthesize heparin-based nanoparticles[1-3,14-18]; but from all of them there is only one in which heparin is used directly as a reducing and stabilizing agent to synthesize gold nanoparticles [3]. In the rest

of them, non-metal nanoparticles are made of heparin conjugated to another material [14-17]; heparin has been modified to synthesize metal nanoparticles [1,2], or it has been used directly but to synthesize silver nanoparticles [21].

In this section, the work done on this thesis concerning gold nanoparticles synthesis using heparin as the reducing and stabilizing agent is compared to the one done by Guo et al [21], for being the closest one regarding conditions, this is, heparin was not modified in any way, the only difference being that instead of using a thermal approach, Photochemistry was used. The chart below (figure 1.15) shows the differences.

In that work [18], heparin concentration was varied (from 0.01 to 4 mg/mL) whereas the gold precursor one was fixed (0.1 mg/mL),and the shapes obtained were quasispherical ranging from 12 up to 52 nm (decreasing heparin concentration). On the other hand, in this thesis results concentrations of both heparin and gold were varied using both heparin types and as it can be seen in figures 1.15b ,reactive-grade heparin AuNPs results show that when decreasing gold concentration, the nanoparticles go from wires and triangles to quasispherical products and when decreasing heparin concentration, wires are formed once more but the nanoparticles within them are become bigger in size. As for the experiments with pharmaceutical-grade heparin AuNPs, shapes are different from those obtained with reactive-grade heparin and when the gold concentration decreases, the nanoparticles grow smaller and when decreasing heparin concentrations they grow big, these results are in agreement with the ones obtained by Guo et al because as the heparin concentration (at a fixed gold one) decreases nanoparticles are bigger, the differences observed are in the shapes obtained, because even though quasispherical products were obtained, other shapes are present as well.

a)

Yanli Guo et al [18]

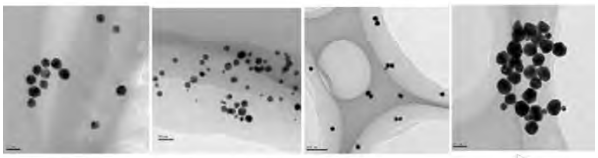

Decreasing heparin concentration

Gold precursor concentration:0.1 mg/mL

b)

Reactive-grade heparin results [20]

Decreasing gold concentration

Heparin concentration:0.5 mg/mL

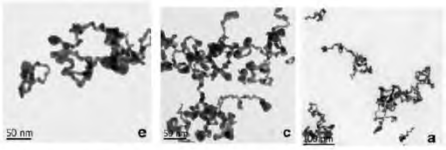

Decreasing heparin concentration.

Gold concentration:0.32 mg/mL

c)

Pharmaceutical-grade heparin results [20]

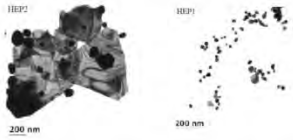

Decreasing gold concentration

Heparin concentration:0.370 mg/mL

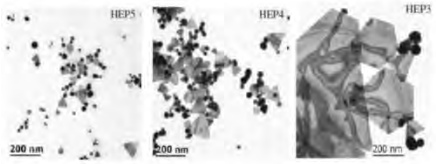

Decreasing heparin concentration

Gold concentration:0.328 mg/mL

Figure 2.16a, b and c. Comparison with Guo et al. work on heparin-based gold nanoparticles.

References.

[1] Gandhi N.S., Mancera R.L.,(2008), The Structure of Glycosaminoglycans and their Interactions with Proteins, Chemical Biology and Drug Design, 72, 6, 455-482.

[2] Murugesan S., Xie J, Linhardt R.J.,(2008), Immobilization of Heparin: Approaches and Applications, Current Topics in Medicinal Chemistry, 8, 80-100.

[3] Hirsh J., Warkentin T.E., Shaughnessy S.G., Anand S.S., Halperin J.L., Raschke R., Granger C., Ohman E.M., Dalen J.E., (2001), Heparin and Low-Molecular-Weight Heparin Mechanisms of Action, Pharmacokinetics, Dosing, Monitoring, Efficacy, and Safety, Chest ;119;64S-94S.

[4] Ghasemi J., Niazia A., Ghobadib S.,(2005), Simultaneous Spectrophotometric Determination of Benzyl Alcohol and Diclofenac in Pharmaceutical Formulations by Chemometrics Method, Journal of the Chinese Chemical Society, 52, 1049-1054

[5] Balazs E.A., Laurent T.C., Howe A.F., Varga L.,(1959), Irradiation of Mucopolysaccharides with Ultraviolet Light and Electrons, Radiation Research 11, 149-164.

[6] Sushko N.I., Firsov S.P., Zhbankov R.G., Tsarenkov M., Marchewka M.,Ratajczak C. (1994) Vibrational spectra of heparins. Journal of Applied Spectroscopy 61:5–6.

[7] Oliveira G.B., Carvalho L.B. Jr., Silva M.P.C. (2003) Properties of carbodiimide treated heparin. Biomaterials 24:4777–4783.

[8] Grant D, Long WF, Moffat CF, Williamson FB (1991) Infrared spectroscopy of heparins suggests that the region 750–950 cm-1 is sensitive to changes in iduronate residue ring conformation. Biochemical Journal 275:193–197.

[9] Grant D, Long WF, Moffat CF, Williamson FB (1991) Infrared spectroscopy of heparins suggests that the region 750–950 cm-1 is sensitive to changes in iduronate residue ring conformation. Biochemical Journal 275:193–197.

[10] Chakrabarti B, Park J.W. (1980), Glycosaminoglycans: structure and interaction, CRC Critical Reviews in Biochemistry, 8(3):225-313.

[11] Qin X, Lu W.,Chang G. ,Luo Y., Asiri A.M., Al-Youbi A.O., Sun X. (2012), Novel synthesis of Au nanoparticles using fluorescent carbon nitride dots as photocatalyst, 45:61–67.

[12] Chakrabarti B, Park J.W. (1980), Glycosaminoglycans: structure and interaction, CRC Critical Reviews in Biochemistry, 8(3):225-313.

[13] Sakamoto M., Fujistuka M, Majima T. (2009), Light as a construction tool of metal nanoparticles: Synthesis and mechanism, Journal of Photochemistry and Photobiology C:Photochemistry Reviews, 10, 33–56.

[14] Li N., Zhao P., Astruc D. (2014), Anisotropic Gold Nanoparticles: Synthesis, Properties, Applications, and Toxicity, Angewandte Chemie International Edition,53, 7, 1756–1789.

[15] Yang S, Zhang T, Zhang L, Wang S, Yang Z, Ding B (2007) Continuous synthesis of gold nanoparticles and nanoplates with controlled size and shape under UV irradiation. Colloid Surface A:Physicochemical Engineering 96:37–44.

[16] Lee K.Y., Kim M., Lee Y.W., Choi M.Y., Han SW (2007) Photosynthesis of gold nanoplates at the water/oil interface. Bulletin of Korean Chemical Society 28(12):4124–4126.

[17] Zhang G., Jasinski J.B., Howell J.L., Patel D., Stephens D.P., Gobin A.M. (2012) Tunability and stability of gold nanoparticles obtained from chloroauric acid and sodium thiosulfate reaction. Nanoscale Research Letters 7:337.

[18] Nuzzo R.G. , Fusco F.A. , Allara D.L.,(1987), Spontaneously organized molecular assemblies.Preparation and properties of solution adsorbed monolayers of organic disulfides on gold surfaces, Journal of the American Chemical Society, 109 (8), 2358–2368.

[19] Ping L., Jing J.,Xiao-Jun H., Deepak G. , Thomas G. ,Jörg V., Hui D. (2012), Adsorption/Desorption of Low-density Lipoprotein on a Heparinized Surface of Gold Sensors, CHEMICAL RESEARCH CHINESE UNIVERSITIES 28(2), 323—328.

[20] Rodríguez-Torres M. del P., Díaz-Torres L.A., Salas P., Rodríguez-Gonzáles C., Olmos-López M. (2014), UV photochemical synthesis of heparin-coated gold nanoparticles, Gold Bulletin, 47:21–31.

[21] Nguyen T.K. Thanha,b, Luke A.W. Greena,b, (2010), Functionalisation of nanoparticles for biomedical applications, Nano Today, 25, 213—230.

[22] Guo Y.,Yan H., (2008), Preparation and characterization of heparin-stabilized gold nanoparticles, Journal of Carbohydrate Chemistry,27,5, 309-319.

Chapter 3.

Surface enhanced Raman spectroscopy of colloids.

This chapter is devoted to explaining Raman spectroscopy principles, the surface enhanced Raman spectroscopy phenomenon and to show the results obtained with heparin-based gold colloids obtained photochemically and with heat, using differently charged analytes (Methylene Blue, Rosebengal and Neutral Red) and proteins (GP120 and Bovine Serum Albumin) to assess their surface enhanced Raman activity.

3.1 Raman scattering.

When a molecule is exposed to an electric field, electrons and nuclei are forced to move in opposite directions and a dipole moment proportional to the electric field strength and to the molecular polarizability, α is induced. A molecular vibration can only be observed in the Raman spectrum if there is a modulation of the molecular polarizability by the vibration as indicated in equation (1):

$$\left(\frac{\partial \alpha}{\partial q}\right)_0 \neq 0 \qquad (1)$$

Where q stands for the normal coordinates describing the motion of the atoms during a normal vibration, and the subscript 0 indicates that the derivative is taken at the equilibrium configuration.

The origin of Raman spectroscopy is an inelastic scattering effect, but in a Raman experiment, the elastic as well as the inelastic scattering of the radiation are observed.

The elastic scattering, which is also called Rayleigh scattering corresponds to the light scattered at the frequency of the incident radiation, ν_0. The molecule absorbs no energy from the incident radiation in this case. The inelastic scattered light, which is known as Raman radiation, is shifted in frequency, and hence energy, from the frequency of the incident radiation by the vibrational energy that is gained or lost in the molecules ($h\nu_0 \pm h\nu_s$).

The Raman scattering process has a much lower probability in comparison with the Rayleigh scattering that is a coherent process. On the other hand, according to Boltzmann´s law, most molecules are in their vibrational ground state at ambient temperature, and a much smaller number in the vibrationally excited state. Therefore, the Raman process, which transfers vibrational energy to the molecules and leaves a quantum of lower energy ($h\nu_0$-hvs) has a higher probability than the reverse process, and the corresponding lines are referred to as Stokes and anti-Stokes lines, respectively. The intensities of the Stokes lines, caused by quanta of lower energy are higher than those of the anti-Stokes lines. Therefore, usually only Stokes radiation is recorded as a Raman spectrum.

To understand the Raman process, virtual states have to be considered. This is because the interaction of the photon with the molecule and the reemission of the scattered photon occur almost simultaneously. The existence of such virtual states also explains why the non-resonance Raman effect does not depend on the wavelength of excitation, since no real states are involved in this interaction mechanism. In fact, the Raman spectrum does not depend on the laser wavelength excitation.

An important aspect to consider in Raman spectroscopy is the appropriate wavelength choice. A large variety of lasers covering a broad range from the visible domain have been used; and in

recent years, infrared diodes at 785, 810 and 830 nm as well as Nd-YAG (1064 nm) have been incorporated. Particularly, the use of near-infrared lasers, which often avoid the excitation of Raman masking fluorescence, has stimulated the area of biospectroscopy [1-3].

3.1.1 Surface enhanced Raman spectroscopy.

Surface enhanced Raman spectroscopy, also known as SERS, is about the enormous enhancement of the common Raman signal of materials (commonly referred to as analytes) which are adsorbed on a metallic surface, such as metal nanoparticle´s. Many of the advantages of Raman scattering, such as molecular specific vibrational spectra, simple versatile sampling, and the ready determination of the presence of analytes in water are applicable to SERS, too. In fact, an increased sensitivity is obtained and very low concentrations of analytes can be detected.

A qualitative understanding of the SERS process is provided by the classical theory of light scattering. It is considered that a beam of incident light induces an oscillation dipole in a particle which reemits or scatters light at the same frequency of the dipole oscillation. For the particular case where the magnitude of the incident electric field E, is not too large, the induced dipole moment can be approximated as follows (equation 2) [2]:

$$\mu = \alpha E \tag{2}$$

Where α is the polarizability of the molecule.

Raman intensity is proportional to the square of the induced dipole, μ, and there are two possible enhancement mechanisms, which are the chemical and electromagnetic ones. Hence, the enhancement effect can influence either the molecular polarizability or the electric field experienced by the molecules. Surface selection rules are available and according to them, the most intense bands are those given by vibrations, which induce a polarization of the adsorbate

electron cloud perpendicular to the metal surface. By using the surface selection rules, the orientations of the adsorbate molecule relative to the metal surface can be predicted [2,3].

3.1.2 Mechanisms of Raman enhancement.

The nature of the mechanism which produces the surface enhanced Raman signal is not elucidated yet and remains as a focus of debate. There are two major contributions to the total enhancement of the Raman signal of adsorbed molecules as mentioned in the previous section:

Electromagnetic enhancement.

It is sometimes referred to as an electric field effect in which the molecule experiences large local fields caused by electromagnetic resonances occurring near metal surface structures.

The electromagnetic effect is, in turn, based on two enhancements: The first one is the enhancement of the laser electromagnetic field due to the addition of the field provoked by the polarization of the metal particles. The other is due to the molecule radiating an amplified Raman field, which further polarizes the metal particle and in this manner acts as an antenna to amplify the Raman signal even more [2].

Surface roughness is an essential requirement for SERS to occur. On a smooth metal surface, surface plasmons exist as waves of electrons bound to the metal surface and are capable of moving in a direction parallel to the surface. On a roughened metal surface, the plasmons are no longer confined and the resulting electric field can radiate both in a parallel and a perpendicular direction to the surface. When an incident photon falls on the roughened surface, excitation of the plasmon resonance of the metal may happen and this allows scattering . Additionally, due to the difference in dielectric constants between the roughened surface and the surrounding media, a concentration of electric field density takes place at sharp points on the surface. Metal colloids

and colloidal aggregates provide a particularly rich example of such electromagnetic enhancement [2].

The charge transfer mechanism enhancement.

It results when molecules physisorb or chemisorb directly on the roughened surface forming an adsorbate-metal complex. If chemisorption arises, the molecular orbitals of the adsorbate are broadened by an interaction with the conduction bands of the metal surface resulting in a ready transfer of electrons and excitation from the metal to the adsorbate and viceversa. As a consequence, the SERS spectra of chemisorbed molecules are significantly different from the Raman spectrum of free species, although those of the physisorbed species are not changed. The spectrum of physisorbed molecules is practically the same as that of free molecules, small changes being observed only for the bandwidths. This situation corresponds to a relatively larger distance between the metal surface and adsorbed molecules [3]. The charge-transfer mechanism is restricted by its nature to molecules directly adsorbed on the metal, as opposed to the electromagnetic effect which extends a certain distance beyond the surface. Thus, it effectively operates only on the first layer of the adsorbate [4, 5].

3.1.3 SERS active substrates.

SERS substrates enable the identification of different molecules at low concentrations based on Surface Enhanced Raman Scattering effect. The original SERS substrates were electrochemically roughened metal electrodes [6]. Metallic nanoparticles were used after the discovery of the SERS effect and became the most studied class of substrates. The emphasis on nanostructures for SERS is justified by the wide possibilities of optimization parameters, since both the frequency and magnitude of the maximum field enhancement are strongly dependent on the shape, size and arrangement of the metallic features at the nanoscale [7]. SERS substrates can be classified in

three categories: (1) Metal nanoparticles in suspension; (2) Metal nanoparticles immobilized on solid substrates and (3) Nanostructures fabricated directly on solid substrates, which includes nanolithography and template synthesis of nanostructures. The SERS effect is observed from a number of limited roughened metals, for example, silver, gold, aluminium, lithium, copper and sodium. The intensity of scattering from adsorbed analytes is no longer proportional to the frequency fourth power (ν^4) as in the case of conventional Raman. In fact, the intensity of the bands is related to the frequency of the surface plasmon resonance and the laser excitation frequency. The exact dependence is related to the nature of the metal substrate, particularly, to the identity of the metal and its roughness. Since SERS was first observed, numerous SERS-active surfaces have been developed [8].

Colloidal suspensions are attractive as SERS substrates since the aggregation of metal nanoparticles leads to the formation of aggregates with the roughness necessary to render intense Raman spectra and they can be reproducible and inexpensive [9]. In fact, the simplest SERS experiments are carried out with metal nanoparticles in suspension in the presence of a certain concentration of the analyte. These colloids are used as SERS substrates due to their high SERS performance, good stability and ease of fabrication.

3.1.4 Selection rule.

The surface selection rule is not a restriction on the symmetries of the excited states, but rather the reduction or increment in the intensities of certain infrared or Raman bands of an adsorbed molecule resulting from the physical proximity of the surface. The most popular enunciation of this selection rule is in terms of image charges, this is,when one considers the vibrating system to be a composite of the adsorbed molecule and its conjugate-charge image in the metal, one can show that vibrations whose transition dipoles in the molecule are directed tangentially to the metal surface would have zero composite transition dipoles, whereas vibrations whose transition

dipoles have a component normal to metal surface would have that component reinforced in the composite system.

There is another way to state the selection rule which is not based on image charges terms: It says that the incident and reflected electric fields at a surface interface interfere in such a way that the tangential component is diminished while the normal component is augmented; consequently, the component of the transition dipole normal to the surface is excited more strongly than the tangential component. In simple words for both approaches the basic statement is that only molecular vibrational peaks giving rise to a dynamic dipole moment perpendicular to the surface will be observed in the spectra [10,11].

3.1.5 SERS enhancement factor.

In normal Raman spectroscopy, the average Raman intensity of a molecule is directly proportional to the laser power density and to the Raman cross section of molecules. This simple fact can be generalized to SERS: The SERS intensity for a given vibrational mode of a given analyte should also be proportional to the laser intensity and to the normal Raman cross section but affected by an enhancement factor (EF), such parameter is the essence of SERS, being the measurement giving an idea of how boosted the Raman signal is.

The complex nature of the SERS effect and SERS substrates makes it impossible to use a single and unique SERS enhancement factor. This implies there is more than one definition depending on the situation and the effects that are being emphasized. There is an approach to classify them:

1. The Single Molecule Enhancement Factor (SMEF).

   This is the SERS enhancement felt by a given molecule at a specific point. It is generally dependent on the Raman tensor of the probe and its orientation on the SERS substrate and with respect to the local field at that point. It is also dependent on the orientation of the SERS

substrate with respect to the incident laser polarization and direction. Hence, it requires the exact definition of the SERS substrate geometry, and the exact position and orientation of the probe on it. Because of these constraints, this definition is much more suited to theoretical estimations of the EF, rather than experimental measurements.

It could be defined in a simple way as the ratio of the SERS intensity of a single molecule I_{SERS}^{SM} to the Raman intensity I_{RS}^{SM} of the same molecule under the exact same conditions, but in absence of the metallic substrate. Since there could be variations of the Raman signal s from the free molecule that could result in an infinite enhancement factor, the Single Molecule Enhancement Factor can be defined as:

$$SMEF = \frac{I_{SERS}^{SM}}{\langle I_{SERS}^{SM} \rangle} \tag{3}$$

Where I_{SERS}^{SM} is the SERS intensity of the single molecule under consideration, while $\langle I_{RS}^{SM} \rangle$ is the average Raman intensity per molecule for the same probe. This average is taken over all possible orientations of the molecule in space [12].

2. The SERS Substrate Enhacement Factor (SSEF).

It is defined as :

$$SSEF = \frac{I_{SERS}/N_{surf}}{I_{RS}/N_{Vol}} \tag{4}$$

Where $N_{Vol} = c_{RS}V$ is the average number of molecules in the scattering volume, V for the Raman (non SERS) measurement, and N_{Surf} is the average number of adsorbed molecules in the same scattering volume for the SERS experiments. Drawbacks posed by this definition

are: First, it requires additional constraints to make it more rigorous, in particular terms of which molecules exactly should be counted in N_{surf}. Secondly, the notion of scattering is nor rigorous in many cases and the exact metallic surface area is not easily measured; the final enhancement factor will depend on how these are estimated. Strongly related to this problem is the fact that the excitation intensity, even the most ideal of situations, is usually not uniform across the scattering volume.

Because of these, this definition is not rigorous enough and could lead to artificial variations by as much as 2 orders of magnitude for the measured EF on a the SERS substrate. In an attempt to overcome this, the SSEF can be defined as:

$$SSEF = \frac{1}{A_M} \int_{A_M} OASMEF(r)\, dS \tag{5}$$

Where A_M represents the surface area of the metallic substrate. This last expression can be rewritten as :

$$SSEF = \{OASMEF\} = \{[SMEF]\} \tag{6}$$

Where $\{[SMEF]\}$ is the spatial-and-allowed-orientation-averaged single molecules EF.This definition is strictly rigorous and well suited to theorethical predictions. This enhancement factor has been used for 2D planar SERS substrates [9,12].

3. The Analytical Enhancement Factor (AEF).

The definitions for the SMEF and SSEF have attempted to emphasize the intrinsic characteristics of the substrates and are not always straightforward to relate to experimental results. For many applications, however, one is mostly concerned with knowing how much more signal can be expected from SERS as compared to normal Raman under given

experimental conditions. To address this problem, another definition for the enhancement factor is given:

$$AEF = \frac{I_{SERS}/N_{SERS}}{I_{bulk}/N_{bulk}} \quad (7)$$

An analyte solution with an N_{bulk} concentration, produces a Raman signal I_{bulk} under non SERS conditions. Under identical experimental conditions (laser wavelength, laser power, microscope objective, spectrometer, and so on), and for the same preparation conditions, the same analyte on a SERS substrate, with possibly different concentration N_{SERS}, now gives an I_{SERS} signal. The Analytical Enhancement Factor (AEF) is useful for specific practical]]applications, and tends to depend strongly on many factors, in particular, on the adsorption properties and surface coverage of the probe; in fact N_{SERS} does not characterize well the number of adsorbed molecules. The AEF in fact ignores that SERS is a type of surface spectroscopy, which means that only the adsorbed molecules contribute to the signal and that the effect is distance dependent. The AEF represents a simple figure for the SERS EF, whose measurement is easily reproducible, and from its definition it is also clear that the AEF is particularly suited to the case of SERS active liquids, that is, colloidal solutions [12].

The enhancement factor used to assess the SERS activity of gold colloids is the Analytical Enhancement Factor (AEF),eq. 7, which is fairly intuitive and particularly relevant for analytical chemistry applications.

This definition, although useful for specific practical applications tends to strongly depend on many factors, in particular, on the adsorption properties and surface converge (monolayer vs multilayer) of the probe; N_{SERS} does not fully characterize the number of adsorbed molecules. It

is also strongly dependent upon the sample preparation procedure for 2D planar substrates (for example, the ones prepared by spin-coating, dipping or drying).

It is normally assumed that submonolayer coverage is ensured, the AEF represents a simple figure for SERS EF, whose measurement is easily reproducible [8].

In SERS it is important to investigate how the analytes interact with metal nanoparticles. Dyes such as rhodamines (B OR 6G,commonly) [13,14] and crystal violet [15] have been already been detected with the aid of gold nanoparticles, yielding good SERS signals, as well as Methylene Blue using plant-synthesized gold nanoparticles [16], and rosebengal by using citrate reduced gold colloids [17]. SERS experiments using heparin-based gold nanoparticles have not been reported so far.

3.2 Glycosaminoglycans and their interactions with chosen analytes.

3.2.1 Interaction with proteins.

Strong ionic interactions are expected between GAGs and proteins. Clusters of positively charged amino acids in proteins form ion pairs with spatially defined negatively charged sulfate or carboxylate groups on heparin chains. Glycosaminoglycans interact with residues that are prominently exposed on the surface of proteins. The main contribution to binding affinity comes from ionic interactions between the highly acidic sulfate groups and the basic side chains of arginine, lysine and to a lesser extent, histidine [18]. The relative strength of heparin binding by basic amino acid residues has been compared and arginine has been shown to bind 2.5 times more tightly than lysine. The guanidino group in arginine forms more stable hydrogen bonds as well as stronger electrostatic interactions with sulfate groups. The ratio of these two residues is said to define, in part, the affinity of a binding site in a protein for GAGs [17].

The interactions of GAGs with proteins also involve a variety of different types of interactions, including Van der Waals forces, hydrogen bonds and hydrophobic interactions with the

carbohydrate backbone. It has also been observed that heparin-binding domains contain amino acids such as asparagine and glutamine which are capable of hydrogen bonding. The affinity of heparin-binding proteins for heparin was also enhanced due to the presence of polar residues with smaller side chains like serine and glycine. These residues provide minimal steric constraints and good flexibility for the interaction with GAGs [19].

The main contribution to binding affinity comes from ionic interactions between the highly acidic sulphate groups and the basic side chains of arginine, lysine and, to a lesser extent, histidine. The relative strength of heparin binding by basic amino acid residues has been compared and arginine has been shown to bind 2.5 times more tightly than lysine. The interactions of GAGs with proteins also involve a variety of different types of interactions, including van der Waals (VDW) forces, hydrogen bonds and hydrophobic interactions with the carbohydrate backbone. It has also been observed that heparin-binding domains contain amino acids such as asparagine and glutamine which are capable of hydrogen bonding. Hydrophobic interactions can also play an important role in heparin-protein interactions: For example, phenylalanine aromatic residues which lie near basic amino acids in the heparin binding domain, make direct contact with the pentasaccharide responsible for heparin´s anticoagulation properties [20]. The Bovine Serum Albumin main aminoacid components are: alanine, phenylalanine, lysine, proline, threonine, cysteine, glycine, leucine, glutamine, valine, aspartic acid, histidine, methionine, arginine, tryptophan, glutamic acid, asparagine, serine, tyrosine and isoleucine.

3.2.2 Interaction with dyes.

There are only studies which focus on glycosaminoglycans interactions with basic dyes (positively charged). Because of their polyanionic nature, glycosaminoglycans interact with a number of basic dyes: alcian blue, methylene blue, ruthenium red, acridine orange ,among others.

The negative electrical field of the GAG attracts the positively charged basic dyes and cations forming a complex with basic dyes [21].

3.3 Raman spectra acquisition.

The Raman experiments were performed using a Renishaw InVia Raman microscope system. Its block diagram is shown in figure 3.1.

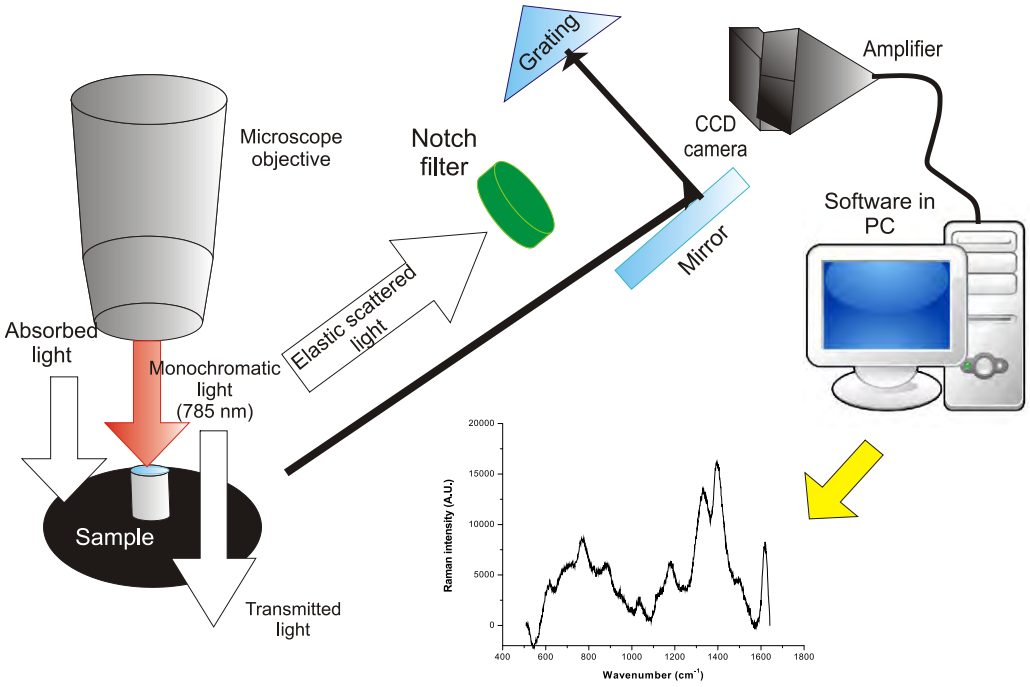

Figure 3.1 Micro Raman system block diagram.

The system comprises the common elements to a Raman microscope system, that is, laser sources, notch filters, mirrors, gratings, a CCD camera, an amplifier and microscope objectives.

The specific parameters for Raman spectra acquisition were the following: 10 s integration time, 20 acquisitions, 3 mW power (785 nm laser line) and usage of the 20X objective.

All SERS measurements were performed in aqueous solutions. Reference samples containing analytes at 1 mM were prepared in aqueous solution: rosebengal (RB, Sigma-Aldrich), methylene blue (MB, Industrial KEM, Mexico) and neutral red (NR, Hycel de 231 Mexico, SA de CV) and

bovine serum albumin (BSA, Alfa-Aessar) and HIV envelope protein (GP120), fragment 421-438 (Sigma-Aldrich). Deionized water was used to prepare them. All reactants were used as received.

The SERS samples were prepared as follows:

A total 500 µL solution is prepared by mixing the gold colloids and the analyte at different ratios to reach different analyte concentrations. Samples are left for incubation for 8 hours.

First, the experiments with heat-synthesized heparin gold nanoparticles and dyes are described; then the experiments using UV- synthesized heparin gold nanoparticles, these are split in two parts: the first one using methylene blue, rosebengal and neutral red at 1.997µM using reactive-grade heparin and pharmaceutical-grade heparin colloids and secondly, experiments for detection limits were carried out with reactive-grade gold nanoparticles and variable analyte concentrations (1 µM, 1 nM, 1 pM, 1 fM, 1 aM and 1 zM) of dyes and proteins.

All measurements were performed by micropipetting a volume of the prepared solution into a stainless steel cylindrical container (Length= 9 mm, radius=7 mm). The container was placed under the microscope objective (20X), then the solution surface was measured to acquire spectra. The reference solution (without nanoparticles) for both, dyes and proteins is 1 mM.

The presented graphs show the average taken from spectra at different points (4 spectra were taken over 6 points on the SERS solution surface).

3.3.1 Dyes used for surface enhanced Raman spectroscopy.

For the initial assessment of the nanoparticles Raman activity, three dyes were chosen as analytes: methylene blue (+), rosebengal (-) and neutral red (+-). The choice was made according to the charge each one of them possesses and to the fact that, in general, dyes are used as probe molecules in SERS, except for neutral red, which is being SERS-analyzed for the first time.

Basic dyes are cationic. This means that the dye molecule has a positive charge; and that they are attracted by proteins and nucleic acids in cells and they penetrate them making it easier for them to have toxic or carcinogenic effects, even at smaller concentrations. It has been found, for example, that methylene blue intercalates into DNA, giving it a special ability to cause damage [22].

Acid dyes possess a negative charge (anionic), these dyes are non-caustic, they are in some cases non toxic, and in others their toxicity ranges from moderate to low depending on the number of acid groups in their structure and are named for the mild acid (such as vinegar) used in dying and for the types of bond they form to the fiber in the textile industry [25].

Neutral dyes show low hazard, in general [26].

3.3.2 Proteins used for SERS.

To prove that nanoparticles are adequate for other applications of more biological interest, bovine serum albumin (BSA) and GP120 were used, too.

They were chosen as probe molecules as examples of typical proteins.

3.4 Surface enhanced Raman spectroscopy experiments.

3.4.1 Surface enhanced Raman spectroscopy of samples synthesized with heat (38°C).

These samples were synthesized as mentioned in chapter 1 at 38°C for seven hours and were centrifuged 4 times at 13,500 rpm and redispersed in water.

Sample labelling:

PGHEPAU38: Gold colloid synthesized at 38°C using pharmaceutical-grade heparin.

RGHEPWAU38: Gold colloid synthesized at 38°C using reactive-grade heparin dissolved in water.

RGHEPBAWAU38: Gold colloid synthesized at 38°C using reactive-grade heparin dissolved in benzyl-alcohol/water.

Raman spectra generated by nanoparticles synthesized with heat are presented to compare the obtained signals with the ones obtained from their UV-irradiated counterparts.

Figures 3.2, 3.3 and 3.4 show the SERS spectra obtained from methylene blue, rosebengal and neutral red in aqueous solution. Black curves indicate the reference solution (normal Raman), green, gray and pink curves are the SERS curves given by the pharmaceutical-grade heparin, reactive-grade heparin in water and reactive-grade heparin in water/benzyl alcohol gold nanoparticles syntheses, respectively.

In figure 3.2 the SERS signals shown by all syntheses (prepared at 38°C) for methylene blue is shown and the colloidal gold solutions that produces the best enhancement is the one synthesized with reactive-grade heparin in benzyl alcohol.

In the case of rosebengal, in figure 3.3 the same thing happens as with methylene blue, the solution that shows peaks is the synthesis prepared with reactive-grade heparin dissolved in benzyl-alcohol/water; the other two syntheses basically show no enhancement. Such results are shown in figure 3.3.

When neutral red is used as the SERS probe with these syntheses, it is observed that the reference solution has a big fluorescence background, and when the dye is mixed with each one of the synthesis, such background is suppressed but the peaks that are typical in the probe are not completely visible.

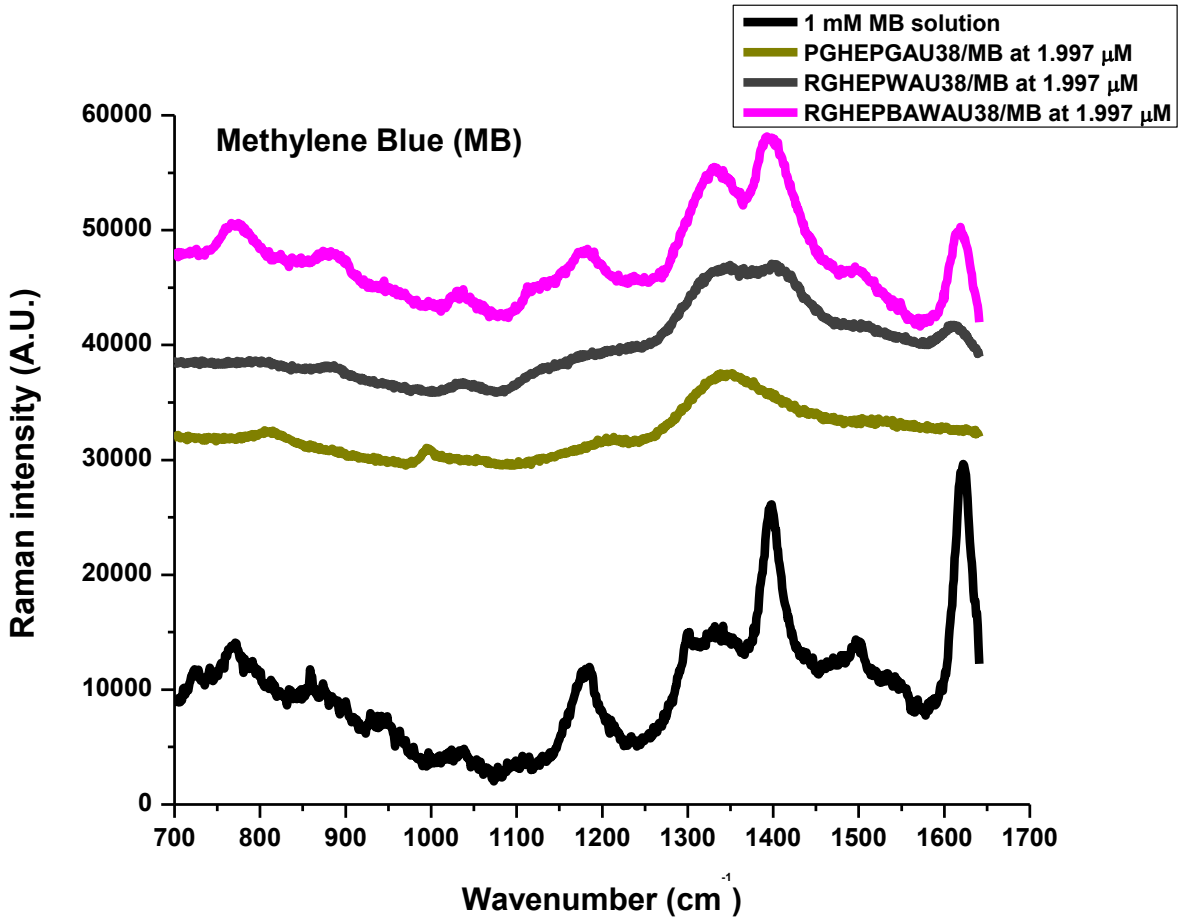

Figure 3.2 Normal Raman(1 mM reference solution, black line) and SERS spectra of methylene blue using the heat-synthesized (38°C) nanoparticles samples.

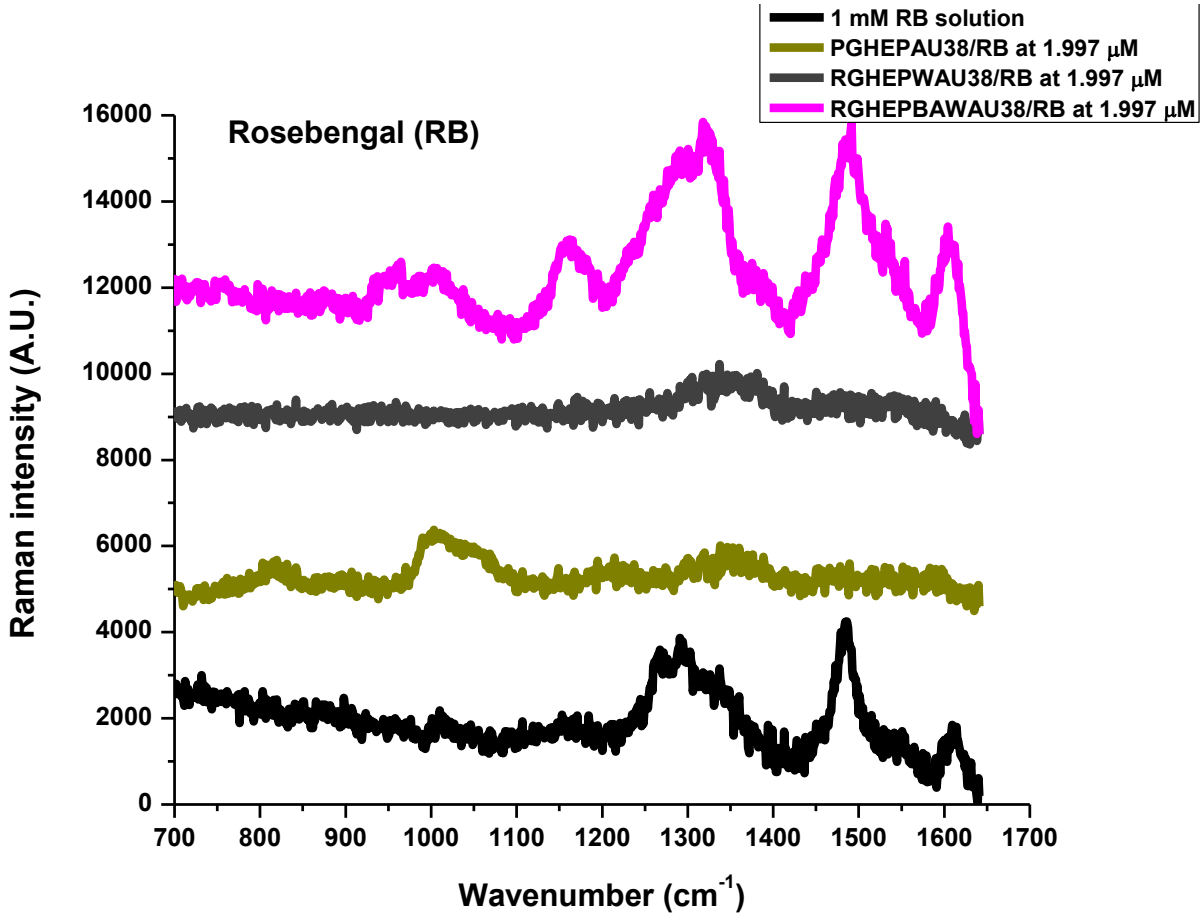

Figure 3.3 Normal Raman (1 mM reference solution, black line) and SERS spectra of rosebengal using the heat-synthesized (38 °C) nanoparticle samples.

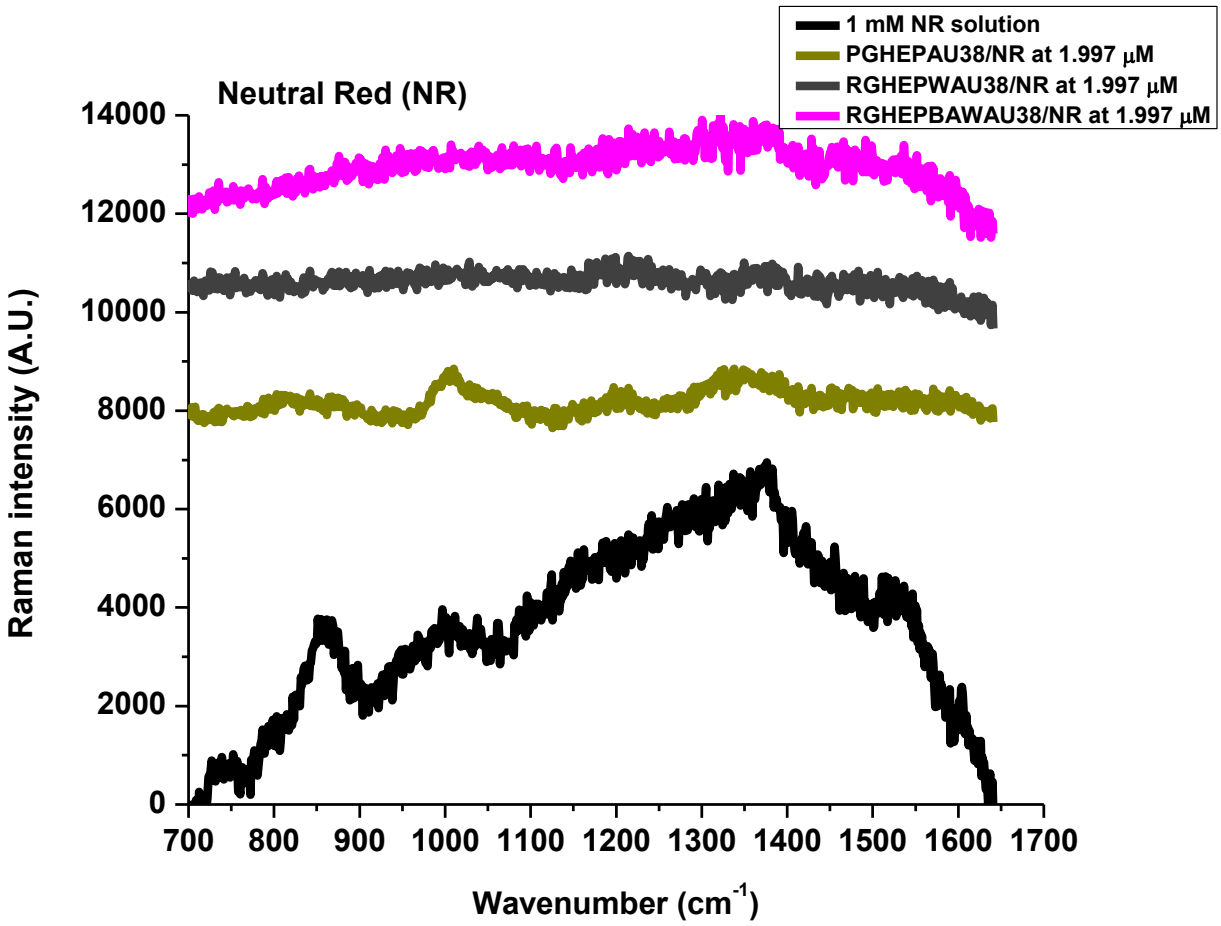

Figure 3.4 Normal Raman (1 mM reference solution, black line) and SERS spectra of neutral red using heat-synthesized nanoparticle samples.

The results obtained in these experiments prove that using temperature (38°C) to synthesize gold nanoparticles is not adequate to generate Raman-active nanoparticles that yield enhanced signals, this is probably due to the fact that nanoparticle formation and functionalization are not attained adequately not permitting the attachment of analytes to the nanoparticle surface to generate a SERS signal. In figure 3.2 the normal spectra for Methylene Blue and the SERS spectra from the three heat-synthesized samples are shown, all the three samples depict some peaks typical to Methylene Blue, but they are not enhanced, this is, their intensity is not higher than the peaks that belong to the reference solution, this is also proved by the enhancement factors in table 1 .The factors were not calculated for Neutral Red because the peaks could not be isolated due to their

weak intensity; in the case of Methylene Blue and Rosebengal they were only calculated for the peaks that show the highest intensity.

Table 1 . Enhancement factors for heat-synthesized samples.

Sample	Dye	Enhancement Factor
PGHEPAU38	Methylene Blue	-
RGHEPWAU38	Methylene Blue	3.8
RGHEPBAWAU38	Methylene Blue	50
PGHEPAU38	Rosebengal	-
RGHEPWAU38	Rosebengal	-
RGHEPBAWAU38	Rosebengal	1213
PGHEPAU38	Neutral Red	-
RGHEPWAU38	Neutral Red	-
RGHEPBAWAU38	Neutral Red	-

3.4.2 Surface enhanced Raman spectroscopy of dyes using UV-irradiation synthesized samples.

Gold nanoparticles synthesized with water as solvent.

The sample from which SERS spectra has been used for this experiment is labelled as RGHEPWAU, which is a gold nanoparticle solution prepared using reactive-grade heparin in water.

Figures 3.4, 3.5 and 3.6 show the normal Raman signal of Methylene Blue, Rosebengal and Neutral Red (black lines) and the their SERS spectra (gray lines). These samples did not depict any Raman enhancement. This could be attributed to the heparin molecules being surrounded by

water (as mentioned in chapter 1) neither letting heparin promote gold reduction properly nor letting nanoparticle growth occur accordingly .

The SERS solution used for Methylene Blue enhancement shows (figure 3.5) that the reference solution has the typical peaks for the dye. Nevertheless, the SERS solution does not show any kind of enhancement, the spectrum is almost flat. The same tendency is followed in the Neutral Red and Rosebengal SERS spectra.

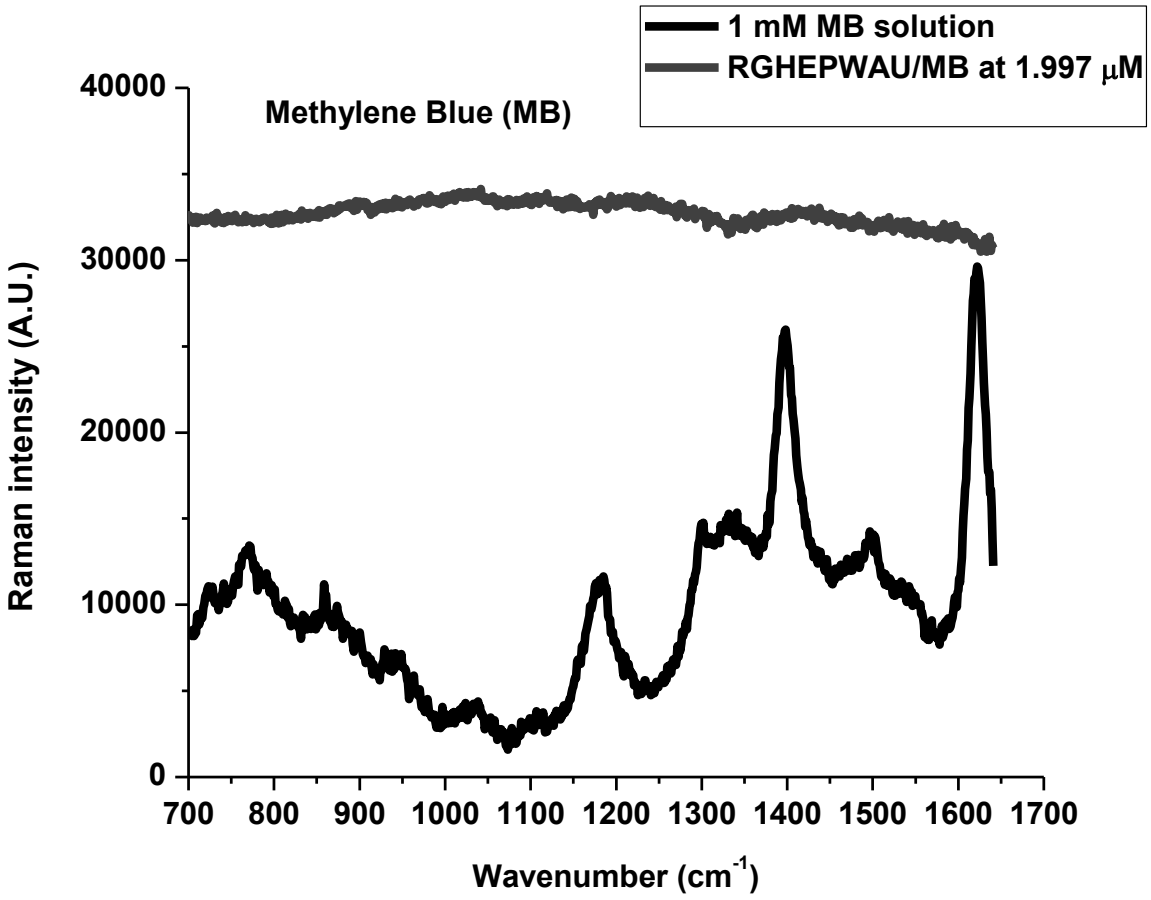

Figure 3.4 Normal and SERS spectra of methylene blue using gold nanoparticles synthesized with reactive-grade heparin dissolved in water.

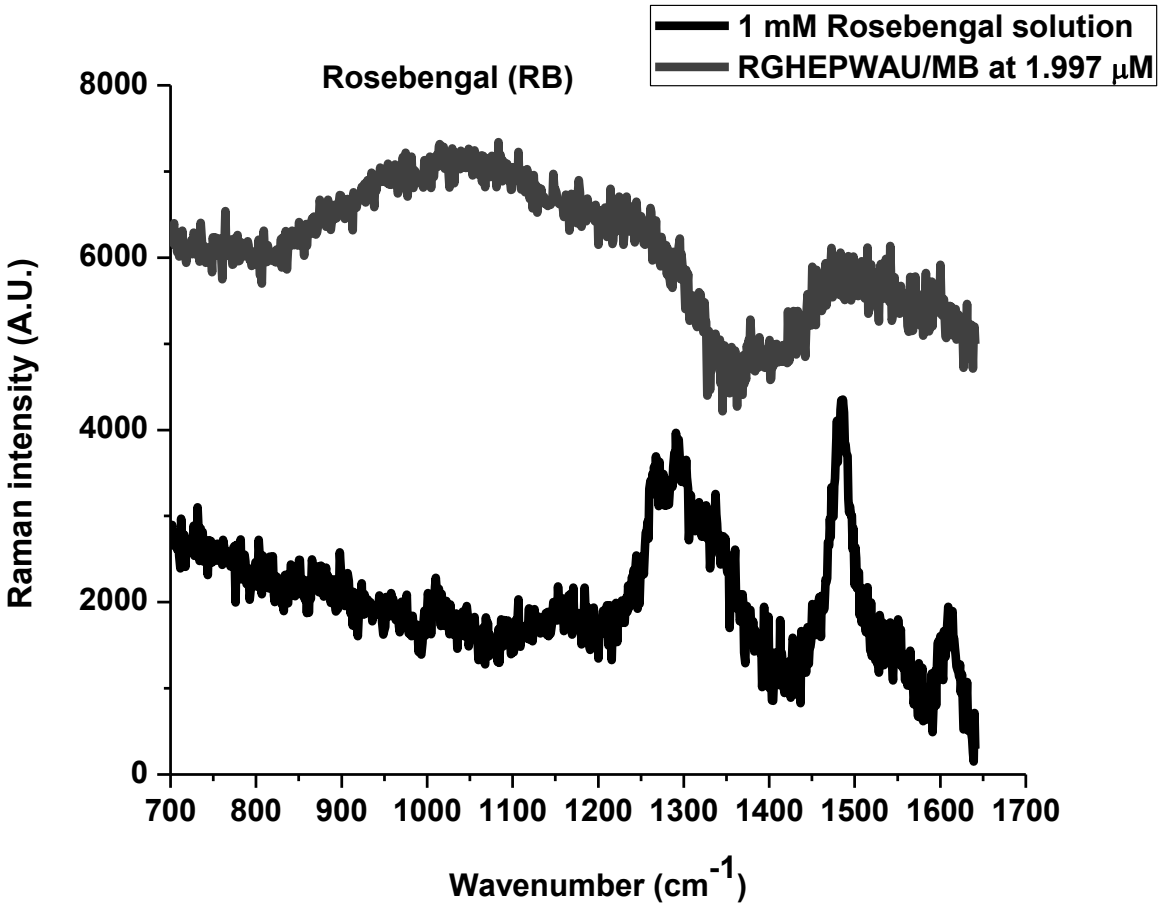

Figure 3.5 Normal and SERS spectra of rosebengal using gold nanoparticles synthesized with reactive-grade heparin dissolved in water.

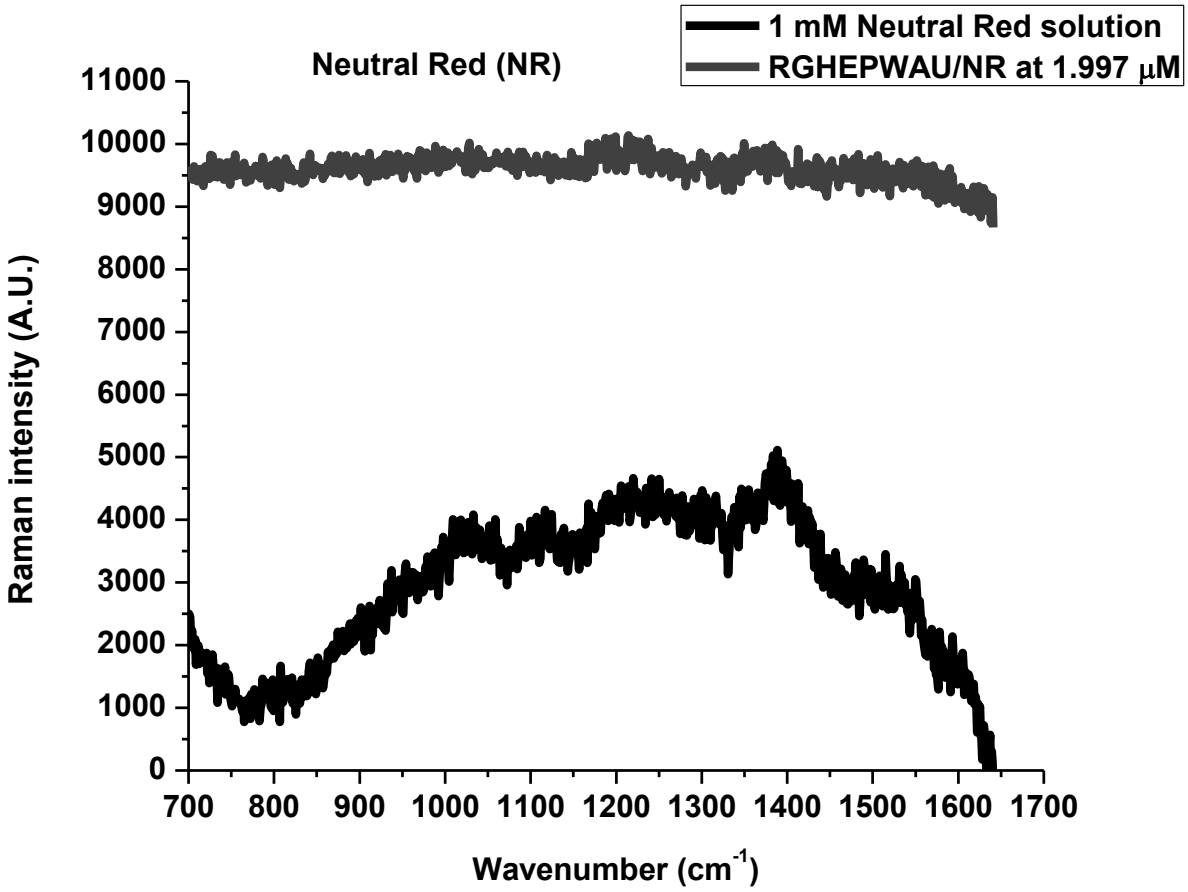

Figure 3.6 Normal and SERS spectra of neutral red using gold nanoparticles with reactive-grade heparin dissolved in water.

Gold nanoparticles synthesized with benzyl alcohol/water as solvent.

As for the synthesis elaborated in pharmaceutical-grade heparin and reactive-grade heparin dissolved in benzyl alcohol/water, there are substantial differences. First, it has to be mentioned that pharmaceutical-grade heparin´s excipient is benzyl-alcohol/water as determined in Chapter 1, and the same solvent was prepared for the reactive-grade heparin to be dissolved in it (1:106). The SERS signals obtained with these samples are shown next, the best enhancement was observed with the reactive-grade heparin-based nanoparticles, weaker SERS signals were observed with the products synthesized with pharmaceutical-grade heparin.

The Raman spectrum from the reference solution as well as the corresponding SERS spectra (with an analyte concentration of 1.997 μM) are shown in figures 3.7 to 3.9 and the corresponding peak assignments in tables from 1 to 3.

The SERS spectra show that reactive-grade heparin prepared nanoparticles (RGHep lines) lead to better SERS signals than the pharmaceutical-grade heparin products (PhGHep lines). The best interactions were obtained from the oppositely charged one (Methylene Blue) while not being the case with same-charged (Rosebengal) and neutral (Neutral Red) molecules. Even though some enhancement is observed which indicates that nanoparticles have made some contact with the metal surface, it has not been good enough to quench such effect [9]; this might be due to the molecule orientation or unbounds parts of it.

In the Methylene Blue SERS spectra, the peaks that result from the most enhanced signals are at 1386 (C-H in plane ring deformation) cm and 1607 cm^{-1} (C-C- ring stretching) (PhGHep AuNPs) and at 1393 (C-H in plane ring deformation) and 1619 cm^{-1}(C-C- ring stretching) (RGHep AuNPs). As for Rosebengal, such peaks are located at 1386 (C-H in-plane ring deformation) and 1607 cm^{-1} (C-C ring stretching) (PhGep AuNPs) and at 1399 (C-H in-plane ring deformation) and 1619 cm^{-1} (RGHep AuNPs). Finally, for Neutral Red, although signal enhancement is not very intense, the strongest interactions are indicated by the peaks at 1336 (PGHep AuNPs) and 1374 cm^{-1}(C-C ring stretching) (RGHep AuNPs). According to the assignment in the case of Methylene Blue, the aromatic rings interact the most with the metal surface, being the same for Rosebengal. Also, the chloride ions belonging to Rosebengal promote some adhesion to the metallic surface by the displacement of ions they induce in addition to the fact that they might also induce some aggregation in the colloid-dye system [25,28], which contributes to the generation of the Rosebengal SERS signal. Lastly, for Neutral Red, the most acute peak corresponds to the C-N stretching vibration and considering that it possesses a NH_2 group

attached to an aromatic ring and is positively charged, then it can be concluded that is the channel through which an interaction, though weak is established.

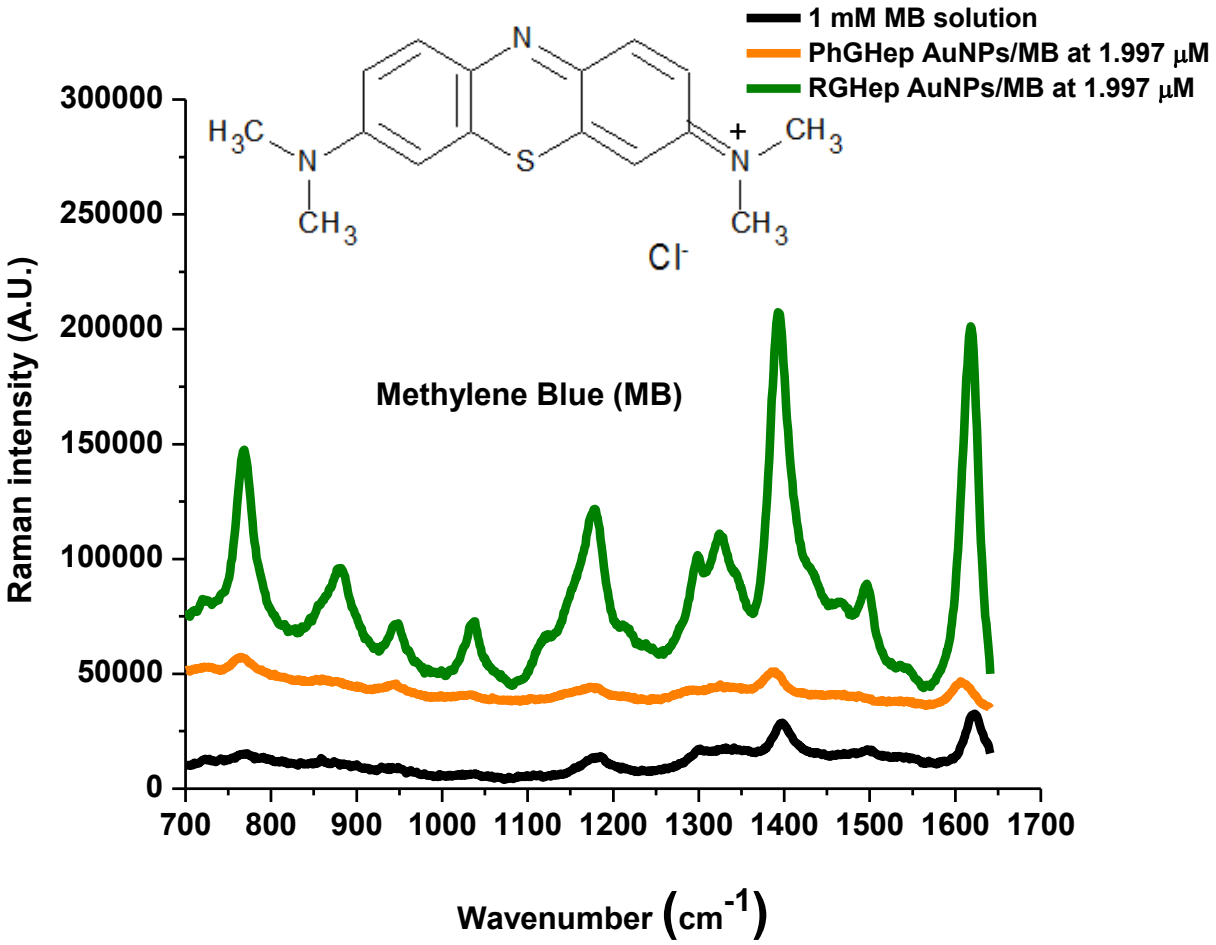

Figure 3.7 Normal (black line) and SERS (orange and green lines) spectra of methylene blue [25].

Table 2. Methylene Blue peak assignment.

Reported Powder Peaks (cm^{-1}) [26]	1 mM Aqueous Solution (cm^{-1})	PG-Heparin AuNPs (cm^{-1})	RG-Heparin AuNPs (cm^{-1})	Band Assignment
1067 (w)	1038 (w)	1033 (w)	1037 (m)	C-H in-plane bending
1121 (w)	-	-	1122 (w)	C-H out-of-plane-bending
1181 (m)	1185 (w)	1181(w)	1178 (m)	C-N stretching
1272 (w)	1299 (w)	1293 (w)	1299 (m)	-
1396 (m)	1393 (m)	1386 (m)	1393 (s)	C-H in-plane ring deformation
1441 (w)	-	-	1464 (w)	C-N asymmetric stretching
1544 (w)	1541 (w)	1537 (w)	1541 (w)	C-C ring stretching
1618 (s)	1620 (m)	1607 (m)	1619 (s)	C-C ring stretching

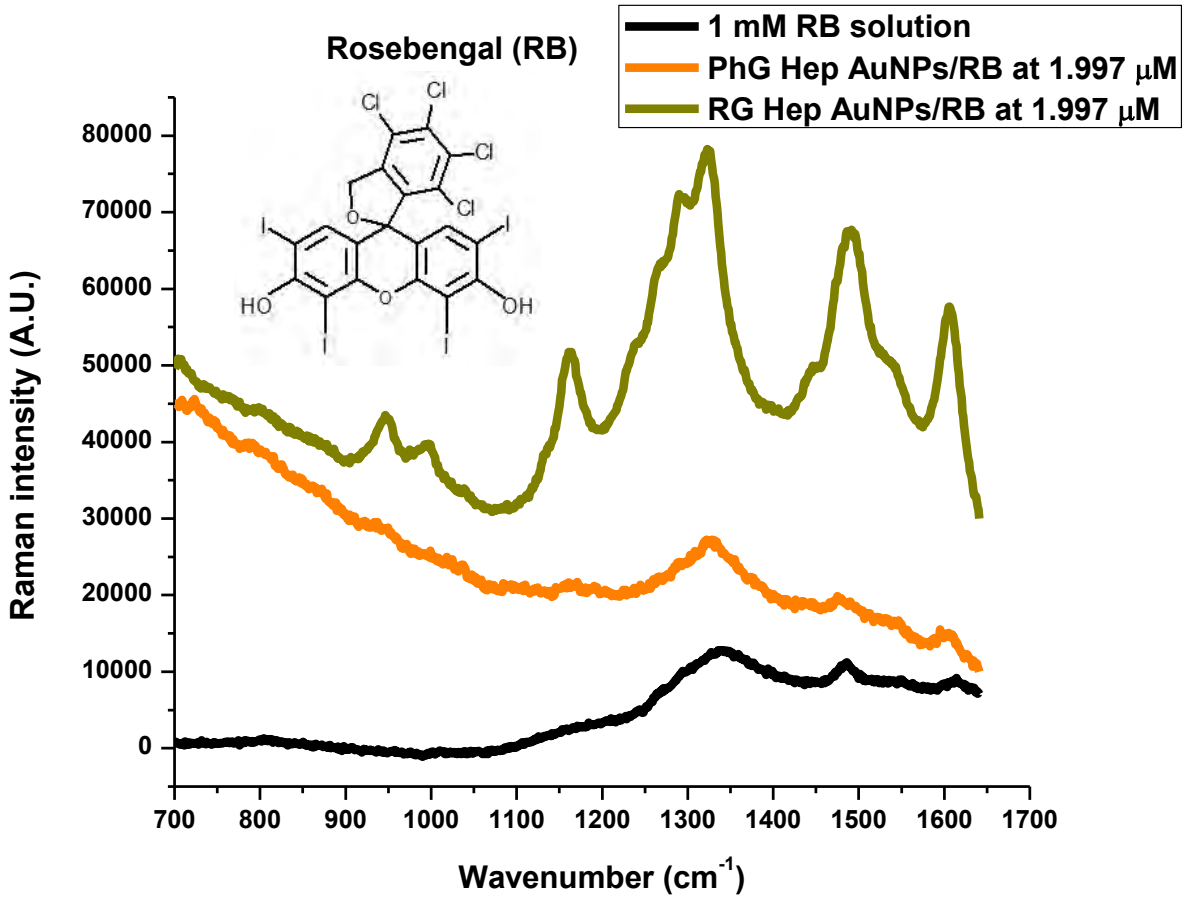

Figure 3.8 Normal (black line) and SERS spectra (orange and green lines) of rosebengal [25].

Table 3. Rosebengal peak assignment.

Reported Powder Peaks (cm^{-1}) [30]	1 mM Aqueous Solution (cm^{-1})	PG-Heparin AuNPs (cm^{-1})	RG-Heparin AuNPs (cm^{-1})	Band Assignment
1067 (w)	1038 (w)	1033 (w)	1037 (m)	C-H in-plane bending
1121 (w)	-	-	1122 (w)	C-H out-of-plane-bending
1181 (m)	1185 (w)	1181(w)	1178 (m)	C-N stretching
1272 (w)	1299 (w)	1293 (w)	1299 (m)	-
1396 (m)	1393 (m)	1386 (m)	1393 (s)	C-H in-plane ring deformation
1441 (w)	-	-	1464 (w)	C-N asymmetric stretching
1544 (w)	1541 (w)	1537 (w)	1541 (w)	C-C ring stretching
1618 (s)	1620 (m)	1607 (m)	1619 (s)	C-C ring stretching

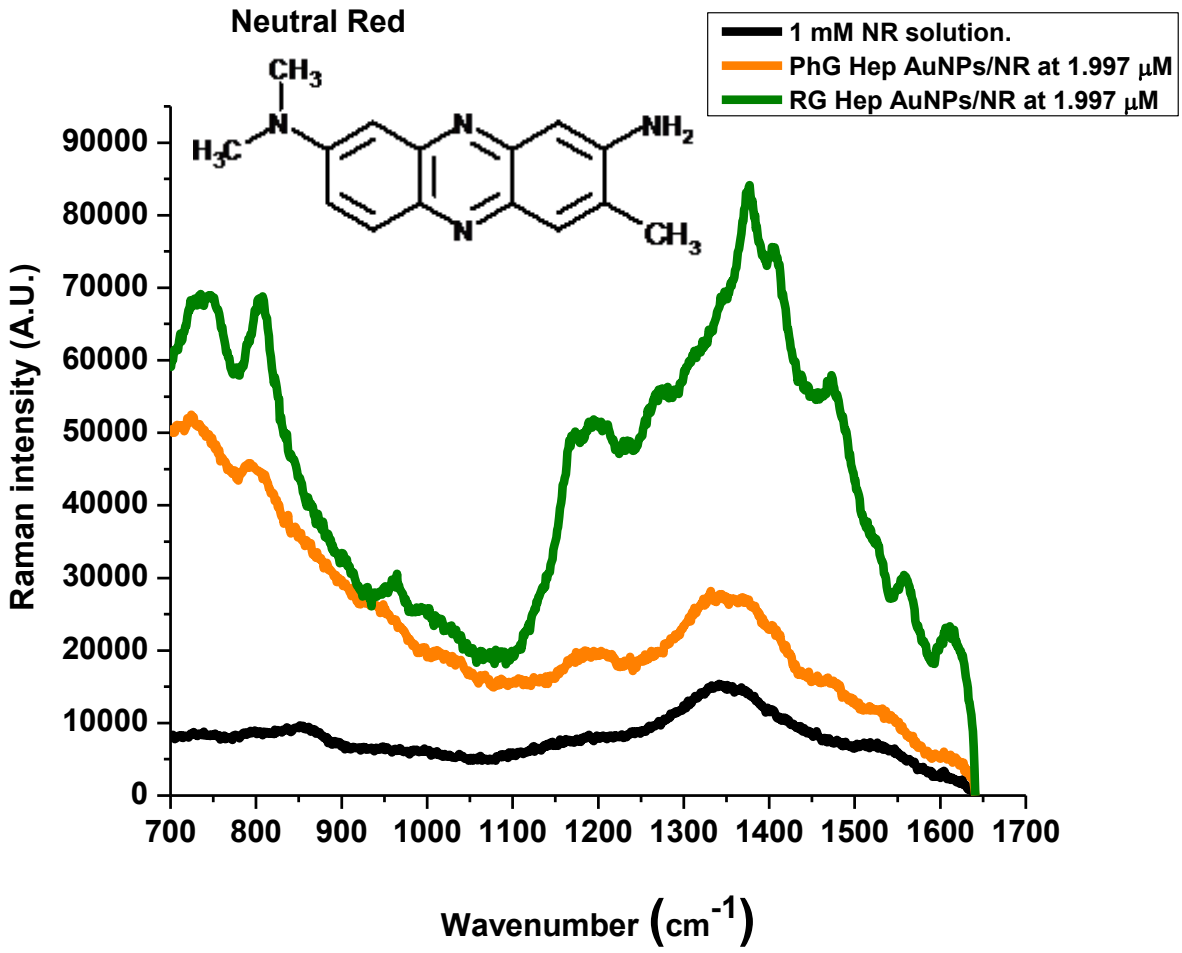

Figure 3.9 Normal (black line) and SERS (orange and green lines) spectra of neutral red [25].

Table 4. Neutral Red peak assignment.

1 mM Solution (cm^{-1})	PG Heparin Au NPs (cm^{-1})	RG Heparin Au NPs (cm^{-1})	Band Assignment [29]
1605 (w)	1618 (w)	1609 (m)	Scissor vibration of primary amines
1341 (vw)	1336 (w)	1374 (m)	C-N stretching vibration.
1370 (w)	1370 (w)	1403 (w)	C-N stretching vibration
1459 (vw)	1470 (w)	1472 (w)	CH_3 deformation vibration

Pharmaceutical-grade heparin AuNPs show a weak SERS signal at the concentrations used contrary to the reactive-grade heparin AuNPs, this could be due to the fact that reactive-grade heparin is more sulphated.

Detection limits.

Experiments were performed as already mentioned in section 3.2. The results are displayed from figures 3.10 to 3.12. Also, the only samples taken for analysis were the gold nanoparticles synthesized with reactive-grade heparin because they were the nanoparticles that showed the best interactions with analytes. The peak assignments in the previous section will be taken as a reference for these experiments.

Figure 3.10 shows the spectra obtained when measuring SERS for Methylene Blue, which is positively charged, the concentrations used are listed (color lines) as well as the reference solution (black line).

It can be seen that at 1 μM, peaks are sharp and noticeable, but when the Methylene Blue concentration begins to decrease, the SERS spectrum changes, the peak at 1393 cm^{-1} (the most intense in the SERS spectra) which corresponds to the C-H in plane ring deformation loses intensity. The one at 1619 cm^{-1}(C-C ring stretching) is sharp at 1 μM but then it starts broadening and blue shift. The rest of the peaks which are less intense continue to be medium and weak, but they are not so noticeable.

There are other peaks that do not have a specific assignment but they do appear in the SERS spectra as well, for example, at 1002 cm^{-1} which blue shifts and the one at 952 cm^{-1} in the SERS spectrum of Methylene Blue at 1 μM that disappears from the 1 nM concentration and below. Peaks at 1299 and 1329 cm^{-1} are acute in the 1 μM SERS spectrum but as the analyte concentration declines they get broad and almost overlap.

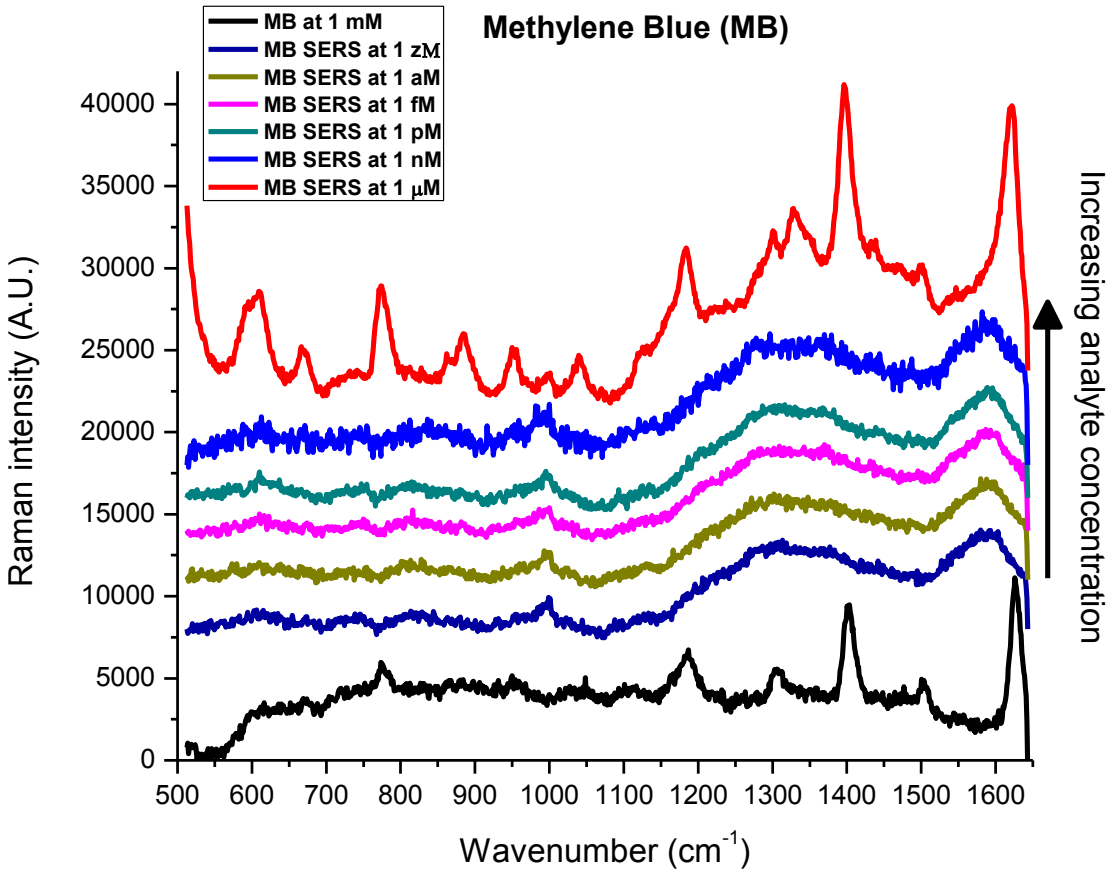

Figure 3.10 Normal and SERS spectra (at various concentrations) of methylene blue.

Rosebengal follows almost the same trend as Methylene Blue because as its concentration lowers, the peaks at 1489 (C=C asymmetric stretching in ring), 1172 (C-O and C-C stretching,C-H skeletal deformation) cm^{-1} basically dissapear. The rest of them diminish their intensities and tend to broaden or suffer blue-shifting. Intensities of Raman peaks go down as the Rosebengal concentration decreases.

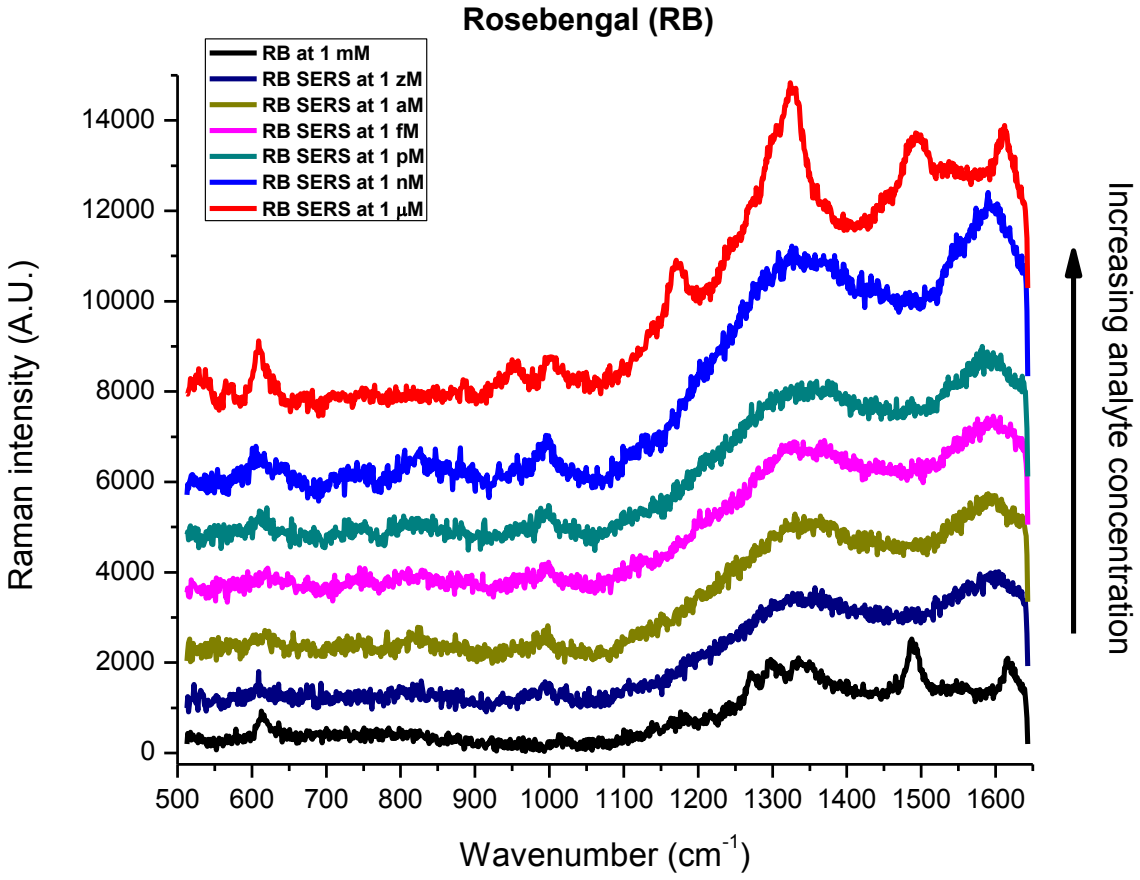

Figure 3.11 Normal and SERS spectra (at various concentrations) of rosebengal.

Neutral Red normal Raman spectrum depicts a broad background due to fluorescence. Its SERS spectra, on the other hand, do not show it. Even at the highest Neutral Red concentration, 1 µM, and the following one,1 nM, enhancement is still visible, but from 1 pM and below, SERS spectra do not vary much, there are no big differences among them. Also, the enhancement does not seem to be quite visible, the peaks at 1374 and 1609 cm^{-1} blue-shift but do not vary in intensity. Such peaks (without assignment) in all spectra from the three studied dyes may behave in such way due to the fact that the SERS signals intensities from analytes depend on adsorptivities and the solution concentrations and even when the Raman spectrum of water is weak [30], it hinders the SERS signals at very low concentrations [31].

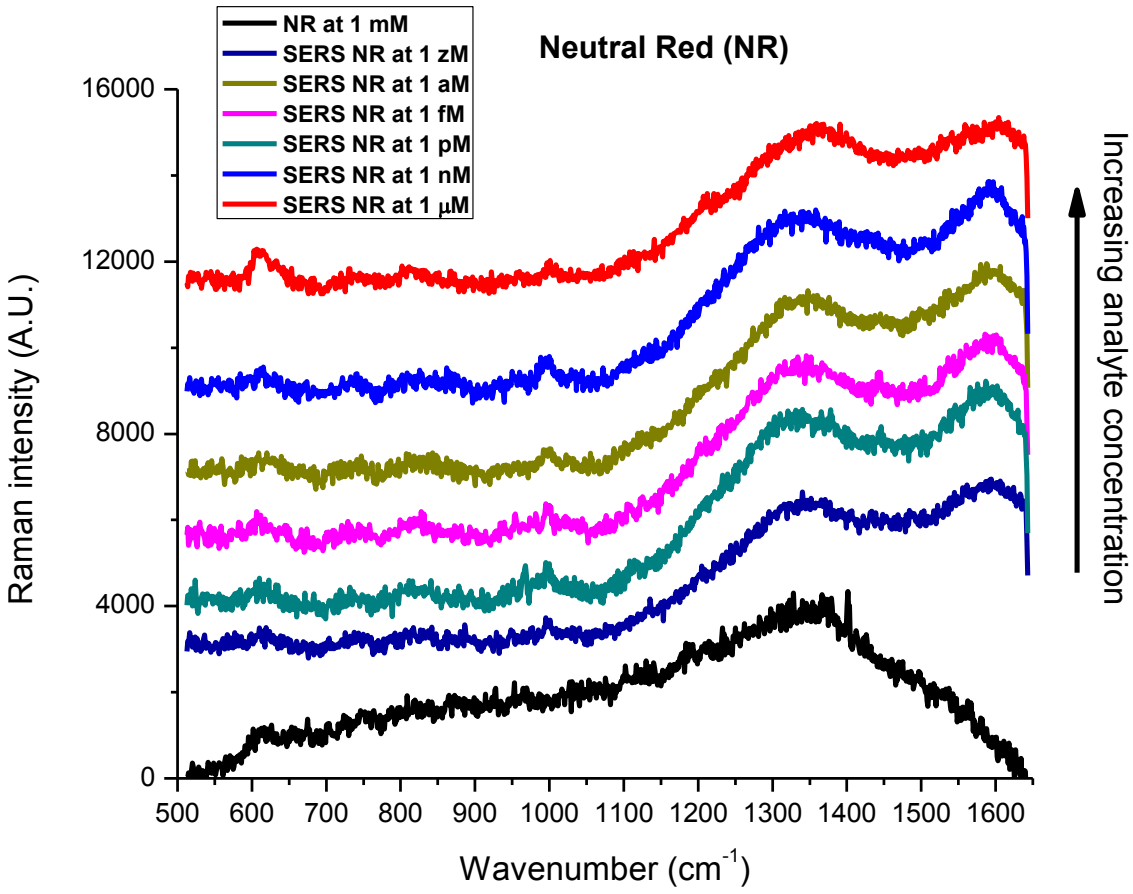

Figure 3.12 Normal and SERS spectra (at various concentrations) of Neutral Red.

In both cases, for Methylene Blue and Rosebengal, the peaks that are enhanced are related to the rings belonging to the dyes structures, this means that they are the groups most involved in the Raman signal enhancement and that they are closer to the nanoparticles surface. According to surface selection rules the strong intensities of the bands assigned to the rings, the in-plane deformation modes imply both the proximity of the rings plane to the gold surface and their strong interaction with the surface as well as the perpendicular orientation of the rings plane with respect to the nanoparticle surface [3].

The calculated enhancement factors, for the selected peaks that show enhancement are in table 4. They were calculated using the analytical enhancement factor formula (3).

The enhancements factors were calculated up to the micromolar concentration because these are the peaks that are the sharpest and show the best enhancement. Such calculations were carried out only for Methylene Blue and Rosebengal which showed the strongest interactions.

Table 5. Enhancement factors calculated for Methylene Blue and Rosebengal.

Analyte	Concentration	Enhancement factor
Methylene Blue	1.997 μM	8.6×10^5
	1 μM	1.6×10^4
Rosebengal	1.997 μM	3.7×10^5
	1 μM	2×10^4

The photochemical method proposed in this thesis work in order to get Raman active products has been justified because when acquiring Raman spectra using nanoparticles either synthesized with water as a solvent or just without UV-irradiation, the obtained results showed that either no peaks were observed or that they did not present improvement in Raman signal whatsoever, compared to their normal Raman spectra.

On the contrary, when using nanoparticles synthesized with UV light, SERS was observed with the only restriction that pharmaceutical-grade heparin based particles did not yield a good enhancement and reactive-grade heparin nanoparticles did, being them the chosen products to work with. Enhancement factors on the order of 10^5-10^6 were the highest obtained for Methylene Blue and Rosebengal in this work.

3.4.3 Surface enhanced Raman spectroscopy of proteins using UV-irradiation synthesized samples.

Bovine Serum Albumin normal Raman and their SERS spectra is shown in figures 3.13. The amino acids highlighted in red are the ones who have shown a good affinity when binding to heparin according to Hileman et al [19]. In the case of their SERS spectra, they did prove their interaction with the protein used.

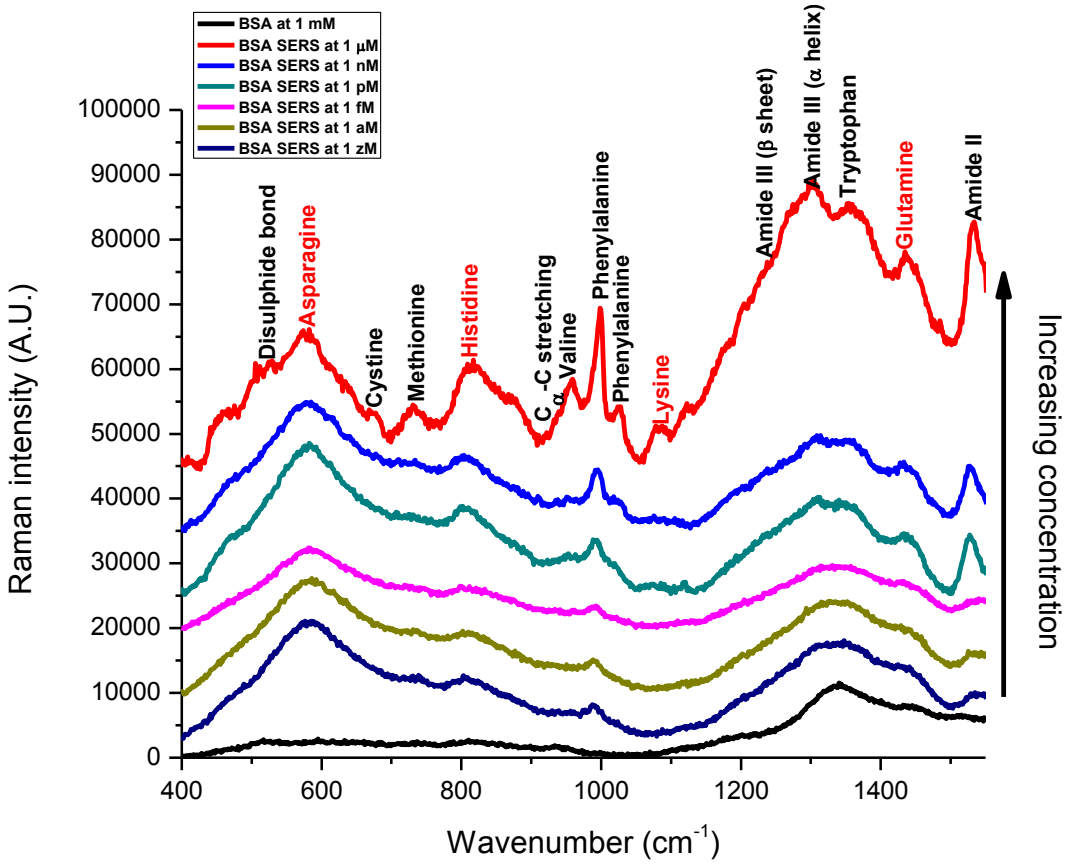

Figure 3.13 Normal and SERS spectra (at various concentrations) of Bovine Serum Albumin.

Unlike the interactions exhibited by dyes, BSA and GP120 still keep a little of their relevant peaks up to 1 pM concentration.From 1 zM and below, the spectra peaks begin to lose their characteristic shape and peaks intensity.

The enhancement factors obtained for BSA are indicated below, the peak chosen for calculations was the one corresponding to Phenylalanine at approximately 1000 cm^{-1}:

Table 6 .Enhancement factors calculated for Bovine Serum Albumin.

Concentration	Enhancement factor
1 µM	3.4×10^4
1 nM	9×10^3

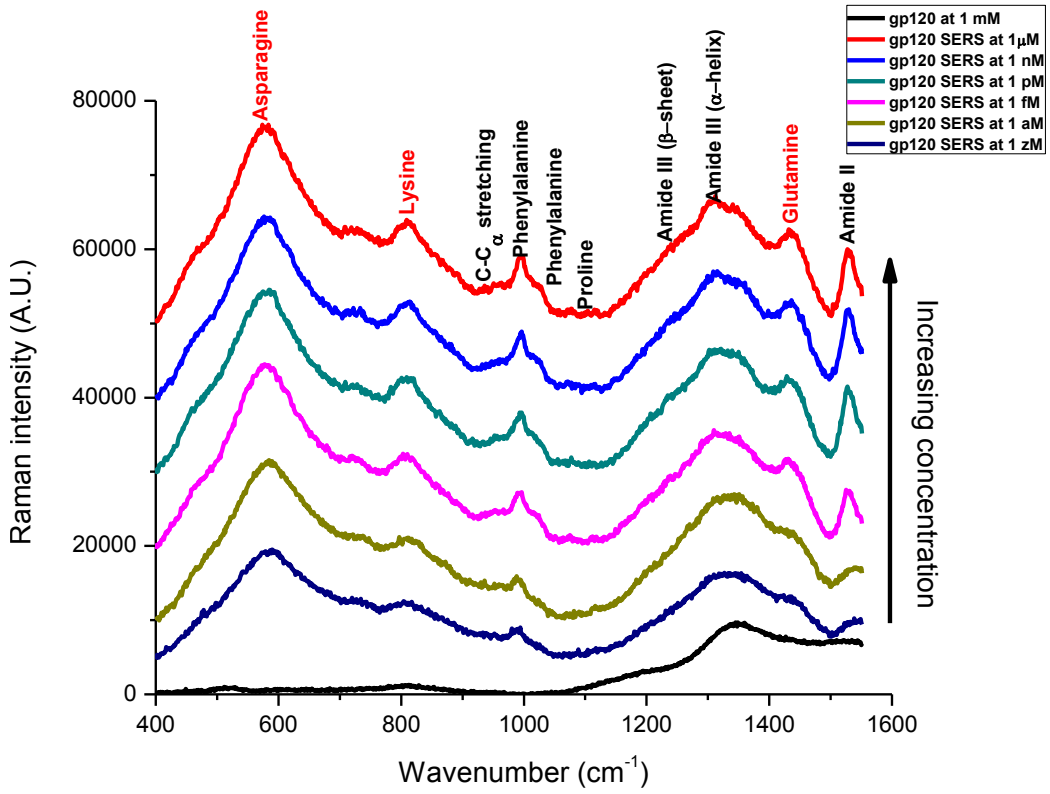

Figure 3.13 Normal and SERS spectra (at various concentrations) of GP120.

From the results obtained using proteins, it was proved that SERS phenomena can be observed and to assess that heparin-based nanoparticles can be used for more biological-oriented purposes given the advantage that heparin has a good affinity with proteins.

3.5. Heparin, dyes, proteins and gold colloid spectra.

The reactive-grade heparin and the reactive-grade heparin gold nanoparticles Raman spectra are shown along with the Methylene Blue (1.997 μM) SERS spectrum are shown in figure 3.15a. Heparin´s main peaks have already been assigned by Atha et al [32], specifically: In the range of 750-1100 cm^{-1}, which is the region of interest for heparin: the 1039 and 1055 cm^{-1} peaks belong to the S-O stretchings of the sulfate residues, in the case of this work, the are located at 1046 and 1060 cm^{-1}; 827 and 893 cm^{-1} are assigned to the C-H deformation of the glucosamine residues, in

this thesis they are at 820 and 895 cm^{-1} and finally, the 1000 cm^{-1} peak corresponding to the C-N stretching is located at 1004 cm^{-1} in this work. The Raman spectrum of the gold colloid shows that the heparin bands corresponding to the 1049 and 1060 cm^{-1} present but with very weak intensity and shifted, this is, the first one is located at 1029 cm^{-1} and the other one at 1067 cm^{-1} ; as for the 820 cm^{-1} band, it is absent in the colloid, this could be due to the existence of a direct interaction between sulphate groups and the glucosamine in heparin with the gold surface [3].

The gold colloid spectrum as well as the dyes´s are also shown for comparison in figure 3.15b, in it, the vertical lines indicate the main peaks already investigated for heparin and they are compared to the analytes´s peaks. From this figure, it is observed that heparin´s peaks do not hinder none of the dyes SERS spectrum, the intensity of the peaks that are related to sulphate groups (1049 and 1060 cm^{-1}) and the C-H deformation (895 cm^{-1}) of the glucosamine residue do demonstrate it.

In the case of the proteins, Bovine Serum Albumin (BSA) and GP120, other comparisons are made in figure 3.15c- BSA interacts with the colloids surface through heparin´s sulphate groups and the CH_3 groups of Valine [3], also the acute peak of Phenylalanine may interact with the nanoparticle surface via hydrophobic interactions [20], something similar happens to the GP120 protein, but in its case what is going on is that even though the same groups interact, the GP120 SERS signal is weaker, and according to the selection rule, this may be due to the protein being in an unfavorable position, this is not perpendicular to the nanoparticle surface [3,10,11] and farther away from it than in the Bovine Serum Albumin´s case.

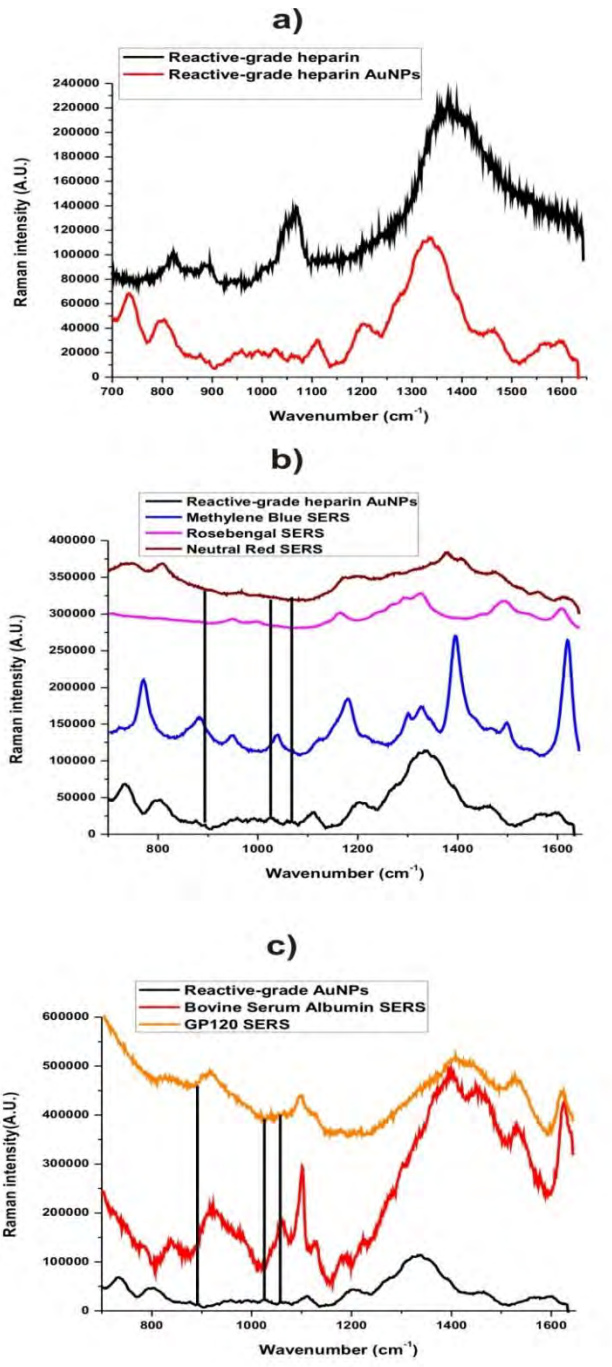

Figure 3.15a, b and c a) Raman spectra reactive-grade heparin and the reactive-grade heparin AuNPs, b)Raman spectrum of the reactice-grade heparin AuNPs and the probed dyes SERS spectra, c)Raman spectra of reactive-grade AuNPs and proteins.

3.5 Comparison with other SERS work.

Gold nanoparticles have been used for SERS purposes, in the case of methylene blue, its detection has not been carried out using gold nanorods and a 10 μM concentration obtaining enhancement factors between 10^4-10^5 according to the desposition angle of the arrays on a substrate [16].

For rosebengal, there is a study by Gabudean et al. [28], in which gold nanorods are synthesized by a seed-mediated growth protocol, and then they are used for SERS measurements and the enhancement factor calculated is $1.7x10^5$ for 10^{-6} M rosebengal concentrations versus $3.7x10^5$ for 1.997 μM and $2x10^4$ for 1 μM concentrations in this work.

As for Neutral Red, no SERS reports have been found so far.

When it comes to Bovine Serum Albumin, the work by Davida et al. [33] has reported 10^5 enhancement factors for 1 mM concentration. In this thesis work a 10^4 enhancement factor was found for 1 μM concentration.

As for the GP120 protein, there are no proper SERS studies for its detection, but protocols based on the identification of bio/chemical material composed of multi-component materials such as viruses, including bovine leukemia virus (BLV), respiratory syncytial virus (RSV) and HIV [].

All comparisons to published works, except for GP120 and neutral red are presented in figures 3.16a,b and c.

Reactive-grade heparin gold nanoparticles synthesized with UVA light are useful for surface enhanced Raman purposes, being this the first time this photochemical procedure is proposed, obtaining10^4- 10^5 enhancement factors for methylene blue, rosebengal and bovine serum

albumin, still they possess values which are in the acceptable ranges that have been reported so far for gold nanostructures It has also been demonstrated that and neutral red show less SERS signal enhancement.

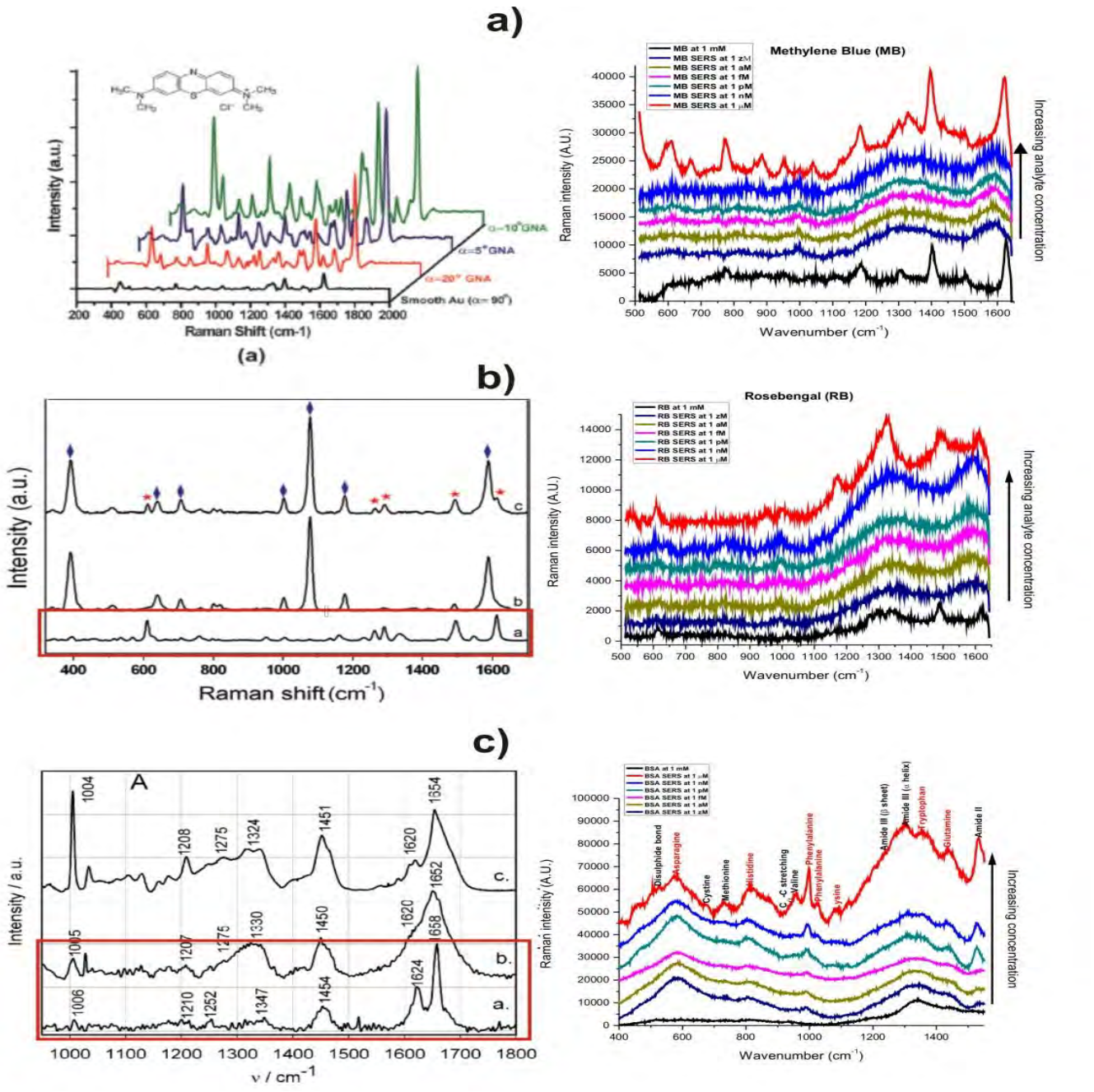

Figure 3.16a,b and c Comparison of published work on SERS [16,28,33] and this thesis work for a)Methylene Blue ,b)Rosebengal and c)Bovine Serum Albumin.

References.

[1] Introductory Raman Spectroscopy, R.L. Ferraro, Academic Press U.S.A. (1994).

[2] Smith W.E., Dent G.,(2005), *Modern Raman Spectroscopy – A Practical Approach*, 1st John Wiley & Sons, Ltd, West Sussex,England.

[3] Baia M., Astilean S., Iliescu T., (2008), *Raman and SERS Investigations of Pharmaceuticals*. 1st Edition, Springer, Berlin Heidelberg.

[4] Stiles P.L., Dieringer J.A., Shah N.C.,Van Duyne R.P.,(2008), Surface-Enhanced Raman Spectroscopy, Annual Review of Analytic Chemistry, 1:601–26.

[5] Moskovits M.,(2005), Surface Enhanced Raman Spectroscopy: A brief retrospective, Journal of Raman Spectroscopy, 36,485-496.

[6] Fleischmann M., Hendra P.J., McQuillan A.J., (1974), Raman spectra of pyridine adsorbed at a silver electrode, Chemical Physics Letters 26,163.

[7] Kelly K., Coronado E., Zhao L., Schatz G., (2003), The Optical Properties of Metal Nanoparticles: The Influence of Size, Shape, and Dielectric Environment, The Journal of Physical Chemistry B,107,668.

[8] Sharma B., Frontier R.R., Henry A.I., Ringe E., Van Duyne R.P.,(2012), SERS: Materials, applications and the future, Materials Today,15 (1-2),16-25.

[9] Le Ru E.C., Etchegoin P.G. (2009), Principles of Surface-Enhanced Raman Spectroscopy: and related plasmonic effects, 1st Edition, Elsevier, Oxford, UK.

[10] Moskovits M.,(1982), Surface selection rules, Journal of Chemical Physics 77(9),4408-4416.

[11] Moskovits M,(2005), Surface-enhanced Raman spectroscopy: a brief retrospective, Journal of Raman Spectroscopy; 36: 485–496

[12] Le Ru, E.C., Blackie E., Meyer M., Etchegoin P.G. (2007), Surface Enhanced Raman Scattering Enhancement Factors: A Comprehensive Study, Journal of Physical Chemistry C ,111, 13794-13803.

[13] Michaels A.M., Nirmal , Brus L.E.,(1999), Surface Enhanced Raman Spectroscopy of Individual 333 Rhodamine 6G Molecules on Large Ag Nanocrystals, Journal of the American Chemical Society , 121, 9932-9939. 334

[14] Mullane A.P, Selvakannan P.R., Bhargava S.K.,(2010), Honeycomb nanogold networks 335 with highly active sites, Chemical Communications,46, 9182-9184.

[15] Kudelsky A., (2005) Raman studies of rhodamine 6G and crystal violet sub-monolayers on electrochemically roughened silver substrates: Do dye molecules adsorb preferentially on highly SERS-active sites?, Chemical Physics Letters ,414 (4-6),271–275.

[16] Yilmaz M., Senlik E., Biskin E., Yavuz M.S.,Tamere U., Demirel G.,(2014), Combining 3-D plasmonic gold nanorod arrays with colloidal nanoparticles as a versatile concept for reliable, sensitive, and selective molecular detection by SERS Physical .Chemistry Chemical Physics, 16, 5563-5570.

[17] Suarasan S., Focsan M., Maniu D., Astilean S., (2013), Gelatin-nanogold bioconjugates as effective 343 plasmonic platforms for SERS detection and tagging, Colloids and Surfaces B: Biointerfaces,103:475-481.

[18] Gandhi N.S., Mancera R.L., (2008), The Structure of Glycosaminoglycans and their

Interactions with Proteins, Chemical Biology and Drug Design;72: 455–482.

[19] Hileman R.E., Fromm J.R., Weiler J.M., Linhardt R.J. (1998) Glycosaminoglycan–protein interactions: definition of consensus sites in glycosaminoglycan binding proteins. BioEssays;20:156–167.

[20] Caldwell E.E., Nadkarni V.D., Fromm J.R., Linhardt R.J., Weiler J.M. (1996) Importance of specific amino acids in protein binding sites for heparin and heparan sulfate. International Journal of Biochemical Cell Biology; 28: 203–216.

[21] Varma R., Varma S.R.,(1989), *Mucopolysaccahrides-Glycosaminoglycans of body fluids in health and disease,* Walter de Gruyter & Co., Berlin, Germany.

[22] Burch P.E. (1989), DNA Damage and Cell Lethality by Photodynamically Produced Oxygen Radicals, PhD thesis, Rice University, Houston, Texas.

[23] Paula Burch´s All about hand dyeing, (2013), About dyes, http://www.pburch.net/dyeing/basic_dyes.shtml, April 2014.

[24] Barbosa P, Peters T.M.,(1971), The effects of vital dyes on living organisms with special reference to Methylene Blue and Neutral Red, The Histochemical Journal, 3, 1,71-93.

[25] Schlücker S,(2011),Surface enhanced Raman Spectroscopy:Analytical, biophysical and life science applications, Wiley VCH Verlag GmbH & Co, Weinheim,Germany.

[26] De Nicolai, S.H.A.; Rodrigues, P.R.P.; Agostinho, S.M.L.; Rubim, J.C. (2002) Electrochemical and spectroelectrochemical (SERS) studies of the reduction of methylene blue on a silver electrode, Journal of Electroanalytical Chemistry , 527, 103–111.

[27] Rodríguez-Torres M. del P.,Díaz-Torres Luis Armando, Romero-Servin S (2014), Heparin assisted photochemical synthesis of Gold nanoparticles and their performance as SERS substrates, International Journal of Molecular Sciences 2014, 15.

[28] Gabudean, A.M.; Focsan, M.; Astilean, S.(2012), Gold Nanorods performing as dual-modal Nanoprobes via metal-enhanced fluorescence (MEF) and surface-enhanced raman scattering (SERS), Journal Physical Chemistry C , 116, 12240−12249.

[29] Socrates G. (2001), *Infrared and Raman Characteristics Group Frequencies: Tables and Charts*, 3rd Edition, Wiley, West Sussex, England.

[30] Perkin Elmer, 2008, *Advantages of Raman Spectroscopy when Analyzing Materials Through Glass or Polymer Containers and in Aqueous Solution*, Waltham, MA, USA

[31] Ruperez A., Laserna J.J.,(1994), Solvent Effects on Surface-Enhanced Raman Activity of Adsorbates on Colloidal Silver, Applied Spectroscopy, 48, 2.

[32] Athax D.H., Gaigalas A.K, Reipa V,(1996), Structural Analysis of Heparin by Raman Spectroscopy, Journal of Pharmaceutical Sciences,85, 1, 52-56.

[33] Davida C.,Guillota N., Shenb H., Touryb T. ,De la Chapellea M.L. (2010), SERS detection of biomolecules using lithographed nanoparticles towards a reproducible SERS biosensor, Nanotechnology, 21(47):475501.

Chapter 4.

Summary.

4.1 Conclusions.

A new, simple while flexible strategy to synthesize colloidal gold anisotropic nanoparticles has been shown. Moreover, the obtained products are synthsized by taking advantage of an inexpensive home-made black light reactor and heparin as a reducing and stabilizing agent, and which is a biomolecule used as an anticoagulant that is also reactive in the UV range.

It was found that low heparin concentrations trigger nanoparticle growth in preferential directions contrary to the case when its concentrations is higher than the gold precursor one, which restrains this growth.

It was also shown that these heparin functionalized nanoparticles exhibit Raman activity which varies according to the heparin type used as well as to the charge of the analytes under study. These results suggest this as-produced heparin functionalized gold nanoparticles could be used in biological applications, taking into account that such functionalization allows a good affinity for a huge variety of organic molecules (methylene blue and rosebengal) and proteins (BSA and GP120), especially because there are no reports on surface enhanced Raman spectroscopy using heparin-based nanoparticles.

The developed photochemical synthesis approach has the following advantages:

1. It respects and follows the Green Chemistry principles.
2. It is inexpensive.
3. It is highly reproducible.

4. Nanoparticles are directly functionalized and they can be used in the future for biomedical applications.

5. It is not necessary it is carried out under very controlled conditions. The UV radiation used is not harmful for the most part.

4.2 Future work.

This work has been extensive, everything from the photochemical approach development, synthesis optimization, colloid selection and the surface enhanced Raman signal acquiring. There is still room for the development of planar and capillary substrates which can be used for SERS development using these hydrophilic heparin-based nanoparticles or either to have them functionalized for turning them hydrophobic as well.

Also, the products obtained may be used for detection of other analytes besides the ones used here, or be improved as drug carriers, which is another use of the heparin-based nanoparticles. Tailoring of the synthesis can also be done.

Original work has been done in proposing and developing the photochemical method based on the usage of UV-light using heparin, for the first time, as a reducing and stabilizing agent and it has also been proved the nanoparticles synthesized this way are useful in Surface Enhanced Raman Spectroscopy when synthesizing nanoparticles with reactive-grade heparin.

4.3 Contributions from this work.

All throughout these four years, three contributions, 2 articles and a proceeding came out. They are listed below.

1. UV photochemical synthesis of heparin-coated gold nanoparticles.
Gold Bulletin,May 2014, Volume 47, Issue 1-2, pp 21-31.

M. del P. Rodríguez-Torres, Luis Armando Díaz-Torres, Pedro Salas, Claramaría Rodríguez-González, Martin Olmos-López.
Cited by 1 (so far as of March 2015):
Muddineti O.S., Ghosh B., Biswas S.,(2015), Review:Current trends in using polymer coated gold nanoparticles for cancer therapy, International Journal of Pharmaceutics (Available online).

2. Heparin Assisted Photochemical Synthesis of Gold Nanoparticles and Their Performance as SERS Substrates.

Int J Mol Sci. 2014 Oct 23;15(10).
Del Pilar Rodríguez-Torres M, Díaz-Torres LA, Romero-Servin S.

3. UVA mediated synthesis of gold nanoparticles in pharmaceutical-grade heparin sodium solutions

SPIE NanoScience+ Engineering/Optics and Photonics Proceedings
August 11, 2013
2013 SPIE Travel grant (O+P conference 2013) Grant

This thesis work was supported by the National Council for Science and Technology (CONACyT)

through the scholarship grant: 166107 for PhD studies at Centro de Investigaciones en Óptica A.C.

(CIO) in the period: September 2010 – August 2014..